d'Collection

A THESIS
FOR THE DEGREE OF DOCTOR OF PHILOSOPHY

Triboelectric Nanogenerator for Powering Portable/Wearable Devices and its Smart Self-Powered Applications

ARUNKUMAR CHANDRASEKHAR

Department of Mechatronics Engineering

GRADUATE SCHOOL
JEJU NATIONAL UNIVERSITY

February 2018

Triboelectric Nanogenerators for Powering Portable/Wearable Devices and its Smart Self-Powered Applications

Arunkumar Chandrasekhar

(Supervised by Professor Sang Jae Kim)

A thesis submitted in partial fulfillment of the requirement for the degree of Doctor of Philosophy

2017.12

The thesis has been examined and approved.

Thesis Director,
Prof. Kwang Man Lee

Professor, Department of Electronics Engineering,
College of Engineering, Jeju National University

Thesis Committee Member,
Prof. Young Sun Mok

Professor, Department of Chemical Engineering,
College of Engineering, Jeju National University
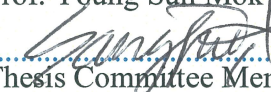
Thesis Committee Member,
Prof. Sang Jae Kim

Professor, Department of Mechatronics Engineering,
College of Engineering, Jeju National University

Thesis Committee Member,
Prof. Soo Seok Choi

Assistant Professor, Department of Energy Engineering,
College of Engineering, Jeju National University

Thesis Committee Member,
Prof. Woo Young Kim

Assistant Professor, Department of Electronics Engineering,
College of Engineering, Jeju National University

December, 2017

Department of Mechatronics Engineering
GRADUATE SCHOOL
JEJU NATIONAL UNIVERSITY
Republic Korea

Dedicated to

My Dear Mother

Mrs. V. Padmavathy

&

My Beloved Wife

Mrs. Deepa Katti

&

All My Family, Teachers

&

Friends

Acknowledgement

நீங்கள் உறங்கும் போது வருவது கனவு அல்ல,

உங்களை உறங்க விடாமல் செய்வதே கனவு,

Dream is not the thing you see in sleep

but is that thing that doesn't let you sleep.

Dr. A.P.J. Abdul Kalam

It is my great pleasure to thank so many people who have made this thesis possible. I sincerely acknowledge all the people who helped and supported me during my doctoral course.

Foremost, I express my sincere gratitude to my research supervisor, **Prof. Sang Jae Kim** for making it possible for me to realize my hopes and dreams of my research career. I am also grateful to him for guiding me to gain some expertise in the exciting field of nanomaterials research. With a broad sense of gratitude, I would like to thank for his guidance, happiness, support, encouragement, and suggestions. During some of my initial critical times in the research, he is the real guardian for me to overcome.

I would like to thank **National Institute for International Education (South Korea)** for inviting me in the **Korean Graduate Scholarship Program** and for their effort to teach Korean language. This gave an opportunity to interact with Korean people that transformed my life with a doctorate also mastering in Korean language.

I extend my sincere thanks to the thesis committee members **Prof. Kwang Man Lee**, **Prof. Young Sun Mok**, **Prof. Soo Seok Choi** and **Prof. Kim Woo Young** for their excellent suggestions and support to finish my thesis. I would like to thank Prof. Young Sun Mok for his constant support in collaboration work.

I extend my sincere thanks to **Dr. Ananthakumar Ramadoss** and **Dr. Suresh Kannan Balasingam** for their help, guidance, and encouragement to complete my thesis successfully. I would like to thank **Dr. Kaliannan Thiyagarajan**, for his valuable support, to achieve this thesis. I would like to express my sincere thanks to my friends **Dr. Rengarajan Baskaran**, **Dr. Govindan Rajapriya** and **Mr. Saravanan Govindan** for their encouragement and motivation throughout my research career. I would like to thank **Mr. Cho In Ho,** Mechatronics department staff for assisting in official process also **Mrs Lee Hyun Sook**, Brain Korea 21+ project staff for guiding me participate in various technical events.

Staying away from home country is always challenging. My immense sense of gratitude to my friends **Dr. S. Dharaneedharan** and **Mrs. Pooornima Dharaneedharan** for their constant help, advice, care and encouragement in research as well as in life. Without my senior, I couldn't be able to finish this degree. I sincerely thank **Dr. Saravanakumar Balasubramaniam** for his valuable support. I also thank him for his continuous encouragement in both profession and personal life during my research career. I am very much grateful to my friends and colleagues **Dr. Nagamalleswara Rao Alluri**, **Dr. Sophia Selvarajan**, **Ms. Yuvasree Purusothaman**,

Mr. Vivekananthan Venkateswaran, **Mr. Gaurav Khandalwal**, **Mr. Nirmal Prasanth**, **Mr. Rajagopal, Mr. Oh Gil Seop**, **Ms. Shin So Yoon**, **Mr. Kim Taehyun**, **Ms. Park Minhee** and **Mr. Seong Mingeon** for their help and support. I would like to thank **Dr. K. Anil Kumar**, **Dr. Roshini Arivazhagan, Mr. Sravan Kumar**, **Mr. Nilojan**, **Mr. Pavithran** and **Mr. Kugapreethan** for giving me so many memories to cherish during my stay in Jeju.

I also thank all the JISO members who have been very co-operative and supportive during my stay in Jeju. I am very much thankful to Research Instrument Center at JNU for providing the instrumental facilities during my study.

Last but certainly not least, I would like to express my deepest gratitude to my parents **Mrs. V. Padmavathy and Mr. K. Chandrasekhar** for their motivation, advise and support for my studies. Esspecially to thank my grandfather **late Dr. S. Venkatasan** for inspiring me to become a doctrate and my grandmother **Mrs. V. Bhagya Lakshmi** for her continuous prayers to make me strong, my dear brother **Dr. C. Gowtham Kumar**, and sister **Ms. L. Gayathri**, my uncle **Mr. V. Lakshmi Narayanan,** aunt **Dr. K.P.S. Komalavali** and family.

I would like to thank my wife **Mrs. Deepa Katti,** for her love, patience, support, for all the late nights and early mornings,and for keeping me healthy over the past few years. Thankyou, for being my editor, muse, proofreader and moral adviser. Above all thank you for being my best friend.

Finally, I want to thank my grand mother **late Mrs. K. Adilakshmi** for her blessings and her belives on me to achieve this doctrate, **Er. K. Raveendrababu,** mother-in-law **Mrs. K. Saritha Raveendrababu**, brother-in-law **Mr. K. Vamsipradeep,** sister **Dr. G. Deepthi Krishna** and the new addition to our family **Miss. Monvi Brinda,** for their continuous support, cheering and compassion. My thanks are bountiful for their wholehearted love and care.

Arunkumar Chandrasekhar

Thesis Overview

Contents

CHAPTER -1

Introduction

CHAPTER -2

Materials Characterization and Electrical Measurement Techniques

CHAPTER -3

Human Interactive Triboelectric Nanogenerator as a Self-Powered Smart Seat

CHAPTER -4

Smart Mobile Pouch as a Biomechanical Energy Harvester towards Self-Powered Smart Wireless Power Transfer Applications

CHAPTER - 5

Microcrystalline Cellulose Ingrained Polydimethylsiloxane Triboelectric

Nanogenerator as a Self-Powered Locomotion Detector

CHAPTER - 6

Sustainable Freestanding Biomechanical Energy Harvesting Smart Back Pack as a Portable-Wearable Power Source

CHAPTER - 7

Sustainable Biomechanical Energy Scavenger towards Self-Reliant Kids' Interactive Battery-Free Smart Puzzle

CHAPTER - 8

Summary and suggestions for the future work

List of Table

List of Figures

10, 15 and 20 Hz.

xiv

xv

초록

우리 사회의 지속 가능한 발전은 우리의 기본적인 필요를 충족시키기에 충분한 에너지의 양으로 정의된다. 하지만 기술의 급속한 발전은 에너지 위기로 이어지고 있다. 최근 특히 국방 분야에서 병사들이 다양한 착용 가능한 통신 및 실시간 상태 감시 장비를 사용하면서 착용 가능하고 휴대할 수 있는 기기의 사용이 급증하고 있다. 이러한 기기는 연속적인 작동을 위해 배터리를 자주 충전하거나 교체해야 한다. 전 세계의 연구원들은 물질의 엔지니어링, 혁신적인 디자인, 높은 전력 밀도 및 안정성과 같은 다양한 측면을 가진 에너지 수집 및 저장 분야에 대해 연구하고 있다. 그러나 여전히 이동하는 동안 휴대용 및 착용 가능한 기기에서 전원 문제에 직면해 있다. 이 시나리오는 생체 역학 에너지를 절약함으로써 교체할 수 있다. 에너지 수집 장치는 가벼운 중량, 압축 가능한, 휴대용, 착용 가능하고 환경 친화적이어야 한다. 이 점은 그러한 전자 기기에 전력을 공급하기 위해 생체 역학 에너지를 흡수하는 혁신적인 기술을 추구하기 위한 것이며, 또한 이 검색은 프로세스를 수행할 수 있는 기기를 설계하기 위해 자체적으로 설계된다. 최근에, 마찰 전기 나노 발전기가 물, 바람, 진동과 같은 다양한 출처에서 에너지를 흡수하기 위해 연구원들에 의해 개발되었다. 이 마찰 전기 나노 발전기를 발견하기 전까지, 마찰 전기 현상은 다양한 전자 및 항공 우주 분야에서 원치 않는 간섭으로 여겨졌다. 하지만 이 시나리오는 이제 중합체 필름에 전극을 부착함으로써 바뀌었다. TENG의 작동 원리는 정전기 유도 및 접점 전화에 기반하며, 이러한 TENG 장치는 높은 에너지 변환 효율에 적합한 네가지 모드에서 작동합니다. 또한, 특정한 애플리케이션 분야의 혁신적인 아이디어는 똑똑한 자체적으로 작동하는 장치를 발명하게 할 것이다.

이 논문의 주된 초점은 스마트 폰, 가방, 좌석, 신발 등과 같은 기기가 내장된 새로운 마찰 전기 나노 발전기를 고안하는 것이다. 본 논문의 제3장에서는 스마트 시트를 기반으로 하는 경량의, 유연한, 비용 효과적이고 강력한 단일 전극의 제작에 대해 다룬다. 이는 생활 환경에서 에너지를 거둬들이고, 통합된 자가 전력 시스템에 사용할 수 있는 유망한 친환경적 접근 방식이다. 폭넓게 조정 가능한 일상적인 접촉 소재(신문, 데님, 폴리 에틸렌 커버 및 버스 카드)를 사용하여 걷고, 뛰고, 앉는 것과 같은 인간의 움직임에서 생체 역학 에너지를 채취하는 효과적인 방법이 입증되었다. SS-TENG의 작동 메커니즘은 능동 층과 사용자 친화적인 접촉 물질 사이의 마찰 전하 캐리어의 생성과 전송에 기초합니다. SS-TENG 복합 SS-TENG 의 경우 52V및 5.2μA)의 성능은 체계적으로 연구되고 있으며, 간단한 STOP INC를 사용한 셀프 파워 조수석 시트 숫자 표시기를 포함한 애플리케이션에서 입증되었다.

Harvested 에너지는 상용 LED 60개와 녹색의 LED및 단색 LCD를 구동하기 위한 직접 전원으로 사용됩니다. 이 실행 가능성 연구는 마찰 전기 나노 발전기가 수송을 하는 동안 인간의 움직임으로부터 에너지를 채취하는 적합한 기술이라는 것을 확인하는데, 이는 다양한 무선 장치, GPS, 전자 기기를 사용하는 동안에 사용될 수 있다. 스마트 이동식 전기 이동식 전기 발전기(SMP-TENG)는 차세대 지능형 장치와 스마트 폰을 구동하기 위한 생체 역학 에너지 청소기로 제4장에서 논한다. 이는 인간의 움직임에서 에너지를 얻을 수 있는 비용 효과적이고 강력한 방법으로, 마모된 직물을 접촉 소재로 활용합니다. SMP-TENG은 측면 슬라이딩과 수직 접촉 및 분리라는 두가지 작동 모드에서 에너지를 수집할 수 있습니다. 게다가, SMP-TENG 는 또한 정상적인 인간의 움직임 동안 자체적으로 동력을 공급하는 비상 손전등과 자체적으로 동력을 공급하는 만보계의

역할도 할 수 있다. SMP-TENG과 통합된 무선 전송 설정이 입증되었습니다. 이를 통해 전통적인 에너지 수집 장치를 자체적으로 작동하는 무선 전력 전송 SMP-TENG으로 업그레이드할 수 있습니다. 무선으로 전송되는 전력은 리튬 이온 배터리와 LED를 충전하는 데 사용할 수 있습니다. SMP-TENG은 자체적으로 작동하는 장치와 휴대용 및 착용 가능한 전자 기기를 위한 낮은 유지 관리 에너지 수집 시스템 분야에서 광범위한 기회를 제공합니다.

주변의 비산 된 기계적 에너지를 청소하면 보조 전압원을 제공하여 기존 배터리의 한계를 극복함으로써 자체 전력 및 마모성 전자 장치의 잠재력을 크게 높일 수 있다. 챕터-5에서는 알루미늄 소재의 접점과 복합 소재로 구성된 전극 사이의 셀룰로즈 열 전달 물질(PDMS)삼지성 나노 발전기(C-TENG)모드를 시연합니다. 5 W의 복합 필름으로 제작된 기기는 28 V의 개방 회로 전압과 2 µA의 단락 전류를 발생시키며, 기계적인 피크 전력이 576 µW이고, 32.16 N의 기계적 보안 기기로 작동하는 것을 체계적으로 입증할 수 있다. C-TENG은 또한 인간이 다양한 동작 범위에서 리튬 이온 배터리 충전 회로를 내장한 착용 가능한 전원으로 사용할 수 있습니다. 다음으로, 혁신적이고 비용 효율적이며 환경 친화적인 스마트 백 트리비전 형 나노 발전기(SBP-TENG)가 6장에 제시된다. 폴리 에틸렌/실록산 필름에 불규칙한 표면을 만드는 새로운 접근법은 실험실 사용 후 버려진 플라스틱 페트리 접시를 재활용하는 것으로 증명되었습니다. SBP-TENG 는 PDMS필름과 접촉 물질(양모, 종이, 면, 데님, 폴리 에틸렌)사이의 접촉 및 분리 전화에 의존한다. 단일 및 복수 호기 SBP-TENG의 성능은 걷기, 작동 및 휨 입증된 것과 같은 인간의 움직임에서 실시간 에너지 수집과 체계적으로 연구된다. 이 연구에 따르면 SBP-TENG는 글로벌 포지셔닝 시스템(GPS)시스템, 착용감 있는 센서, 플래시 등

과 같은 다양한 저전력 전자 장치를 구동할 수 있는 생체 역학적 에너지를 청소하는 탁월한 기술이다.

7장은 표면 수정 필름 사이의 접촉과 분리 모드에 기초한 스마트 퍼즐 삼원자 나노 발전기(SP-TENG)를 제공한다. SP-TENG은 출력 전압이 70 V이고 전류가 6.5 µA인 간단한 구조(얇고 가벼움)를 보여 주며, 이는 손가락으로 누르면 액체 결정 디스플레이를 구동할 수 있습니다. SP-TENG에 대한 체계적인 조사는 상용 축전기를 충전하고 액체 결정 표시 장치를 구동할 수 있는 잠재력을 가진 실용적인 에너지 수확기라는 것을 입증했다. SP-TENG 도 검출 감도가 2.605 µA/kPa^{-1}인 순간 힘 센서로 작동합니다. 그 다음, 우리는 퍼즐 조각으로 6개의 SP-TENG를 만들어 냈고, 간단한 논리 회로에 연결함으로써 스스로 힘을 얻은 스마트 퍼즐을 만들었습니다. 이 접근법은 단순한 전통적인 퍼즐을 향상시켜, 상호 작용적인 스마트 퍼즐로 변환시켰습니다.

Abstract

Sustainable development of our society is defined by the amount of sufficient energy to fulfill our basic needs. But the rapid development in the technology drives to the energy crisis. Recently, the usage of wearable and portable gadgets are rapidly increasing, especially in defense sectors soldiers are using various wearable communications and real time health monitoring equipments. These gadgets require frequent charging or replacement of batteries for its uninterrupted working. Researchers across the globe are working on energy harvesting and energy storage sectors with various aspects such as engineering of materials, innovative design, high power density and stability. However, still we are facing power issues in portable and wearable gadgets while travelling; this scenario can be replaced by scavenging the biomechanical energy. It is important that the energy harvesting device should be light weight, compactable, portable, wearable, and also eco-friendly. This point drives in search of an innovative technique to scavenge biomechanical energy to power those electronic gadgets, also with this search the concept of self-powered systems fascinate to engineer a device which is capable of doing dual process simultaneously. Recently, Triboelectric Nanogenerator (TENG) has been developed by the researchers to scavenge energy from various sources such as water, wind, vibration. Until the discovery of this triboelectric nanogenerator, the triboelectric phenomenon was considered an unwanted interference in various electronic and aerospace applications. But this scenario has now changed by attaching electrodes to the polymer films. The working principle of TENG is based on electrostatic induction and contact electrification, and these TENG devices works in four different modes, which are adaptable for high energy conversion efficiency. In addition, an innovative idea with a specific field of application will drive to invent a smart self-powered device.

The main focus of this thesis is to engineer a novel triboelectric nanogenerator embedded with a gadget such as smart phone, bag, seat, shoes, and so on. Chapter 3 of this thesis covers the fabrication of a lightweight, flexible, cost effective and robust, single electrode based Smart Seat–Triboelectric Nanogenerator (SS-TENG). It is a promising eco-friendly approach for harvesting energy from the living environment, for use in integrated self-powered systems. An effective method for harvesting biomechanical energy from human motion such as walking, running, and sitting, utilizing widely adaptable everyday contact materials (newspaper, denim, polyethylene covers, and bus cards) is demonstrated. The working mechanism of the SS-TENG is based on the generation and transfer of triboelectric charge carriers between the active layer and user-friendly contact materials. The performance of SS-TENG (52 V and 5.2 μA for a multi-unit SS-TENG) is systematically studied and demonstrated in a range of applications including a self-powered passenger seat number indicator and a STOP-indicator using LEDs, using a simple logical circuit. Harvested energy is used as a direct power source to drive 60 blue and green commercially available LEDs and a monochrome LCD. This feasibility study confirms that triboelectric nanogenerators are a suitable technology for energy harvesting from human motion during transportation, which could be used to operate a variety of wireless devices, GPS systems, electronic devices and other sensors during travel. A Smart Mobile Pouch Triboelectric Nanogenerator (SMP-TENG) is discussed in Chapter- 4 as a biomechanical energy scavenger for powering next generation intelligent devices and smart phones. This is a cost-effective and robust method for harvesting energy from human motion, by utilizing worn fabrics as a contact material. The SMP-TENG is capable of harvesting energy in two operational modes: lateral sliding and vertical contact and separation. Moreover, the SMP-TENG can also act as a self-powered emergency flashlight and self-powered pedometer during normal human motion. A

wireless power transmission setup integrated with SMP-TENG is demonstrated. This upgrades the traditional energy harvesting device into a self-powered wireless power transfer SMP-TENG. The wirelessly transferred power can be used to charge a Li-ion battery and light LEDs. The SMP-TENG opens a wide range of opportunities in the field of self-powered devices and low maintenance energy harvesting systems for portable and wearable electronic gadgets.

Scavenging of ambient dissipated mechanical energy addresses the limitations of conventional batteries by providing an auxiliary voltaic power source, and thus has significant potential for self-powered and wearable electronics. Chapter- 5 demonstrates a cellulose/polydimethylsiloxane (PDMS) triboelectric nanogenerator (C-TENG) based on the contact and separation mode between a cellulose/PDMS composite film and an aluminium electrode. The device fabricated with a composite film of 5 wt% generates an open circuit voltage of 28 V and a short circuit current of 2.8 µA with an instantaneous peak power of 576 µW at a mechanical force of 32.16 N. The C-TENG was systematically studied and demonstrated to be a feasible power source that can commute instantaneous operation of LEDs and act as a self-powered locomotion detector for security applications. The C-TENG can also be used as a wearable power source with an in-built lithium ion battery charging circuit during a range of human motion. Next, an innovative, cost-effective and eco-friendly freestanding smart backpack-triboelectric nanogenerator (SBP-TENG) is presented Chapter- 6. A new approach to creating irregular surfaces on polydimethylsiloxane (PDMS) film is demonstrated by recycling a plastic petri dish discarded after laboratory usage. The SBP-TENG relies on contact and separation electrification between the PDMS film and the contact materials (wool, paper, cotton, denim and polyethylene). The performance of single- and multi-unit SBP-TENGs is systematically studied and real-time energy harvesting from human motions, such as walking,

running and bending demonstrated. This study confirms that the SBP-TENG is an excellent technology for scavenging bio-mechanical energy, capable of driving a variety of low-power electronic devices such as Global Positioning System (GPS) systems, wearable sensors and flash lights.

Chapter-7 presents a smart puzzle triboelectric nanogenerator (SP-TENG) based on the contact and separation mode between a surface-modified polydimethylsiloxane film and a paper contact material. The SP-TENG exhibits a simple structure (thin and lightweight), with an output voltage of 70 V and a current of 6.5 µA, which can drive a liquid crystal display at the press of a finger. A systematic investigation of the SP-TENG demonstrated it to be a practical energy harvester with the potential to charge a commercial capacitor and drive a liquid crystal display. The SP-TENG also acts as an instantaneous force sensor with detection sensitivity of 2.605 µA kPa^{-1}. Next, we fabricated six SP-TENGs as puzzle pieces and formed a self-powered smart puzzle by connecting it to a simple logic circuit. This approach improved a simple traditional puzzle, transforming it into an interactive smart puzzle.

CHAPTER-1

Introduction

1.1 Background

The recent development of the electronic technology creates a trend of miniaturization, simplicity, portability, and multi-functionality. The increase of wearable and portable electronic gadgets in the last decade made the energy industry to think wide about the need of renewable energy harvester. In general, electrical energy usually means the energy required to power an industry or a city but in other hands powering the portable electronic gadgets also plays a vital role in the present situation. In the next few decades, the world will be integrated with sensors, navigation systems and so on. The development of smaller size electronics needs ultra low power to their operation. So making a small electrical energy from our daily activity will be a huge advantage for these low-power electronic gadgets.

Recent technologies that can scavenge energy from our living environment as a self-sufficient power source are newly emerging in the field of nano energy. In the last decade, various research groups are developing nanogenerators (NG) for developing self-powered systems. Mainly two energy harvesting principle was used for this small-scale energy scavenging: piezoelectric effect[1], [2] and triboelectric effect[3], [4]. Compared to piezoelectric nanogenerator the impact of triboelectric nanogenerator (TENG) in our society is more. The development of TENG is simple, cost-effective and it is an eco-friendly approach to develop a sustainable renewable energy harvester.

1.2 Importance of Triboelectric Nanogenerator

From very long years till now we mainly depend on fossil fuels for various energy applications, even though we have developed lots of other energy sources, all these techniques have many disadvantages that cause a threat to the mankind in various ways such as, global warming, nuclear radiation, chemical reaction, carbon emission and soon . From the last few decades, we are mainly utilizing thermal and nuclear energy to fulfill our daily needs. These power plants are expensive in initialization and maintenance and high threat to the environment. Also, installation of these power plants consumes the finance of the nation and threat to sustainable development. **Figure 1.1** shows the impact of energy sectors on economy and social life. Maximum utilization of fossil, nuclear, and thermal energy for producing electrical energy paves a path towards

- World energy crisis

- Carbon emission

- Global warming

- Threat to sustainability

- Inflation in the economy
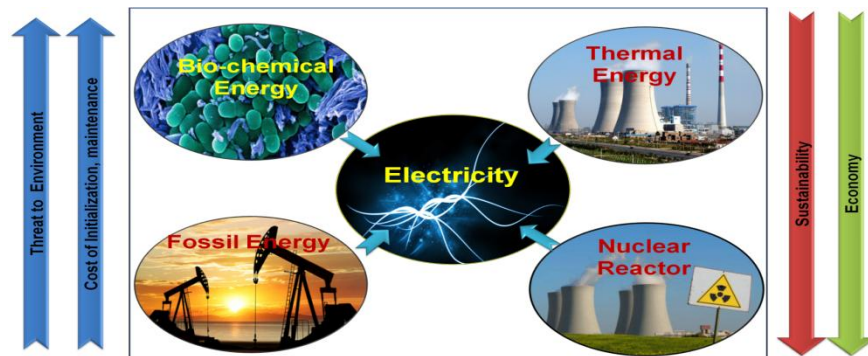
Figure 1.1 Impact of energy sectors on economy and social life.

To fulfill the energy needs of mankind, governments are forced to commission some nuclear power reactor and other power projects. However, all these are driving towards environmental pollution, inflation in the electric bill, energy crisis, inflation in the cost of consumer products, finally harmful to our future generation. Importance of this research is to open a new path to utilize the biomechanical energy, which will help to develop an eco-friendly environment and sustainable development of our society. The recent research approach focuses on developing various eco-friendly energy harvesters to scavenge the renewable energies. TENG is a multi-functional device which can scavenge energy from various modes of vibration, and it can act as a self-powered device in various applications.

1.3 Principle of Triboelectric Nanogenerator

The name "Tribo" comes from the Greek language for "rubbing." Triboelectric effect is a common cause of our day today activity called electrostatics. It is a contact electrification effect in which a material comes in contact with other materials will electrically charge. This effect was known as a noise signal from very long years. When the Van de Graaff generator was developed to generate the voltage by the electrostatic induction and triboelectrification, the concept of triboelectric effect was widely identified.
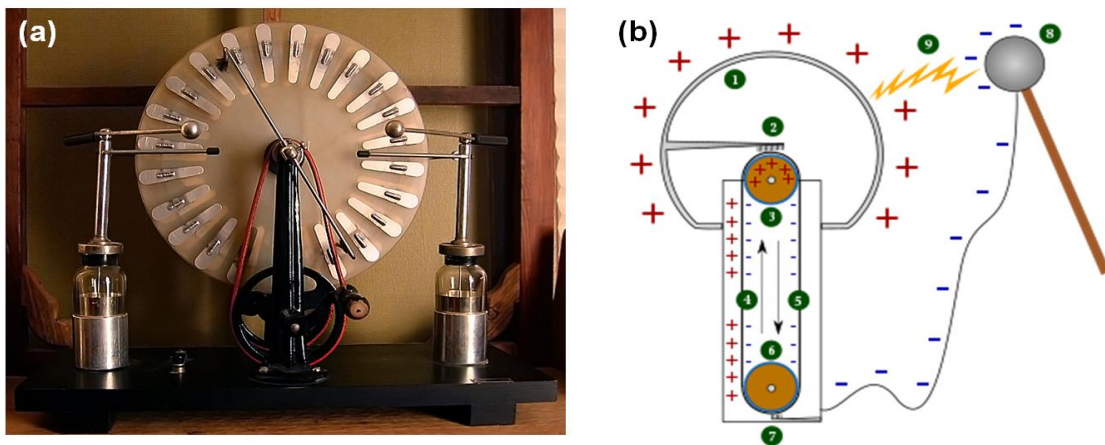
Figure 1.2 (a, b) Wimshurst and Van De Graaff triboelectric generator.

3

The **Figure 1.2 (a, b)** presents the triboelectric generator developed by Wimshurst and Van De Graaff. The basic working mechanism in this triboelectric generator is simple when materials with two different surfaces charge rub together; a charge generated.

Recently, using the electrostatic charges created on the surfaces of two dissimilar materials when they brought into physical contact attracted the researcher. The contact-induced triboelectric charges can generate a potential drop when the two surfaces separated by mechanical force, which can drive electrons to flow between the two electrodes built on the top and bottom surfaces of the two materials. This was the starting of triboelectric nanogenerator (TENG). Since the first report on the TENG in January 2012, the area power density reaches 500 W m^{-2} volume power density reaches 15 MW m^{-3} and an instantaneous power conversion efficiency of 70 %. For low-frequency motion, a total energy conversion efficiency of up to 85% has been shown experimentally[5]. The TENG can be used to scavenge any kinds of mechanical energies that are wasted in our daily life, such as biomechanical, vibration, wind, mechanical triggering, flowing water, rotating tire, and more. Also, a TENG can also be used as a self-powered sensor for actively identifying the static and dynamic processes during mechanical motion using the output electrical signals of the TENG, respectively, with potential applications as mechanical sensors, smart skin technologies, and touchpad. The TENG also has the potential of scavenging ocean wave energy, which could be a new approach for large-scale energy[6]–[8].

1.4 Four fundamental working modes of the TENG

Triboelectrification is a phenomenon that is known to each and everyone probably ever since the Greek time, but usually it is taken as negative effect and avoided in many technologies. Discharges caused by triboelectricity have caused many disastrous damages to industrial processes, electronics, human life, and nature, such as wildfire. However, this effect is seen

4

almost everywhere in our daily life and for any material that we use. Our aim here is to utilize this triboelectricity by converting mechanical energy into electrical energy based on new materials and new designs. To develop an open-circuit condition, two electrodes are attached to the polymer films, by the coupling of electrostatic induction and triboelectrification. The triboelectric charges generated due to the charge transfer between polymer films that shows distinct surface electron affinity and the potential difference is obtained from the separation of the triboelectric charges. During short-circuit conditions, electrons are driven to flow between two electrodes attached on the back side of the films through the load to balance the potential difference resulting from mechanical action. There are mainly four modes of the TENG, which are the basis for various TENGs.[9]
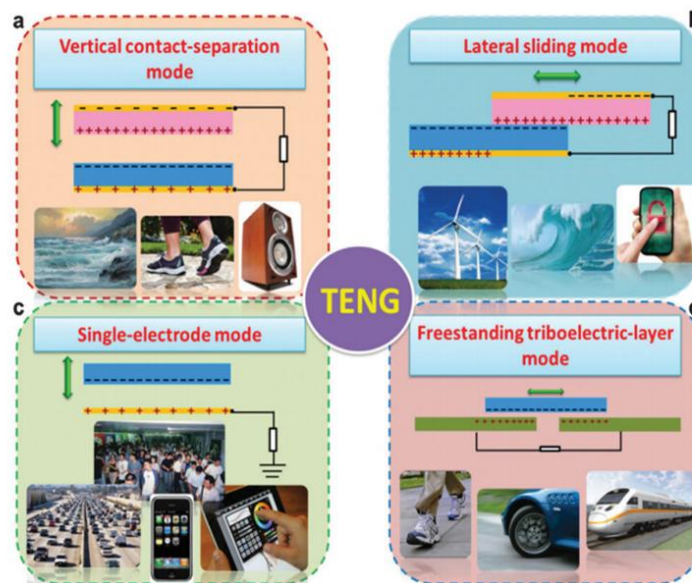
Figure 1.3 The four fundamental working modes of the triboelectric nanogenerators. (a) The vertical contact-separation mode. (b) The lateral sliding mode. (c) The single-electrode mode. (d) The free-standing mode. (Image source: Faraday Discussion, 2014, 176, 447-458)

1.4.1 Vertical contact-separation mode

The vertical contact-separation mode was the initial operation mode for TENGs. A physical contact between the two polymer films with different electron affinity creates oppositely

charged surfaces. Once a gap separates the two surfaces, a potential drop is occurred between the electrodes on the top and bottom surfaces of two polymer films, as shown in **Figure. 1.2 (a)**. If a load electrically connects the two electrodes, free electrons in top electrode would flow to the bottom electrode to balance the electrostatic field. Once the air gap is closed, the potential drop generated by the triboelectric charges disappears, the induced electrons flow back. A continuous contact and separation between these materials moves the induced electrons to flow back and forth between the electrodes, resulting in an AC output signal in the circuit. Here, the electricity generation process depends on a continuous switching between the contact and separation process of the two contact surfaces, and the output is AC signal. Various structural designs were developed, including arch-shaped, cantilever based, zig-zag, spring-supported and so on to scavenge the mechanical energy. TENGs devices based on this mode of operation shows excellent performance in cyclic motions, intermittent impact. This mode is highlighted as a simple design, great robustness, and high power density. However, the design of the vertical contact separation mode is a cavity with constantly changing volume, which is a challenge for the packaging of the TENG. The vertical contact-separation mode has been widely used to scavenging energy from finger typing,[10] engine vibration,[11] human walking[12] and biomedical systems.

1.4.2 In-plane sliding mode

As shown in **Figure. 1.2 (b)**, when two materials with opposite triboelectric polarities, for instance, Kapton film and aluminum, are brought into contact, surface charge transfer takes place due to the triboelectrification effect. Since Kapton film holds a higher electron affinity than aluminum, electrons are injected from aluminum into Kapton film. When the Kapton film and Al are fully aligned, the electric field created by the triboelectric charges does not produce a

potential drop, because the positive charges on aluminum adequately compensated by the negative ones on Kapton film. Once an externally applied force introduces a motion in the direction parallel to the interface, triboelectric charges are not adequately compensated at the mismatched areas; this results in the creation of a useful dipole polarization in parallel to the direction of the displacement. Therefore, a potential difference across the two electrodes generated. A sliding back and forth between the two electrodes results in a periodical change in the electric potential difference, which drives free electrons to flow alternatively across the electrodes. The in-plane sliding mode holds several essential advantages compared to the vertical contact-separation mode. The development of triboelectric charges from the sliding between two surfaces is much more efficient than the simple contact, which contributes to a significantly enhanced output power for real-time applications. Furthermore, the in-plane sliding mode is easy to fabricate an advanced design for high-performance TENGs. Through a grating structure, the total amount of charges is increased. With a stable sliding velocity, finer grating shortens the time to transport induced charges between the electrodes, which enable substantial enhancement of both the magnitude and frequency of the output current. The in-plane sliding mode excels in harvesting energy from planar motions, disc rotation, and cylindrical rotation. Moreover, it was demonstrated to harvest wind energy,[13] rotational kinetic energy, hydropower, and so on. Moreover, it was also developed to function as a velocity sensor, motion sensor, and so on.

1.4.3 Single-electrode mode

In vertical contact-separation mode and in-plane sliding mode triboelectric nanogenerators, the moving objects need to be attached with an electrode and a lead wire. This device configuration largely limits TENGs' performance and applicability for scavenging energy from an arbitrary, freely moving object, because the object should be connected to the entire

제주대학교 중앙도서관
JEJU NATIONAL UNIVERSITY LIBRARY

device by a linker. A single electrode mode TENG was developed to solve these problems.[14], [15] As demonstrated in **Figure. 1.2 (C)**, this mode consists of, for instance, a Kapton film moving object and an aluminum layer electrically connected to the ground. During the initial state, Kapton and aluminum are in contact with each other, which results in electrons being injected from aluminum to Kapton since Kapton has higher surface electron affinity than aluminum. Once the negatively charged Kapton slides apart, a decrease of the induced positive charges on Al occurs, and the electrons will flow from the ground to aluminum till the two plates are entirely separated, to balance the electric potential. Then, when Kapton slides backward or comes into contact again, the induced positive charges on the aluminum increase, driving the electrons to flow from the electron to the ground till the two plates are entirely overlapped to develop an electrostatic equilibrium. This process contributes a full cycle of the electricity generation process of the single electrode mode TENG. Although the induced electron transfer across the electrode is not efficient due to the electrostatic screening effect, one of the triboelectric layers can move freely without any restriction. With this feature, the single electrode mode has been used to scavenge energy from rotating tire, air flow, raindrop, and turning the book pages. It was also used as self-powered touch sensor, displacement vector sensors, biosensors, velocity sensors, active tactile sensors, pressure sensors, self-powered trajectories, angle measurement sensors, acceleration sensors, water/ethanol sensors, sensors for healthcare monitoring, body motion sensors, self-powered distress signal emitters, self-powered identification systems, and

1.4.4 Free-standing triboelectric-layer mode

The freestanding triboelectric-layer mode triboelectric nanogenerator is capable of harvesting energy from the mechanical motion without an electrode attached, as shown in **Figure.**

8

1.2 (d). A pair of electrodes under a dielectric layer and the size of the electrodes are of the same other electrode as the size of the moving object, and there is a small air gap between the object and the electrode, the object's approaching to and/or departing from the electrodes create an charge distribution via induction in the media. The object will be prior-charged by a triboelectric process, which causes the electrons to flow between the two electrodes to balance the potential difference. The movement of electrons between the electrodes in response to the motion of the object produces an AC output.[16] Compared to the single-electrode mode, there is no screening effect in this mode, and the electrostatically-induced electron transfer can reach the same amount of the triboelectric charges on the free-standing layer. In this working mode, there can be on direct contact between the two triboelectric layers, compared to the in-plane sliding mode, and it cause no physical abrasion and heat generation under long-term continuous working. This distinguishes the free-standing mode with ultra robustness as well as high energy conversion efficiency. This freestanding triboelectric-layer mode TENG has been demonstrated to harvest energy from vibration, rotation motions, computer mouse operation, air flow, a walking human or a moving automobile. Moreover, it was developed into self-powered vibration sensor and active micro-actuators.

1.5 Materials for Triboelectrification

Almost any materials we know have triboelectrification effect, from polymer to metal, to silk and wood, almost everything. All of these materials can be a potential candidate for fabricating TENGs so that the materials choices for TENG are broad in range. However, the potential of a material for gaining/losing electron mainly depends on its polarity. John Carl Wilcke published his research on triboelectric series in a 1757 on static charges. Table 1.1 gives such a series for some conventional materials. A material towards the end of the series, when

interacted to a material near the top of the series, will gain more negative charge. The further distance of two materials on the series, the higher the charge transferred. Recently, using the contact between a liquid metal and solid, such as Hg, a methodology has been developed to measure the surface charge density as a result of triboelectrification. Apart from the choice of the materials in the triboelectric series, the surface morphologies can be modified by physical techniques with the creation of pyramids, square- or hemisphere-based micro- or nano-patterns, which are valid for enhancing the contact area and possibly the triboelectrification. The surfaces of the materials can be functionalized chemically using various nanoparticles or nanowires, nanotubes, to enhance the triboelectrification effect. Surface functionalization can mostly change the surface potential. The introduction of nanostructures on the surfaces can change the local contact characteristics between the active layers. The contact materials can be made of composites, such embedding nanoparticles in polymer matrix. This not only changes the surface electrification but also the permittivity of the materials so that they can be useful for electrostatic induction.

Positive			Negative
	Polyformaldehyde 1.3-1.4	(continued)	
	Etylcellulose	Polyester (Dacron)	
	Polyamide 11	Polyisobutylene	
	Polyamide 6-6	Polyuretane flexible sponge	
	Melanime formol	Polyethylene Terephthalate	
	Wool, knitted	Polyvinyl butyral	
	Silk, woven	Polychlorobutadiene	
	Aluminum	Natural rubber	
	paper	Polyacrilonitrile	
	Cotton, woven	Acrylonitrile-vinyl chloride	
	Steel	Polybisphenol carbonate	
	Wood	Polychloroether	
	Hard rubber	Polyvinylidine chloride (Saran)	
	Nickel, copper	Polystyrene	
	Sulfur	Polyethylene	
	Brass, silver	Polypropylene	
	Acetate, Rayon	Polyimide (Kapton)	
	Polymethyl methacrylate (Lucite)	Polyvinyl Chloride (PVC)	
	Polyvinyl alcohol	Polydimethylsiloxane (PDMS)	
	(continued)	Polytetrafluoroethylene (Teflon)	

(continued)

Table 1.1 Triboelectric series for some commonly materials following a tendency of easy losing electrons (positive) to gaining electrons (negative) (Source: J.Phys. D Appl. Phys. 9 (10), 1445)

Table 1.1 (continued)

Positive ↑		Negative ↓
	Aniline-formol resin	Polyvinyl alcohol
	Polyformaldehyde 1.3-1.4	Polyester (Dacron) (PET)
	Etylcellulose	Polyisobutylene
	Polyamide 11	Polyuretane flexible sponge
	Polyamide 6-6	Polyethylene terephthalate
	Melanime formol	Polyvinyl butyral
	Wool, knitted	Formo-phenolique, hardened
	Silk, woven	Polychlorobutadiene
	Polyethylene glycol succinate	Butadiene-acrylonitrile copolymer
	Cellulose	Nature rubber
	Cellulose acetate	Polyacrilonitrile
	Polyethylene glycol adipate	Acrylonitrile-vinyl chloride
	Polydiallyl phthalate	Polybisphenol carbonate
	Cellulose (regenerated) sponge	Polychloroether
	Cotton, woven	Polyvinylidine chloride (Saran)
	Polyurethane elastomer	Poly(2,6-dimethyl polyphenyleneoxide)
	Styrene-acrylonitrile copolymer	Polystyrene
	Styrene-butadiene copolymer	Polyethylene
	Wood	Polypropylene
	Hard rubber	Polydiphenyl propane carbonate
	Acetate, Rayon	Polyimide (Kapton)
	Polymethyl methacrylate (Lucite)	Polyethylene terephtalate
	Polyvinyl alcohol	Polyvinyl Chloride (PVC)
	(continued)	Polytrifluorochloroethylene
		Polytetrafluoroethylene (Teflon)

Table 1.1 (cont) Triboelectric series for some commonly materials following a tendency of easy losing electrons (positive) to gaining electrons (negative) (Source: J.Phys. D Appl. Phys. 9 (10), 1445)

1.6 Self-powered systems and sensors

The ultimate goal of nanogenerators is to build up self-powered systems, in which

multifunctional electronic devices can be powered up by the nanogenerators through collecting

ambient mechanical energies. To achieve this goal, energy storage devices and power transformers are indispensable to store the harvested energy and to regulate the output power into a constant DC power to drive electronic devices. The concept of self-powered system has been applied in many fields owing to the high output of TENGs, including powering portable electronics, electrochemical reactions, logical electronic circuitry, sensor networks, biomedical devices, etc.

A sustainable power source is critical for the operation of implanted biomedical devices, especially considering the limited lifetime of the traditional battery power supply since the replacement of drained batteries usually require additional surgery with more risk and pain to the patients. In this regard, Zheng et al. developed the first in vivo biomechanical energy harvesting system with an implanted triboelectric nanogenerator (iTENG) to power up a prototype pacemaker by harvesting energy from the periodic breathing of a living rat.

The recent development of internet of things (IoTs) requires wireless, multi-functional, and independent operation of sensor networks. The implementation of large number of small-scale sensors, and use of traditional power supply is a big challenge. Hence, developing a self-powered sensors[17] that can employ the ambient environmental energy is highly desired. In this regard, the self-powered active sensors based on TENGs will be an optimum solution. As a new power generation technology, TENGs can be used to scavenge the mechanical energy; on the other hand, by analyzing the electrical output signals of TENGs, the information on the mechanical input (magnitude and frequency) can be successfully analysised. Since this sensing technology originates from the output signals of the TENG itself, no external power source is required to apply onto the device, which is a unique advantage over conventional sensor technologies. By correlating the mechanical input with many other parameters, many prototypes

제주대학교 중앙도서관
JEJU NATIONAL UNIVERSITY LIBRARY

have been realized for various applications, including pressure detection, security check, motion sensing, environmental monitoring, and acoustic sensing, and so on.

1.7 Scope of this present work

The literature studies depicts that the TENG are one of the prominent renewable energy scavenging device for high energy conversion efficiency and its recent applications demonstrates that it is a potential candidate to develop a sustainable energy system for portable and wearable gadgets. Also, the need of self-powered devices has been increasing day by day; developing a TENG with a possible self-powered application is a significant challenge. Hence, evaluating all these factors the objective of this research has been designed to fabricate a portable/ wearable device, which are capable of harvesting biomechanical energy with a self-powered application. In this aspect, few industrial materials as an active polymer, other cloth materials were chosen, and devices were fabricated using various sophisticated techniques. The detailed objective of this work are briefly outlined as follows,

- To develop a cost-effective, eco-friendly and easy fabricating technique for bio-mechanical energy harvesting application.

- To fabricated a device which can utilize the materials that we use in our daily life for harvesting energy

- To develop a sustainable energy source to support portable and wearable gadgets

- Development of an integrated system to harvest biomechanical energy and wireless power transfer to charge a lithium-ion battery.

- To develop a dual operational mode TENG and investigate its electrical performance for self-powered applications.

14

- Finally to develop commercial gadgets that can be used in our day today life to meet the power requirement. Moreover, a simple platform to develop a self-powered devices.

1.8 References

[1] R. Yang, Y. Qin, L. Dai, and Z. L. Wang, "Power generation with laterally packaged piezoelectric fine wires.," *Nat. Nanotechnol.*, vol. 4, no. 1, pp. 34–9, Jan. 2009.

[2] Z. L. Wang and J. Song, "Piezoelectric nanogenerators based on zinc oxide nanowire arrays.," *Science*, vol. 312, no. 5771, pp. 242–6, Apr. 2006.

[3] F. Yi, L. Lin, S. Niu, P. K. Yang, Z. Wang, J. Chen, Y. Zhou, Y. Zi, J. Wang, Q. Liao, Y. Zhang, and Z. L. Wang, "Stretchable-Rubber-Based Triboelectric Nanogenerator and Its Application as Self-Powered Body Motion Sensors," *Adv. Funct. Mater.*, vol. 25, no. 24, pp. 3688–3696, Jun. 2015.

[4] S. Niu and Z. L. Wang, "Theoretical systems of triboelectric nanogenerators," *Nano Energy*, vol. 14, 2014.

[5] Y. Xie, S. Wang, S. Niu, L. Lin, Q. Jing, J. Yang, Z. Wu, and Z. L. Wang, "Grating-Structured Freestanding Triboelectric-layer Nanogenerator for Harvesting Mechanical Energy at 85% Total Conversion Efficiency," pp. 6599–6607, 2014.

[6] J. Chen, J. Yang, Z. Li, X. Fan, Y. Zi, Q. Jing, H. Guo, Z. Wen, K. C. Pradel, S. Niu, and Z. L. Wang, "Networks of triboelectric nanogenerators for harvesting water wave energy: a potential approach toward blue energy.," *ACS Nano*, vol. 9, no. 3, pp. 3324–31, Mar. 2015.

[7] X. Wang, Z. Wen, H. Guo, C. Wu, X. He, L. Lin, X. Cao, and Z. L. Wang, "Fully

Packaged Blue Energy Harvester by Hybridizing a Rolling Triboelectric Nanogenerator and an Electromagnetic Generator," *ACS Nano*, vol. 10, no. 12, pp. 11369–11376, Dec. 2016.

[8] Z. L. Wang, L. Lin, J. Chen, S. Niu, and Y. Zi, "Harvesting Large-Scale Blue Energy," Springer, Cham, 2016, pp. 283–306.

[9] Z. L. Wang, "Triboelectric nanogenerators as new energy technology and self-powered sensors - principles, problems and perspectives.," *Faraday Discuss.*, vol. 176, pp. 447–58, Jan. 2014.

[10] J. Zhong, Q. Zhong, F. Fan, Y. Zhang, S. Wang, B. Hu, Z. L. Wang, and J. Zhou, "Finger typing driven triboelectric nanogenerator and its use for instantaneously lighting up LEDs," *Nano Energy*, vol. 2, no. 4, pp. 491–497, Jul. 2013.

[11] K. C. Aw and S. V. Praneeth, "Low frequency vibration energy harvesting from human motion using IPMC cantilever with electromagnectic transduction," *8th Annu. IEEE Int. Conf. Nano/Micro Eng. Mol. Syst.*, vol. 1, pp. 645–648, 2013.

[12] T. C. Hou, Y. Yang, H. Zhang, J. Chen, L. J. Chen, and Z. Lin Wang, "Triboelectric nanogenerator built inside shoe insole for harvesting walking energy," *Nano Energy*, vol. 2, no. 5, pp. 856–862, 2013.

[13] H. Yong, J. Chung, D. Choi, D. Jung, M. Cho, and S. Lee, "Highly reliable wind-rolling triboelectric nanogenerator operating in a wide wind speed range," *Sci. Rep.*, vol. 6, p. 33977, Sep. 2016.

[14] B. Meng, W. Tang, Z. Too, X. Zhang, M. Han, W. Liu, and H. Zhang, "A transparent single-friction-surface triboelectric generator and self-powered touch

16

sensor," *Energy Environ. Sci.*, vol. 6, no. 11, p. 3235, Oct. 2013.

[15] Y. Yang, H. Zhang, J. Chen, Q. Jing, Y. S. Zhou, X. Wen, and Z. L. Wang, "Single-electrode-based sliding triboelectric nanogenerator for self-powered displacement vector sensor system," *ACS Nano*, vol. 7, no. 8, pp. 7342–7351, 2013.

[16] S. Niu, Y. Liu, X. Chen, S. Wang, Y. S. Zhou, L. Lin, Y. Xie, and Z. L. Wang, "Theory of freestanding triboelectric-layer-based nanogenerators," *Nano Energy*, vol. 12, 2015.

[17] S. Wang, L. Lin, and Z. L. Wang, "Triboelectric nanogenerators as self-powered active sensors," *Nano Energy*, vol. 11. 2015.

CHAPTER-2

Materials Characterization and Electrical Measurement Techniques

This chapter discusses in detail about the experimental methods and other characterization techniques, which are processed for the device fabrication. For the successful completion of this research, the device fabrication experiments were carried out in different laboratories followed by physicochemical characterization and electrical measurements. The typical device fabrication includes laser cutting, dielectric barrier discharge plasma (DBD), electrode deposition and spin coating. For electrical analysis external motion was generated using Electrodynamic shaker, linear motor and electrical measurements using Keithley and Stanford Research Systems are discussed in detail.

2.1 Chemical and apparatus

All materials and chemical were used in these experiments are of high purity research grade. Details on the chemicals and materials used in the experiments are discussed in the respective chapters in detail.

2.2 Fabrication techniques

The fabrication of TENG is a multi-step process, which undergoes different process such as device design, cutting, electrode coating, and development of nanoscale surface roughness on polymer film and so on.

2.2.1 Laser cutting

For the fabrication of interdigitated electrode, laser cutter[1]–[3] was used to cut the PET sheet in the précised dimension. Since the laser cutter was reactive with metals, polymer materials were used as substrate and electrode was coated on it.

2.2.2 Electrode coating

Electrodes were coated using a thermal evaporator (Jeol JEE 4-X).This instrument is main used for coating aluminum, chromium, silver, gold, and copper. It is particularly useful for developing high conductive coating on polymer surfaces. For few devices masking techniques was used to coat electrode.

제주대학교 중앙도서관
JEJU NATIONAL UNIVERSITY LIBRARY

2.2.3 Surface roughness generation

A custom designed DBD plasma reactor chamber was developed to create roughness on the polymer films. The surface treatment was at a power of 100 W for 5 min in an Ar/O_2 atmosphere. The plasma treatment introduced a nanoparticle-like structure over the Kapton surface.
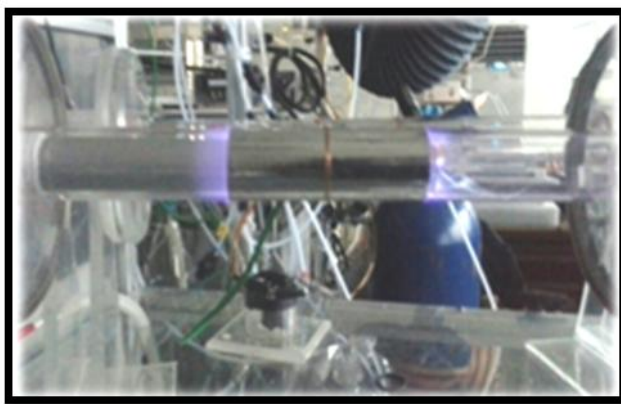
Figure 2.1 Homemade DBD plasma reactor setup.

2.3 Characterization techniques

2.3.1 Field –Emission Scanning Electron Microscopy (FE-SEM)

To analysis, the surface modification on the polymer films FESEM analysis was performed using FE-SEM Zeiss Supra-55vp, Germany and JEOL JSM-6700F, Japan. Here the acceleration voltage of 5 to 10 kV and 10 μA of filament current were applied during the measurement.

2.3.2 Raman spectroscopy

This spectroscopic technique is an efficient approach to analyze the composite materials. Hence, the prepared composite film was analyzed using LabRam HR800 micro Raman

제주대학교 중앙도서관
JEJU NATIONAL UNIVERSITY LIBRARY

spectroscopy (Horiba Jobin-Yvon, France). The Raman spectrum was operated at an excitation wavelength of 514 nm with different laser power.

2.4 Mechanical motion generation techniques

2.4.1. Electrodynamic Shaker

The Labworks ET-126 electrodynamic transducer is small permanent magnet shaker. It is used to generate a mechanical oscillation over the sample. In this instrument, the frequency of the oscillation was controlled using a function generator.[4]–[6]
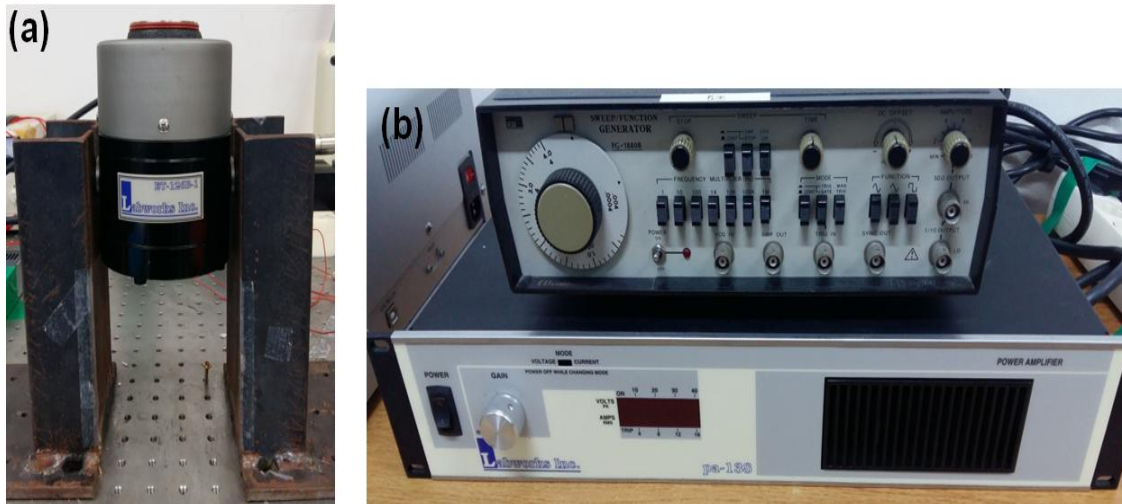
Figure 2.2 (a) Electrodynamic Shaker, (b) Function generator and amplifier.

2.4.1. Linear motor

Here, the external sliding motion, contact and separation motion was generated using a linear motor controlled by a computer (LinMot, USA, Inc) E1100.[7]–[10]   Linear motor is a custom designed setup made according to our research purpose. It can work for more extended period at high speed without any disturbance. A computer program was used to control the motion were

제주대학교 중앙도서관
JEJU NATIONAL UNIVERSITY LIBRARY

acceleration and velocity can be adjusted. **Figure 2.3** (a) shows the linear motor fixed on a vibration free table and (b) the system used to control the linear motor.

Figure 2.3 (a) Linear Motor and (b) controlling system.

2.5 Electrical characterization

To study, the electrical performance of the TENG devices, stability, load resistance, power, capacitor charging and bio-mechanical energy harvesting, Keithley measuring instruments such as 6514 electrometer,[3], [10], [11] 6485 picoammeter[5], [12], [13] and 2184 A nanovoltmeter[13], [14] were used. To obtain the short circuit a low noise current preamplifier (Stanford Research Systems) SR570 [2], [3], [10] was used before measuring the signal. **Figure 2.4** (a, b) shows the instruments used for the electrical analysis.

Figure 2.4 (a) Keithley measuring instruments such as 6514 electrometer, 6485 picoammeter and 2184 A nanovoltmeter (b) low noise current preamplifier.

2.6 References

[1] Z.-H. Lin, G. Cheng, X. Li, P.-K. Yang, X. Wen, and Z. Lin Wang, "A multi-layered interdigitative-electrodes-based triboelectric nanogenerator for harvesting hydropower," *Nano Energy*, vol. 15, pp. 256–265, 2015.

[2] H. Yong, J. Chung, D. Choi, D. Jung, M. Cho, and S. Lee, "Highly reliable wind-rolling triboelectric nanogenerator operating in a wide wind speed range," *Sci. Rep.*, vol. 6, p. 33977, Sep. 2016.

[3] Y. Yang, H. Zhang, J. Chen, Q. Jing, Y. S. Zhou, X. Wen, and Z. L. Wang, "Single-electrode-based sliding triboelectric nanogenerator for self-powered displacement vector sensor system," *ACS Nano*, vol. 7, no. 8, pp. 7342–7351, 2013.

[4]   N. R. Alluri, B. Saravanakumar, and S. J. Kim, "Flexible-Hybrid Piezoelectric Film (BaTi(1-x)ZrxO3)-PVDF Nanogenerator as a Self-Powered Fluid Velocity Sensor.," *ACS Appl. Mater. Interfaces*, Apr. 2015.

[5]   S. Selvarajan, N. R. Alluri, A. Chandrasekhar, and S. J. Kim, "BaTiO3 nanoparticles as biomaterial film for self-powered glucose sensor application," *Sensors Actuators, B Chem.*, 2016.

[6]   N. R. Alluri, S. Selvarajan, A. Chandrasekhar, S. Balasubramaniam, J. H. Jeong, and S. J. Kim, "Self powered pH sensor using piezoelectric composite worm structures derived by ionotropic gelation approach," *Sensors Actuators, B Chem.*, 2016.

[7]   W. Tang, C. B. Han, C. Zhang, and Z. L. Wang, "Cover-sheet-based nanogenerator for charging mobile electronics using low-frequency body motion/vibration," *Nano Energy*, vol. 9, pp. 121–127, 2014.

[8]   Y. Xie, S. Wang, S. Niu, L. Lin, Q. Jing, J. Yang, Z. Wu, and Z. L. Wang, "Grating-Structured Freestanding Triboelectric-layer Nanogenerator for Harvesting Mechanical Energy at 85% Total Conversion Efficiency," pp. 6599–6607, 2014.

[9]   T. C. Hou, Y. Yang, H. Zhang, J. Chen, L. J. Chen, and Z. Lin Wang, "Triboelectric nanogenerator built inside shoe insole for harvesting walking energy," *Nano Energy*, vol. 2, no. 5, pp. 856–862, 2013.

[10]   P. Yang, Z. Lin, Z. L. Wang, K. C. Pradel, L. Lin, X. Li, X. Wen, J. He, M. Science, U. States, E. Engineering, M. Sciences, S. Arabia, B. Engineering, and C. Academy, "Paper-Based Origami Triboelectric," no. Xx, 2015.

[11] L. E. Helseth and X. D. Guo, "Triboelectric motion sensor combined with electromagnetic induction energy harvester," *Sensors Actuators A Phys.*, May 2016.

[12] A. Ramadoss, B. Saravanakumar, and S. J. Kim, "Thermally reduced graphene oxide-coated fabrics for flexible supercapacitors and self-powered systems," *Nano Energy*, vol. 15, pp. 587–597, Jul. 2015.

[13] W. Li, D. Torres, T. Wang, C. Wang, and N. Sepúlveda, "Flexible and biocompatible polypropylene ferroelectret nanogenerator (FENG): on the path toward wearable devices powered by human motion," *Nano Energy*, 2016.

[14] B. Saravanakumar, K. Thiyagarajan, N. R. Alluri, S. SoYoon, K. Taehyun, Z.-H. Lin, and S.-J. Kim, "Fabrication of an eco-friendly composite nanogenerator for self-powered photosensor applications," *Carbon N. Y.*, vol. 84, pp. 56–65, Apr. 2015.

CHAPTER- 3

Human Interactive Triboelectric Nanogenerator as a Self-Powered Smart Seat

Graphical overview
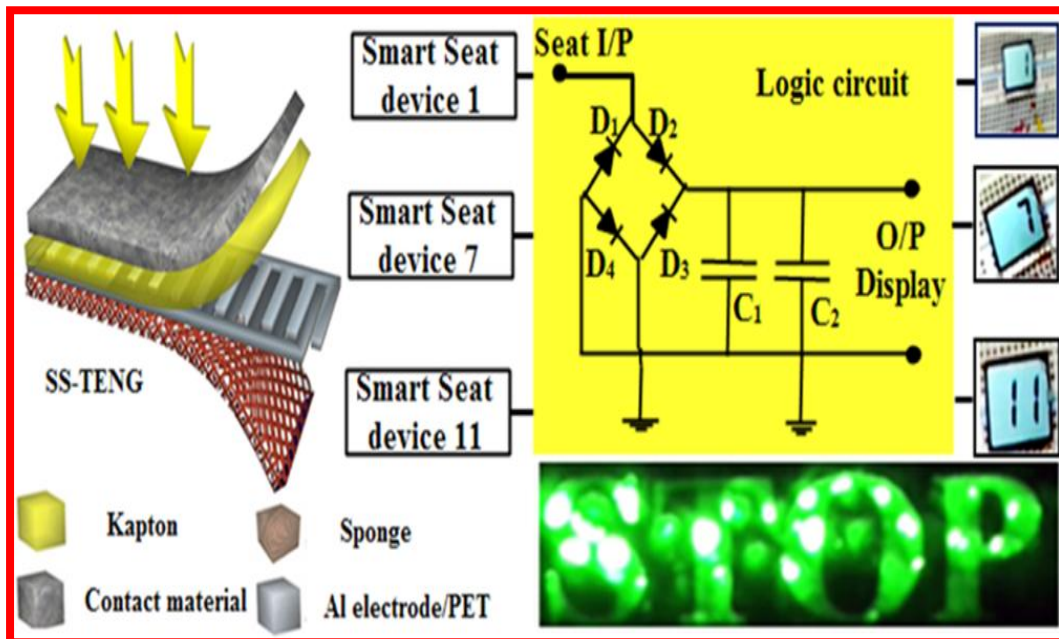
Highlights

> A lightweight, flexible, cost-effective and robust, single electrode based Smart Seat– Triboelectric Nanogenerator (SS-TENG) is introduced as a promising eco-friendly approach for harvesting energy from the living environment, for use in integrated self-powered systems

> An effective method for harvesting biomechanical energy from human motion such as walking, running, and sitting, utilizing widely adaptable everyday contact materials (newspaper, denim, polyethylene covers, and bus cards) is demonstrated

> The performance of SS-TENG (52 V and 5.2 μA for a multi-unit SS-TENG) is systematically studied and demonstrated in a range of applications including a self-powered passenger seat number indicator and a STOP-indicator using LEDs, using a simple logical circuit

> This feasibility study confirms that triboelectric nanogenerators are a suitable technology for energy harvesting from human motion during transportation, which could be used to operate a variety of wireless devices, GPS systems, electronic devices and other sensors during travel

3.1. Introduction

Sustainable development in contemporary society is dependent on obtaining a significant quantity of electrical power from environmental sources, and day-to-day activities are increasingly defined by the use of electronic devices and systems.[1]–[4] Though electricity generation is a two-centuries-old technology, novel methods and mechanisms such as the piezoelectric effect,[5]–[8] the photoelectric effect,[9], [10] the thermoelectric effect,[11], [12] and electrostatic induction,[13]–[15] are still under investigation to meet current requirements, and eco-friendly, cost-effective, reliable energy harvesting technologies are a significant field of interest.[16] Mechanical energy is a natural renewable energy source in the living environment that may originate from human motion, including vibration, rotation, etc.[17]–[20] Recently, a triboelectric nanogenerator (TENG)[21]–[23] has been developed, based on a combination of contact electrification[24] and electrostatic induction[25] to scavenge attenuated mechanical energy using triboelectric materials.[26] Selection of triboelectric pair materials and rational design can increase the rate of energy harvesting[26] and conversion efficiency.[27]TENG systems, which harvest biomechanical energy from human movement, have been reported in some studies.[28]–[32] These devices have been shown to be a promising, highly efficient and eco-friendly technology for harvesting biomechanical energy.[22], [32], [33]

Recently, energy harvesting using biocompatible and biodegradable materials has been extensively studied in the field of biomedical research.[34], [35] Energy harvesting from everyday contact materials together with human activities such as walking, running and heartbeats has also been demonstrated. These technologies can contribute to a reduction in environmental contamination from non-degradable polymer materials. Wearable personal electronics utilizing a self-sufficient power source are increasingly in use;[17], [25]hence,

nanogenerators (triboelectric, piezoelectric and pyroelectric) have been developed for building self-powered systems as active sensors. Numerous applications of TENG technology in self-powered devices have been demonstrated.[7], [26], [34], [36]'[37]

In this work, we present a single-electrode-based highly flexible smart seat tribolelectric nanogenerator (SS-TENG), which can harvest energy using everyday materials present on a person undertaking normal movements. Here, the surface of the contact material acts as the second frictional surface to the SS-TENG. This SS-TENG is fabricated using flexible and highly durable materials, for real-time applications at extremely low cost, and hence presents a potential approach for large-scale human motion energy harvesting. By utilizing the contact interaction between various materials, the device converts biomechanical energy into electrical energy. Here, we show that the SS-TENG can be used in a self-powered passenger seat indicator, which displays a seat number whenever a seat is occupied by a passenger, and in a self-powered stop indicator, which illuminates commercial LEDs. The proposed device can also work as a mobile phone cover that harvests energy from human motion. The working principle of the SS-TENG has been systematically investigated through experimental analysis, and the voltage and current measured between the electrode and the ground reached 13 V and 1.75 μA, respectively, at 20 Hz, with newspaper as the contact material. A multi-unit SS-TENG has also been demonstrated for harvesting mechanical energy from human motion in real time (with the SS-TENG unit fixed on a chair). The SS-TENG has demonstrable capability for both mechanical energy harvesting and use in self-powered electronics.

3.2. Experimental method

3.2.1. Surface modification of Kapton film

To enhance the contact electrification, the Kapton film (25μm) surface was modified through plasma treatment. The surface treatment was carried out in a homemade dielectric barrier discharge (DBD) plasma setup at a power of 100 W for 5 min in an Ar/O_2 atmosphere. The plasma treatment introduced a nanoparticle-like structure over the Kapton surface.

3.2.2. Fabrication of interdigitated electrode

SS-TENG was constructed using a thin layer of polyethylene terephthalate (PET) as the bottom supporting substrate (PET). A large PET sheet was cut to dimensions of 50 mm by 50 mm by 1 mm using a laser cutter. Electrodes were cut into an interdigitate structure with dimensions 50 mm by 2 mm, separated by a gap of 2 mm. A layer of Pt was then deposited using DC sputtering for 180 seconds, followed by a layer of Al on the substrate using a thermal evaporator.

3.2.3. Fabrication of SS-TENG

The surface treated Kapton film was adhered onto the pre-patterned interdigitated electrode as an electrification layer. The electrical contact was taken from the interdigitated electrode through copper wire using silver paste. A thick layer of sponge was attached under the electrode coated PET substrate for support.

3.3. Measurement systems

The morphological analysis of plasma treated, untreated Kapton films and other everyday contact materials were performed by field emission-scanning electron microscopes (FE-SEM Zeiss Supra-55vp, Germany and JEOL JSM-6700F, Japan). For measurement of the electric outputs of the single unit SS-TENG, an external force was applied using an electro-dynamic shaker (Lab works Inc. ET-126-B-1), creating friction between the SS-TENG and contact materials and resulting in contact electrification. The electrical response of the multi-unit SS-TENG was obtained using real-time bio-mechanical energy from human motion. The output voltage and current of the device were measured using a nanovoltmeter (Keithley 2182A) and a picoammeter (Keithley 6485), respectively. Voltage and current measurements were conducted under a roof of grounded homemade faraday cage to avoid the external noise. A logical circuit was designed and constructed on a breadboard for the voltage regulation studies and demonstrations of self-powered applications.

3.4. Results and discussion

3.4.1. SS-TENG design

The basis of the SS-TENG is a plasma-treated Kapton film as an electrification material, with a layer of Al electrode fabricated on a thin layer of polyethylene terephthalate (PET) sheet. The Al electrodes were composed of six pairs of interdigitated electrodes equally spaced with a separation of 2 mm, and a sponge supporting layer for the whole device. The interdigitated electrode layer is entirely embedded and passive. This balanced design demonstrates structural uniformity and excellent performance.
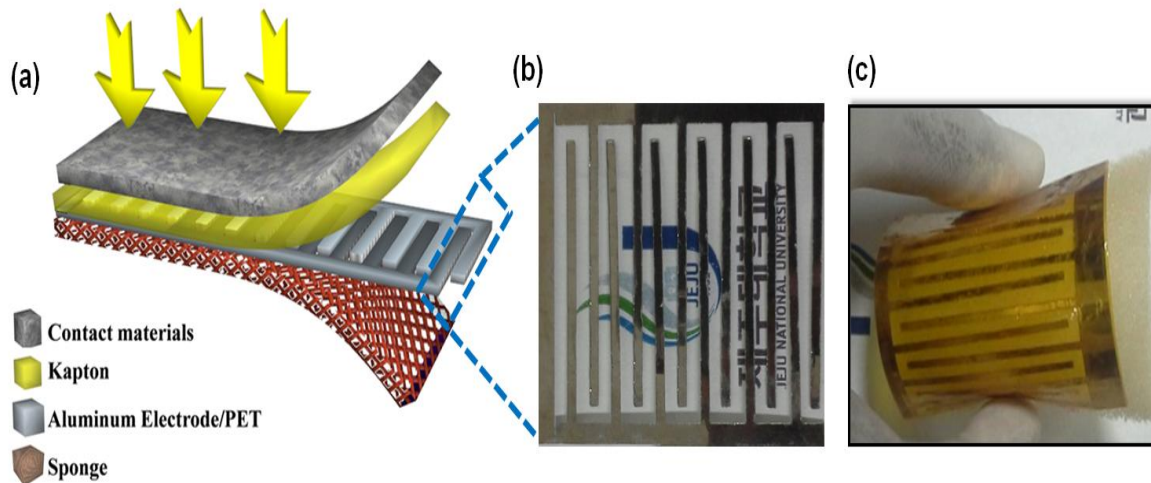
Figure 3.1(a) Schematic illustration of the SS-TENG, (b) The zoomed photograph shows the PET layer with Al electrodes with an interdigitate structured pattern, and (c) digital photograph of the SS-TENG.

The electrodes are schematically illustrated in **Figure 3.1 (a)**, and the enlarged photograph **Figure 3.1 (b)**, shows the interdigitate structured pattern of the PET coated Al electrodes. Finally, a digital image of the fabricated SS-TENG is shown in **Figure 3.1 (c)**,here the PET acts as a bottom supporting substrate.[38]

3.4.2. Morphology analysis of negative and positively charged layers

The mechanism of operation of the SS-TENG is based on electrostatic induction, and contact electrification,[25] Kapton film and a range of everyday materials were selected as contact materials for generating triboelectric charge.[39]**Figure 3.2(a-d)** shows FE-SEM image of the triboelectric active layers – plasma untreated Kapton film and plasma treated surfaces of the Kapton film at various plasma exposure timing, respectively. The surface treated Kapton film is composed of irregular microstructures distributed across the whole surface. Here, the DBD

plasma exposure time has been limited to 5 min because the overexposure of plasma, physically damages the surface of the Kapton film.
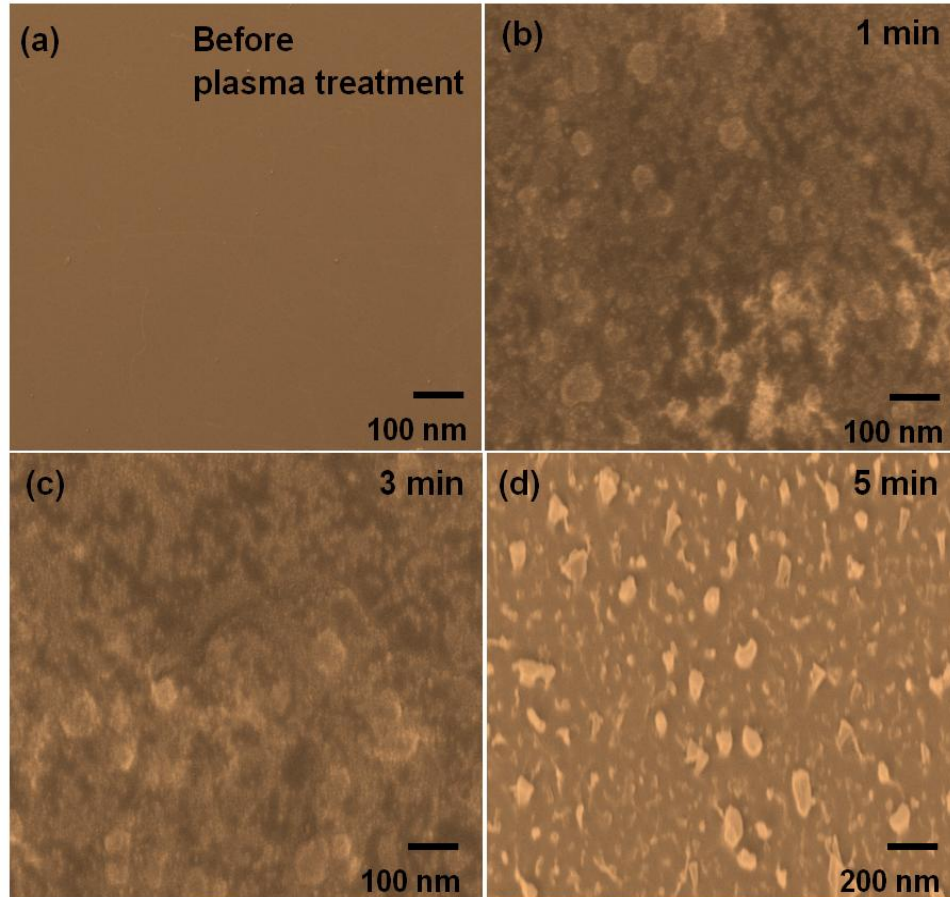
Figure 3.2 FE-SEM images of negatively charged triboelectric active layers: (a)Plasma untreated and Plasma treated Kapton at different time period (b) 1 min, (c) 3 min and (d) 5 min.

The surface of the contact materials also important for triboelectric charge generation. Hence, the surface morphology of the contact materials studied. **Figure 3.3 (a-d)** shows FE-SEM images of different contact materials including newspaper, denim jeans (cotton), a polyethylene cover and a polyvinyl chloride bus card.
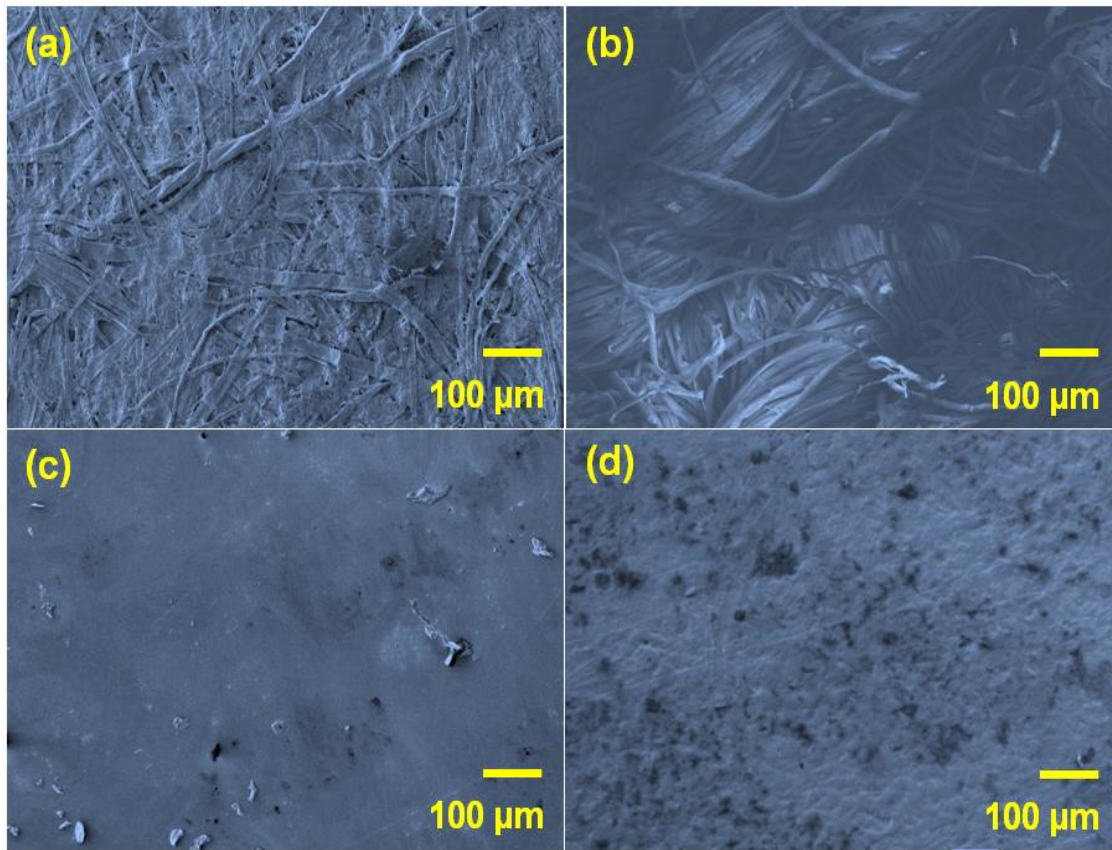
Figure 3.3 FE-SEM image of positively charged triboelectric active layer: (a) newspaper, (b) denim, (c) polyethylene cover and (d) bus card.

3.4.3. Working mechanism of Single electrode SS-TENG

The SS-TENG works in a single electrode mode,[21], [22], [25], [40]'[41] as illustrated in **Figure 3.4**. Here, newspaper, denim, the polyethylene cover and the bus card, all materials commonly carried by a passenger, were selected as contact materials to generate triboelectric charge. These materials come in contact with the active layer of the SS-TENG during a range of physical motions. In the initial state, the contact material is not in touch with the active Kapton layer, and no electrical response is obtained at the output, **Figure 3.4**(a) since there is no triboelectric charge. When an external force is applied to the contact material, it comes into contact with the active layer, and a friction pair is formed between the surfaces. Since polyimide

(Kapton film) is more triboelectrically negative than the contact materials, as shown in the triboelectric series, electrons are transferred from the surface of the contact material to the surface of the Kapton film; hence, friction at the interface generates positive and negative triboelectric charges over the surfaces of the contact material and the active Kapton layer, respectively, shown in **Figure 3.4(b)**. When the applied external force is released, the surfaces separate and a potential difference are formed between them, causing electrons to flow through the Al electrode as shown in Figure. **Figure 3.4(c)**.
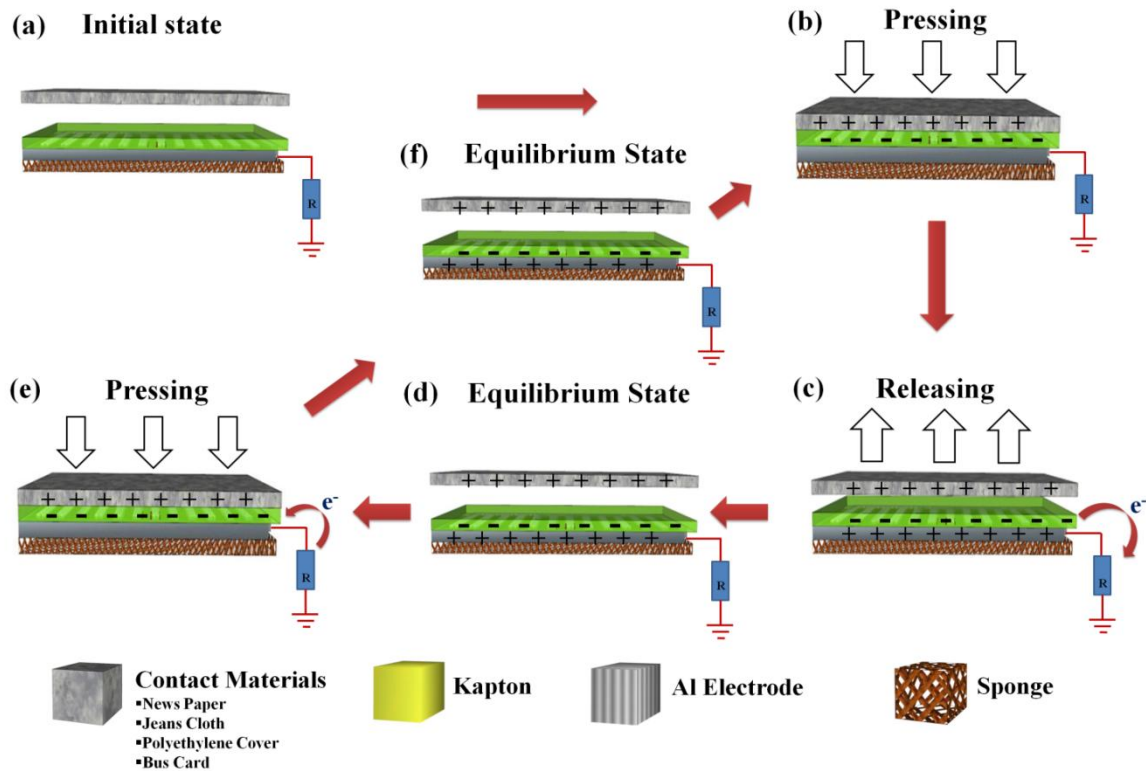
Figure 3.4 Energy harvesting mechanism of the SS-TENG. (a) Initial position of the contact material, Kapton surface with interdigitated electrodes separated by air-gap. (b) An external force causes interaction between the contact material and the Kapton surface, inducing positive triboelectric charges on the contact material and negative triboelectric charges on the Kapton surface. (c) Release of the external force causes electrons to flow from the Al electrode to the external circuit. (d) In the equilibrium state, equal numbers of charge carriers are distributed on both sides of the layers. (e) Electrons are driven back owing to the applied external force, reducing the inductive charge on the Al electrode. (f) Charge carrier distribution of the SS-TENG reaches a new equilibrium state.

35

The charge is then transferred via an external load to the ground, thereby achieving electrostatic equilibrium as shown in **Figure 3.4.(d)**.This operation contributes to the half cycle of the SS-TENG. Inverse charge transfer also occurs, when the contact material again touches the surface of the SS-TENG. Here, electrons flow from the ground to the Al electrode **Figure 3.1.4**. **(e)**, leading to electrical equilibrium. Continuous electric output will be obtained if the contact material interacts with the active layer periodically.

3.4.4. Electrical analysis of SS-TENG

The typical electrical response of the single unit SS-TENG was systematically investigated at a controlled frequency. Initially, to identify the energy harvesting efficiency of the plasma untreated and treated Kapton film, an open-circuit voltage (V_{oc}) was obtained, **Figure 3.5(a)**Output voltage response of SS-TENG using untreated Kapton film as the active layer and (b) plasma treated Kapton film as the active layer.
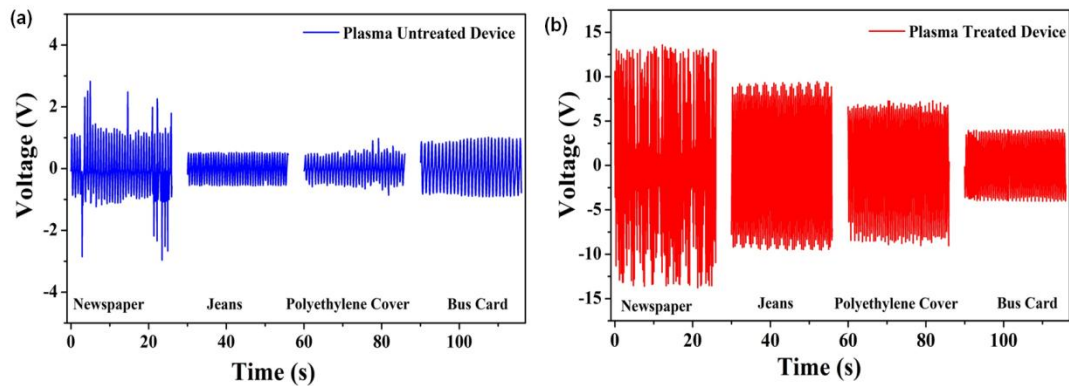
Figure 3.5(a) Output voltage response of SS-TENG using plasma untreated Kapton film and (b) plasma treated Kapton film as an active layer.
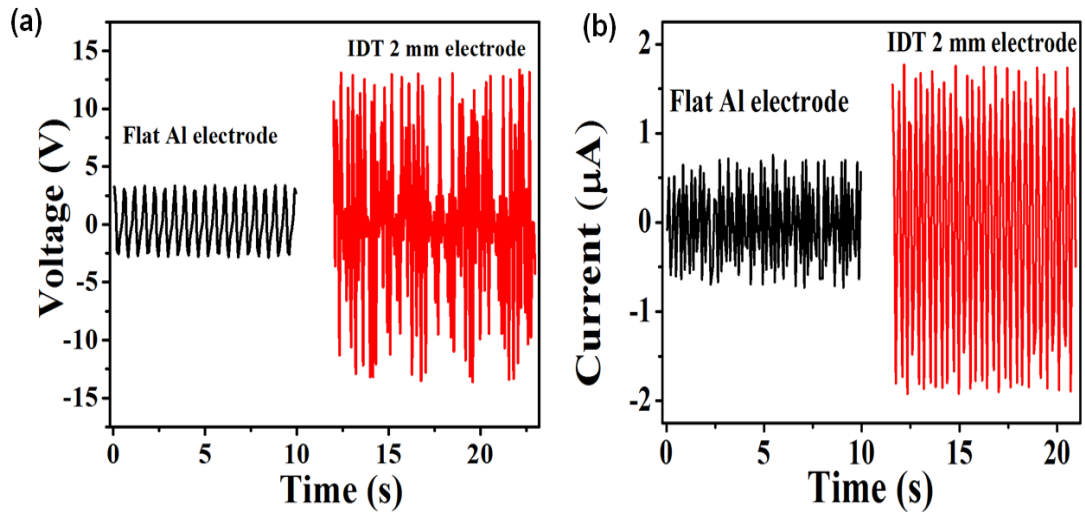
Figure 3.6 (a) Output voltage and (b) current response of SS-TENG using Flat Al electrode and IDT 2 mm electrode.

To ensure the enhanced energy harvesting by interdigitated electrodes SS-TENG, an investigation was performed using newspaper as an interaction material on flat aluminum electrode device under external mechanical load at cyclic-frequencies of 20 Hz shown in **Figure 3.6 (a-b)**. It clesarly states that the use of interdigitated electrode in SS-TENG increases the energy harvesting efficiency. **Figure 3.7 (a-b)** shows the open-circuit voltage (V_{oc}) and short-circuit current (I_{sc}) of the SS-TENG for different contact materials at a cyclic frequency of 20 Hz. Significant contact electrification occurred in all four contact materials, as shown in **Figure 3.7(a)**. A monotonic increase in the electrical output was observed when the contact material was changed from bus card to newspaper.[42],[43] This occurs because the surface-treated Kapton film has a stronger tendency for electron attraction, while the surface of the contact materials tends to donate electrons.[25] At a cyclic frequency of 20Hz, V_{oc} and I_{sc} were measured to be 13 V and 1.75 μA, respectively. An enlarged view of V_{oc} and I_{sc} measurements for denim is shown in the left inset of **Figure 3.7 (a-b)**.

37
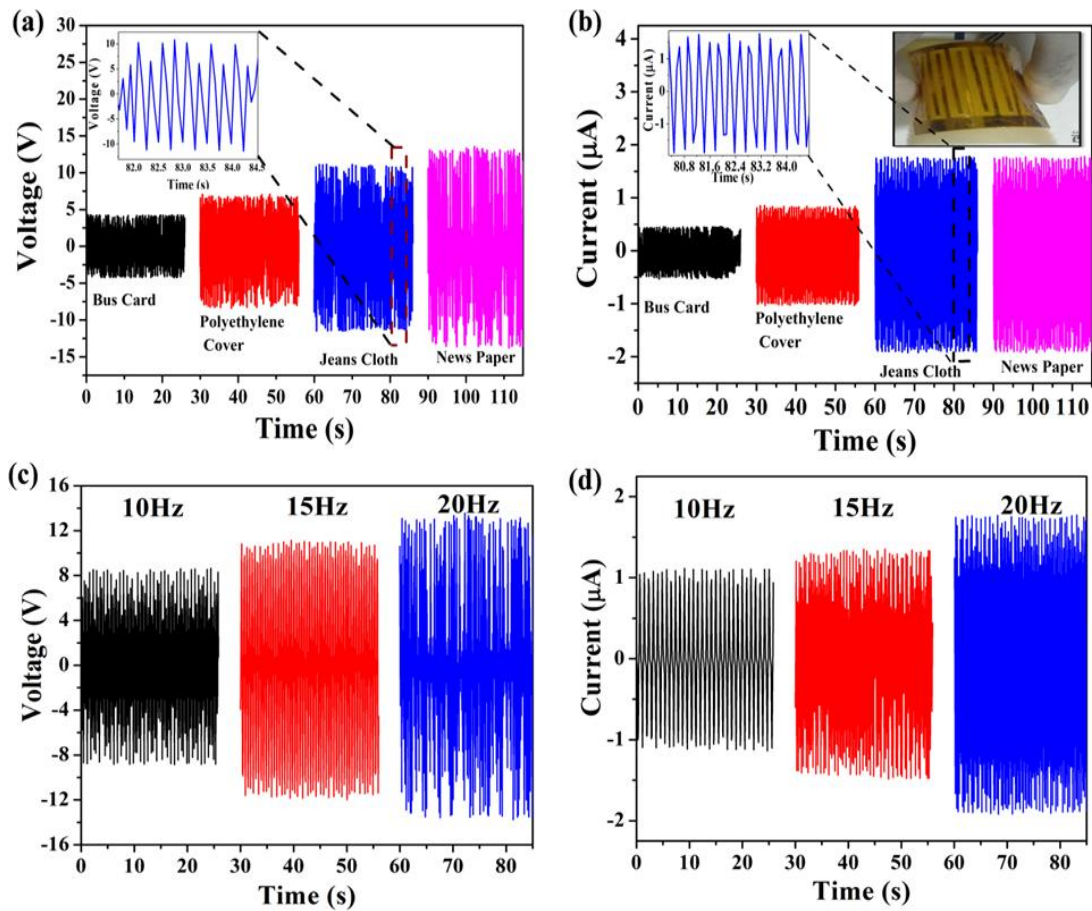
Figure 3.7 Electrical response of SS-TENG: (a) Open circuit voltage of the single unit SS-TENG with different contact materials at a cyclic frequency of 20Hz of mechanical load. The inset shows an enlarged view of the signal when the device interacts with denim. (b) Short circuit current of the single unit SS-TENG during interaction with different contact materials at a cyclic frequency of 20 Hz of mechanical load. The left inset shows an enlarged view of the signal when the device interacts with denim. The right inset shows digital images of the device. (c, d) Electrical response of single unit SS-TENG, newspaper as an interaction material under external mechanical load at cyclic-frequencies of 10, 15 and 20 Hz.

A digital image of the fabricated device is shown in the right inset. **Figure 3.7 (c-d)** shows the V_{oc} and I_{sc} response of the single unit SS-TENG, for newspaper as a interaction material under external mechanical load at cyclic-frequencies of 10, 15 and 20 Hz for a range of cyclic frequencies. The electrical output of the SS-TENG (V_{oc}) increases from 8V to 13V and from 20 Hz V_{oc} almost remains same. The possible reason is that, during open circuit condition

the dynamic process of charge transfer will not involve. The V_{oc} purely depends on triboelectric charge density and the contact separation with respect to given time.[17] During the I_{sc} it exhibits a clear increment from 1μA at 10 Hz to 1.75 μA to 20 Hz, here the possible phenomenon is that at high frequency mechanical agitation the deformation rate increases, leading to a higher flow rate of charges,[17], [33] this results in higher value of current peak.[30]In present work, the mechanical movement (contact and separation) of two triboelectric layers was created by electrodynamic shaker (ET-126) with applied frequency range up to 20 Hz. While increasing the frequency of shaker (11 N), the contact area of SS-TENG will not change, but the number of tappings (contact and separation) has been improved drastically, this increment in frequency of contact between the surfaces causes higher triboelectric charge density over the active materials in a short time span. It was observed that electrical response of SS-TENG is solely dependent on cyclic frequency of mechanical load. This analysis indicates that the proposed device is a potential candidate for frequency-based low power electronic applications.[16], [31], [44]

Load resistance is an important parameter for real-life applications, which directly impacts on device output power. To establish the optimum device load, we performed a systematic study with different load resistances. The effective power and maximum output voltage of the SS-TENG was investigated for a range of external load resistances at a cyclic frequency of 20Hz, and the results are shown in**Figure 3.8 (a)**. The voltage across the load rises with increasing resistance and then becomes saturated for larger load resistances.[21], [45] An instantaneous peak power of 6.45 μW was achieved across the 10MΩ load resistance. The AC signal generated from the SS-TENG cannot drive low-power electronic devices directly and requires regulation with a voltage regulator circuit. **Figure 3.8 (b)** shows the regulated voltage output of the single unit SS-TENG, at a cyclic frequency of 20 Hz, including integration of a

power management circuit to form a power supply system that can deliver a constant DC output voltage within 10 s after the SS-TENG commences operation.
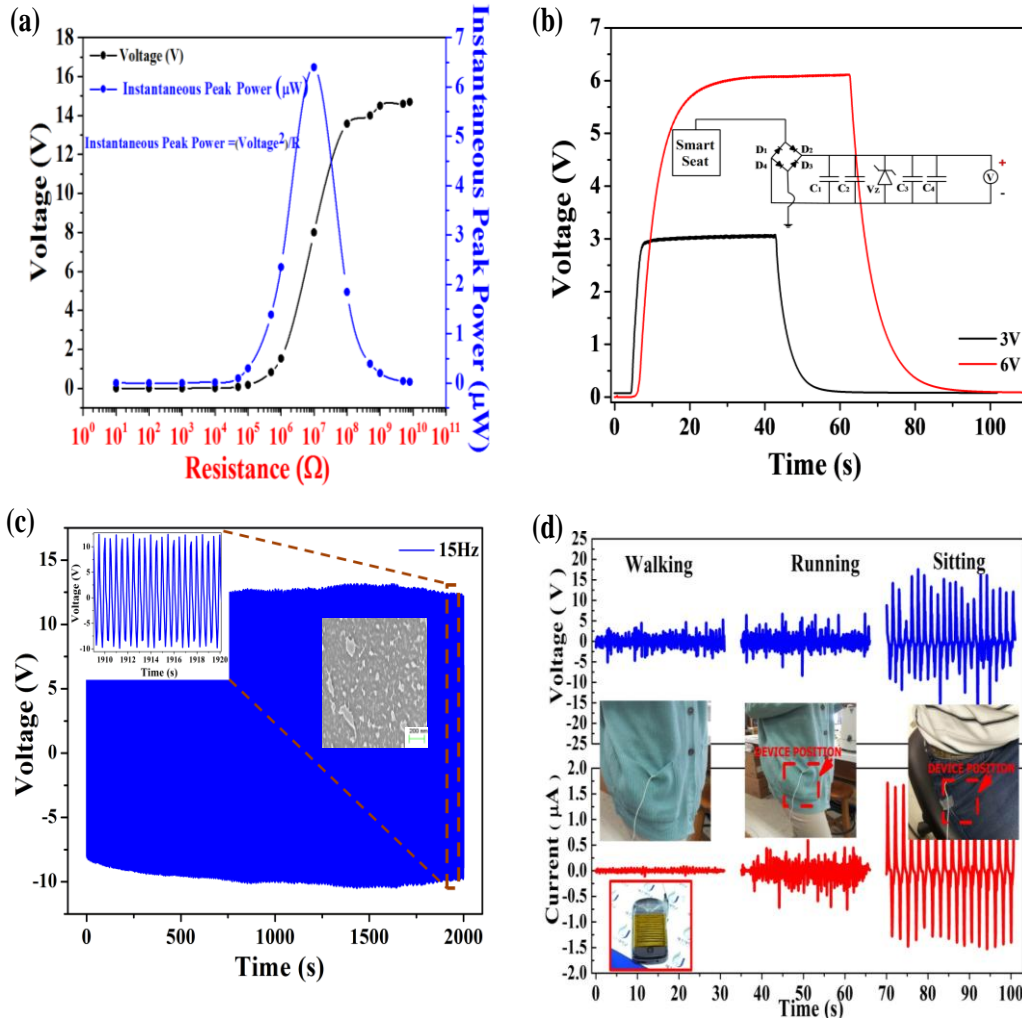
Figure 3.8 (a) Relationship between the output voltage (black), instantaneous peak power (blue) *vs* external load resistance, when newspaper is in contact with the Kapton film surface at a cyclic frequency of 20 Hz of mechanical load. (b) Charging capability and voltage regulation (3 V, 6 V) of the single unit SS-TENG (denim as a contact material) including a power management circuit (inset), at a cyclic-frequency of 20 Hz of mechanical load. (c) Durability test of the SS-TENG at a cyclic-frequency of 15 Hz of load (newspaper as a contact material). The left inset shows an enlarged view of the output voltage signal at the end of the durability test and the right inset shows the FE-SEM image of SS-TENG after few thousand cycle of operation. (d) Energy harvesting of the SS-TENG used as a smart sheet mobile cover when interacting with clothes during a range of physical motions. The center inset shows regular physical motions such as walking, running and sitting. The bottom left inset shows a digital photograph of the SS-TENG used as a smart mobile cover.

40

The power management circuit was designed using commercially available voltage regulator diode (Zener diode: 3.3 V, 1N4728A and 6 V, 1N5234B), capacitors (C_1, C_3= 10nF, C_2, C_4= 47pF) and a full wave bridge rectifier (DF06G). The complete circuit is depicted in Figure. 4(b) inset (centre). This study clearly indicates that a single-unit SS-TENG may be used as a power source for low-power electronic devices. A durability test was performed by repeatedly pressing and releasing the SS-TENG with newspaper at a cyclic frequency of 15 Hz for 2000 cycles. The result indicates the reliability of the output response of the SS-TENG for different external contact materials, shown in **Figure 3.8 (c)**. The left inset presents the enlarged view of the output voltage signal during the final stage of the durability test and right inset shows the FE-SEM image of SS-TENG after few thousand cycle of operation. It clearly shows that the SS-TENG remains stable, even over prolonged cycles, with negligible changes to the output signal. The SS-TENG was driven by a mechanical shaker instrument for these quantitative measurements; normal environmental, mechanical energy was harnessed for subsequent measurements. A compact SS-TENG was attached to the back of a smartphone as a smart mobile cover, to effectively harvest mechanical energy originating from physical motion (walking, running and sitting). **Figure 3.8 (d)**shows V_{oc} and I_{sc} for the smart mobile cover demonstration, and shows that the SS-TENG can harness ambient mechanical energy from normal physical motion. Depending on the nature of the motion, there is a linear increment in V_{oc} and I_{sc}, which clearly shows the importance of physical motion and cloth materials in energy harvesting. The center inset of **Figure 3.8 (d)** depict energy harvesting from regular physical motion exerted by humans using a smart mobile cover. The harvested peak to peak voltage obtained during the various human motions was transformed into frequency domain using Fourier transforms[46] to

confirm the potential of SS-TENG in scavenging energy from low-frequency human motion; the

Figure 3.9 shows the frequency of each motion.
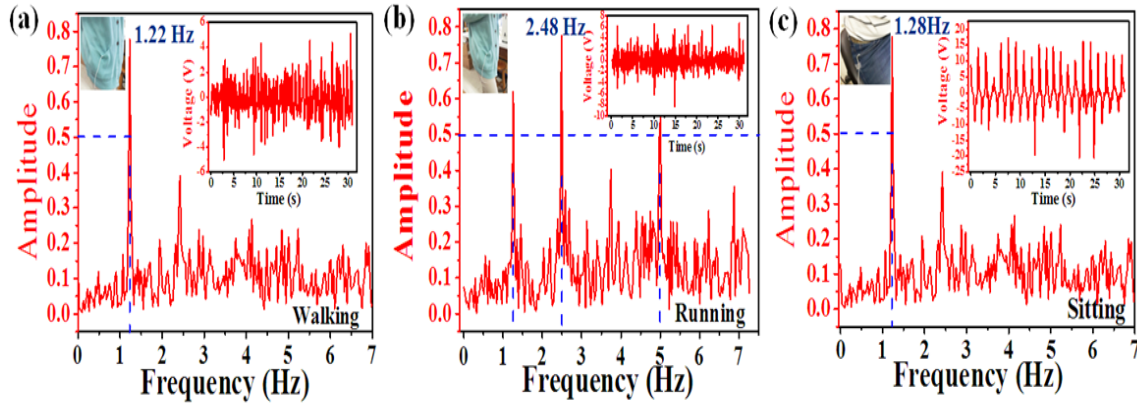
Figure 3.9 (a-b) The frequency components after Fourier transformed of the harvested voltage during human motion (walking, running, sitting).

3.4.4.1. Low power electronics driving analysis

While interacting with various contact materials at a cyclic frequency of 20 Hz, the rectified output of a single unit SS-TENG with was connected to a switching circuit along with a commercial capacitor (10 nF). While pressing the switch, the charge stored in the capacitor drives 100 commercially-purchased blue LEDs connected in series to flash for an instant is shown in **Figure. 3.10 (a-d)**. Likewise the SS-TENG driving a monochrome LCD display, while interacting with contact materials at a cyclic frequency of 20 Hz, is shown in **Figure. 3.10 (e-h)**. This study demonstrates that the SS-TENG is a potential candidate to work as a power source to drive low-power electronic gadgets.
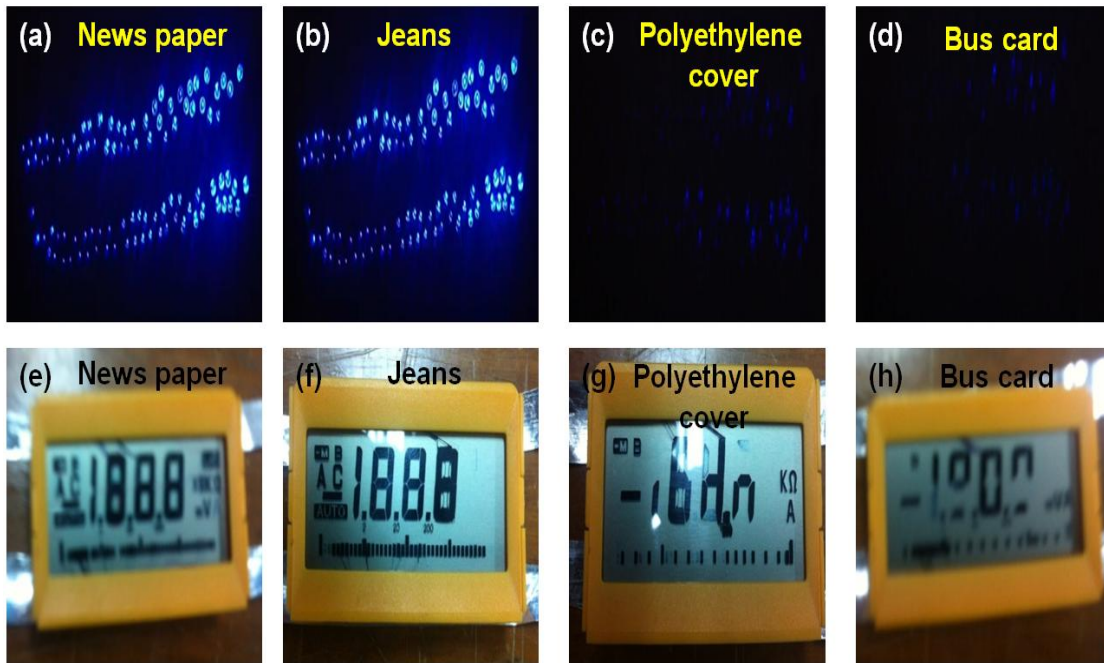
Figure. 3.10 Demonstration of power management system to lit up low power electronic devices. (a-d) Photograph of 100 blue lighted LEDs in complete darkness when a single unit SS-TENG interact with different contact materials at cyclic frequency 20 Hz of mechanical load. (e-h) Photograph of monochrome LCD display powered in ambient background lighting when a single unit SS-TENG interact with different contact materials at cyclic frequency 20 Hz of mechanical load.

3.4.4.2. Multi-unit SS-TENG analysis

The main purpose of the SS-TENG is to harvest electrical energy from everyday materials and mechanical energy in the living environment. In this regard, we have fabricated a multi-unit SS-TENG where each single unit was connected individually to a common output point using a breadboard (the units are electrically connected in parallel).
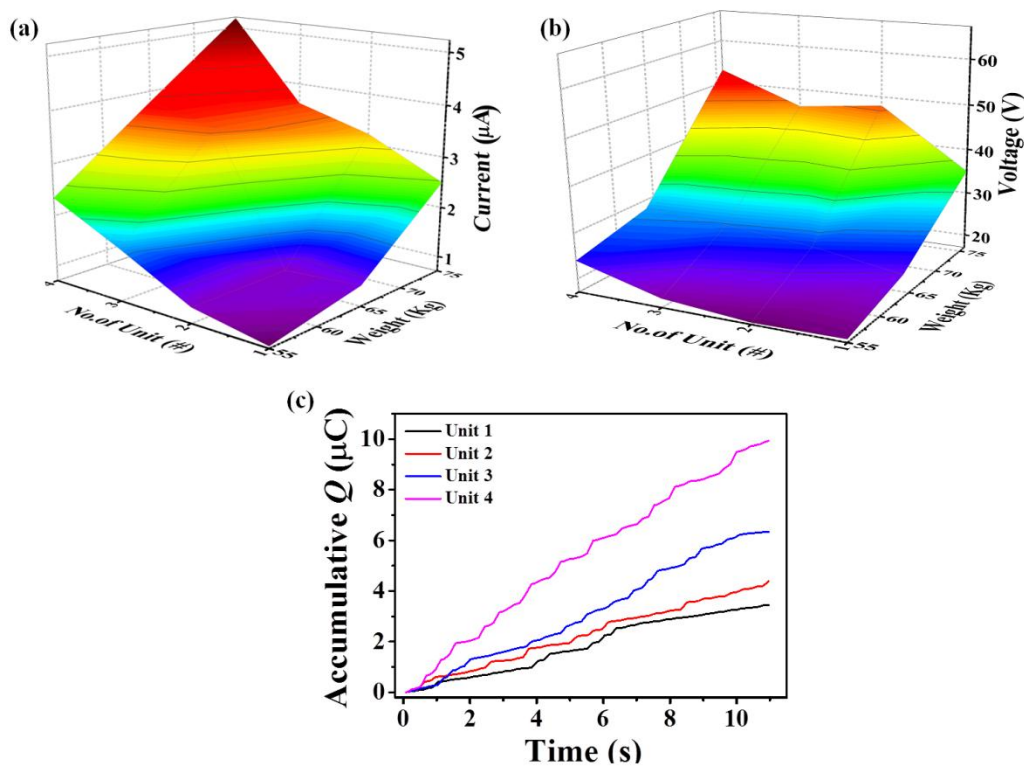
Figure. 3.11 (a) The rectified output current (b) and voltage with respect to the increasing number of units and weight of the person. (c) Accumulative induced charges generated by the SS-TENG with units numbers (1, 2, 3, and 4).

The rectified output characteristics of different number of units were investigated for a normal human motion (sitting) at different weights, with denim as the contact material, and are shown in Figure**. 3.11 (a- b)**. The output voltage and current response of the SS-TENG with increasing the number of units (N= 1, 2, 3, 4) is shown in Figure. 5(b, c). Certain trends can be observed from the evolution of output signals with increasing the number of units and weight of the person. Initially, I_{sc} amplitudes are in increasing function for both addition number of units and weight of the person. The I_{sc} induced by the 75 Kg person when N = 1 is about 2.5 μA which shots up to 5.2 μA at N = 4 as shown in **Figure. 3.11 (a).** An average V_{oc} amplitude was maintained with addition of number of units at various weights, the V_{oc} induced by the 75 Kg passenger when N = 4 is about 52 V as indicated in **Figure. 3.11 (b).** Our next observation

44

shows that, as an attribute to the electrically parallel-connected units, the average amplitudes of voltage peaks almost remains steady with inflated unit numbers and the total peak density was an increasing behavior of the unit number. Also from the above observations, it can be understood that hundreds of units can work together and a direct electrical signal could be obtained from multi unit SS-TENG. This experiment also presents the robustness of multi unit SS-TENG to scavenge energy from human motion. Additionally, the accumulative induced charge also measured using a bridge rectifier (DF06G) as demonstrated in **Figure. 3.11 (c).** Here the rate of charge accumulation and unit number are directly proportional, because multi SS-TENG means more number of contact and separation acted in a unit period of time. Hence with rapid triboelectric charge generation, higher charging accumulation rate was obtained.

3.4.5.   SS-TENG for Self-powered applications

3.4.5.1. Self-powered emergency seat number detection

A single unit SS-TENG was placed on top of a bus seat to act as a self-powered device displaying the occupied seat number. When a passenger occupies a seat, the SS-TENG will generate output energy in the form of an electrical signal through contact electrification between the two triboelectric materials (contact material and active layer). Here, the mechanism of action involves charge carrier transfer between the passenger's clothes, acting as a contact material, and a plasma treated Kapton surface in the SS-TENG acting as an active layer. The output energy generated (at 10 V and 0.75 μA) was collected across the electrodes and connected to the logic-circuit to drive (or display) a monochrome LCD (or LED) displaying the occupied seat number. Here, the simple logical circuit was designed using two commercially available capacitors (C_1= 10nF, C_2= 47pF) connected across a full wave bridge rectifier (DF06G) output. The logical

circuit and operation of a single unit SS-TENG as a self-powered device for displaying the occupied seat number was demonstrated experimentally. Meanwhile, the generated output was measured and is schematically shown in **Figure. 3.12;** the insets show seat LCDs 1, 7 and 11, according to the seat occupied. The above demonstration clearly indicates that the SS-TENG is a potential candidate for self-powered systems in automated vehicles.
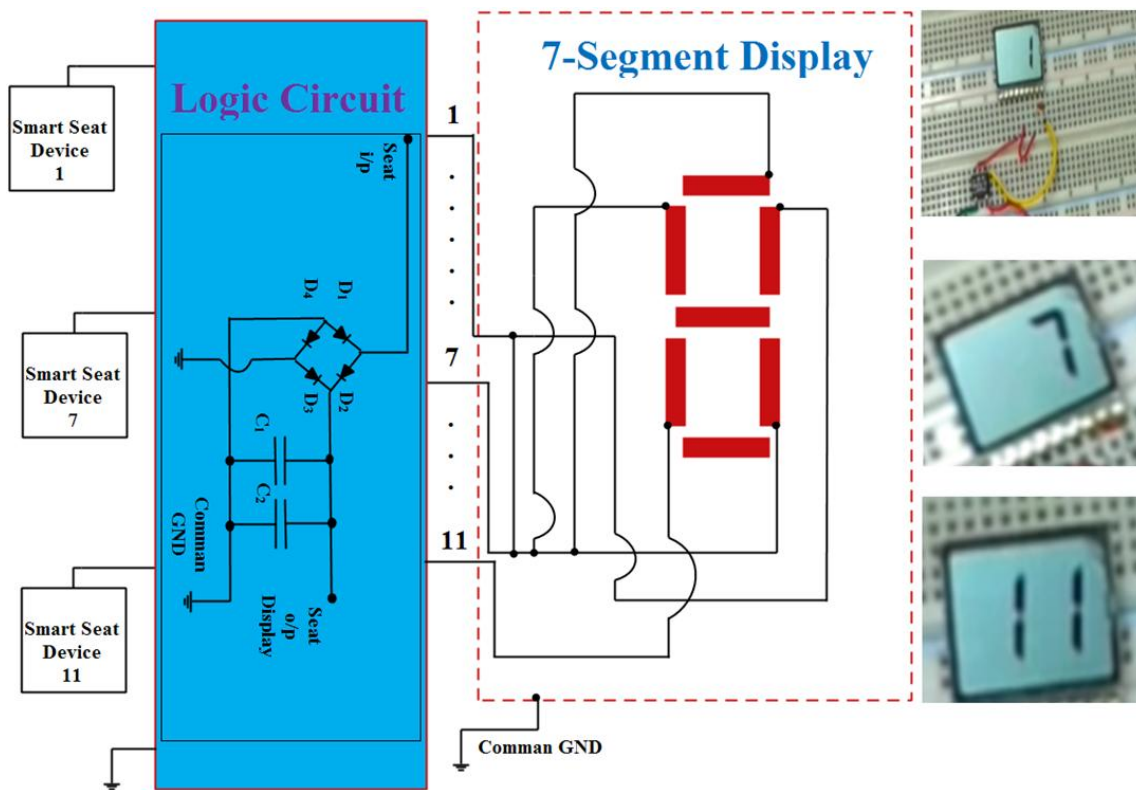
Figure. 3.12 Logic circuit diagram of Self-Powered passenger seat indicator and digital photograph of LCD display of seat number when the passenger occupies the seat.

3.4.5.2. Self-powered stop indicator

To construct a self-powered stop indicator light for a passenger bus, a bridge rectifier (DF06G), capacitor (C_1= 10 nF) and press switch is was used. When a passenger sits on the multi-unit SS-TENG, an electrical output signal is generated and the charge is stored in capacitor C_1. The switching circuit was fitted with 120 LEDs (60 blue and 60 green of 3.0-3.4 V, 20 mA max) connected in series and covered with a mask presenting the word "STOP" as shown in **Figure. 3.13** and the enlarged photograph shows the "STOP" indication LED lit up during its active condition.
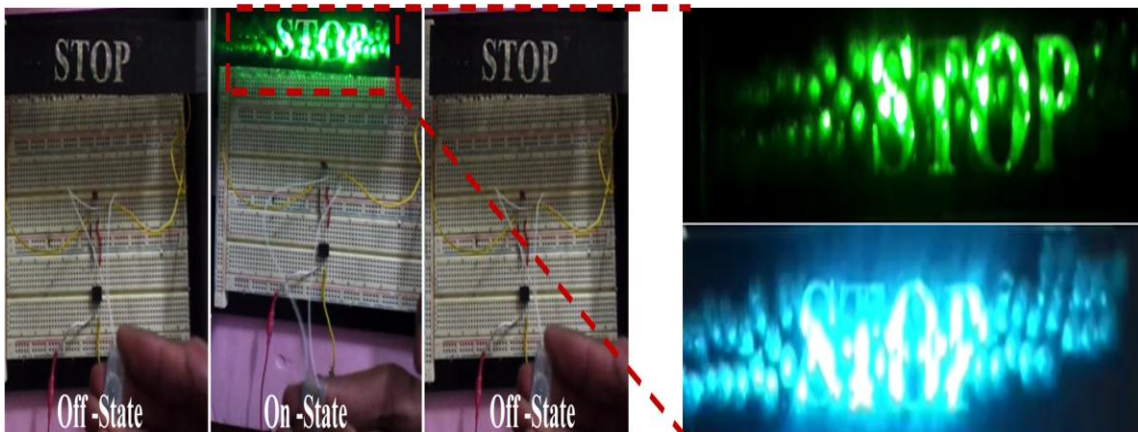
Figure. 3.13 Photograph of the self-powered stop indicator during its operation and its digital images of LED lit up during stop indication.

3.5. Conclusion

An innovative design for electricity-generation was developed using eco-friendly materials found in everyday life. The proposed SS-TENG can effectively harvest electrical energy from physical motion, utilizing materials commonly found on a person. The material in contact with the surface of the SS-TENG produces a significant output power, which may be used to drive low-power consumer electronics using a trigger circuit. The SS-TENG was

demonstrated to work as a self-powered passenger seat indicator and a self-powered stop indicator. It was demonstrated, therefore, that the SS-TENG can be installed as standalone electronic devices in public places, and is capable of illuminating 60(blue and green) LEDs connected in series. Since the SS-TENG is simply fabricated, low cost and robust, it is a promising technology for self-powered electronics, which clearly demonstrates the use of eco-friendly, bio-degradable materials for energy harvesting, and presents a significant opportunity for the extension of degradable organic polymer based triboelectric nanogenerators.

3.6.   References

[1]   D.-H. Kim, N. Lu, R. Ma, Y.-S. Kim, R.-H. Kim, S. Wang, J. Wu, S. M. Won, H. Tao, A. Islam, K. J. Yu, T. Kim, R. Chowdhury, M. Ying, L. Xu, M. Li, H.-J. Chung, H. Keum, M. McCormick, P. Liu, Y.-W. Zhang, F. G. Omenetto, Y. Huang, T. Coleman, and J. A. Rogers, "Epidermal electronics.," *Science*, vol. 333, no. 6044, pp. 838–43, Aug. 2011.

[2]   B. Tian, T. Cohen-Karni, Q. Qing, X. Duan, P. Xie, and C. M. Lieber, "Three-dimensional, flexible nanoscale field-effect transistors as localized bioprobes.," *Science*, vol. 329, no. 5993, pp. 830–4, Aug. 2010.

[3]   W. WZ, W. XN, and W. ZL, "Taxel-Addressable Matrix of Vertical-Nanowire Piezotronic Transistors for Active and Adaptive Tactile Imaging," *Science (80-.).*, vol. 340, no. 6135, pp. 952–957, 2013.

[4]   Z. L. Wang and J. Song, "Piezoelectric nanogenerators based on zinc oxide nanowire arrays.," *Science*, vol. 312, no. 5771, pp. 242–6, Apr. 2006.

[5]   S. Lee, J.-I. Hong, C. Xu, M. Lee, D. Kim, L. Lin, W. Hwang, and Z. L. Wang, "Toward

robust nanogenerators using aluminum substrate.," *Adv. Mater.*, vol. 24, no. 32, pp. 4398–402, Aug. 2012.

[6]   X. Wang, J. Song, J. Liu, and Z. L. Wang, "Direct-current nanogenerator driven by ultrasonic waves.," *Science*, vol. 316, no. 5821, pp. 102–5, Apr. 2007.

[7]   S. Xu, Y. Qin, C. Xu, Y. Wei, R. Yang, and Z. L. Wang, "Self-powered nanowire devices," *Nat. Nanotechnol.*, vol. 5, no. 5, pp. 366–373, Mar. 2010.

[8]   A. Ramadoss, B. Saravanakumar, S. W. Lee, Y.-S. Kim, S. J. Kim, and Z. L. Wang, "Piezoelectric-driven self-charging supercapacitor power cell.," *ACS Nano*, vol. 9, no. 4, pp. 4337–45, Apr. 2015.

[9]   M. Grätzel, "Photoelectrochemical cells.," *Nature*, vol. 414, no. 6861, pp. 338–44, Nov. 2001.

[10] B. Tian, X. Zheng, T. J. Kempa, Y. Fang, N. Yu, G. Yu, J. Huang, and C. M. Lieber, "Coaxial silicon nanowires as solar cells and nanoelectronic power sources.," *Nature*, vol. 449, no. 7164, pp. 885–9, Oct. 2007.

[11] R. Venkatasubramanian, E. Siivola, T. Colpitts, and B. O'Quinn, "Thin-film thermoelectric devices with high room-temperature figures of merit.," *Nature*, vol. 413, no. 6856, pp. 597–602, Oct. 2001.

[12] L. E. Bell, "Cooling, heating, generating power, and recovering waste heat with thermoelectric systems.," *Science*, vol. 321, no. 5895, pp. 1457–61, Sep. 2008.

[13] P. Basset, D. Galayko, A. M. Paracha, F. Marty, A. Dudka, and T. Bourouina, "A batch-fabricated and electret-free silicon electrostatic vibration energy harvester," *J.*

Micromechanics Microengineering, vol. 19, no. 11, p. 115025, Nov. 2009.

[14] S. Meninger, J. O. Mur-Miranda, R. Amirtharajah, A. Chandrakasan, and J. H. Lang, "Vibration-to-electric energy conversion," *IEEE Trans. Very Large Scale Integr. Syst.*, vol. 9, no. 1, pp. 64–76, Feb. 2001.

[15] S. Roundy, P. K. Wright, and J. Rabaey, "A study of low level vibrations as a power source for wireless sensor nodes," *Comput. Commun.*, vol. 26, no. 11, pp. 1131–1144, Jul. 2003.

[16] W. Tang, T. Zhou, C. Zhang, F. Ru Fan, C. Bao Han, and Z. Lin Wang, "A power-transformed-and-managed triboelectric nanogenerator and its applications in a self-powered wireless sensing node.," *Nanotechnology*, vol. 25, no. 22, p. 225402, 2014.

[17] S. Wang, L. Lin, and Z. L. Wang, "Nanoscale triboelectric-effect-enabled energy conversion for sustainably powering portable electronics.," *Nano Lett.*, vol. 12, no. 12, pp. 6339–46, Dec. 2012.

[18] R. Yang, Y. Qin, L. Dai, and Z. L. Wang, "Power generation with laterally packaged piezoelectric fine wires.," *Nat. Nanotechnol.*, vol. 4, no. 1, pp. 34–9, Jan. 2009.

[19] R. Zhang, L. Lin, Q. Jing, W. Wu, Y. Zhang, Z. Jiao, L. Yan, R. P. S. Han, and Z. L. Wang, "Nanogenerator as an active sensor for vortex capture and ambient wind-velocity detection," *Energy Environ. Sci.*, vol. 5, no. 9, p. 8528, Aug. 2012.

[20] G. Zhu, C. Pan, W. Guo, C.-Y. Chen, Y. Zhou, R. Yu, and Z. L. Wang, "Triboelectric-generator-driven pulse electrodeposition for micropatterning.," *Nano Lett.*, vol. 12, no. 9, pp. 4960–5, Sep. 2012.

[21]   Y. Yang, H. Zhang, J. Chen, Q. Jing, Y. S. Zhou, X. Wen, and Z. L. Wang, "Single-electrode-based sliding triboelectric nanogenerator for self-powered displacement vector sensor system," *ACS Nano*, vol. 7, no. 8, pp. 7342–7351, 2013.

[22]   Y. Yang, H. Zhang, Z. H. Lin, Y. S. Zhou, Q. Jing, Y. Su, J. Yang, J. Chen, C. Hu, and Z. L. Wang, "Human skin based triboelectric nanogenerators for harvesting biomechanical energy and as self-powered active tactile sensor system," *ACS Nano*, vol. 7, no. 10, pp. 9213–9222, 2013.

[23]   P.-K. Yang, Z.-H. Lin, K. C. Pradel, L. Lin, X. Li, X. Wen, J.-H. He, and Z. L. Wang, "Paper-based origami triboelectric nanogenerators and self-powered pressure sensors.," *ACS Nano*, vol. 9, no. 1, pp. 901–7, Jan. 2015.

[24]   Q. Liang, X. Yan, X. Liao, S. Cao, X. Zheng, H. Si, S. Lu, and Y. Zhang, "Multi-unit hydroelectric generator based on contact electrification and its service behavior," *Nano Energy*, vol. 16, pp. 329–338, Sep. 2015.

[25]   Z. L. Wang, "Triboelectric nanogenerators as new energy technology for self-powered systems and as active mechanical and chemical sensors.," *ACS Nano*, vol. 7, no. 11, pp. 9533–57, Nov. 2013.

[26]   Z. L. Wang and W. Wu, "Nanotechnology-enabled energy harvesting for self-powered micro-/nanosystems.," *Angew. Chem. Int. Ed. Engl.*, vol. 51, no. 47, pp. 11700–21, Nov. 2012.

[27]   L. S. McCarty and G. M. Whitesides, "Electrostatic charging due to separation of ions at interfaces: contact electrification of ionic electrets.," *Angew. Chem. Int. Ed. Engl.*, vol. 47,

no. 12, pp. 2188–207, Jan. 2008.

[28] Y. Yang, H. Zhang, J. Chen, S. Lee, T.-C. Hou, and Z. L. Wang, "Simultaneously harvesting mechanical and chemical energies by a hybrid cell for self-powered biosensors and personal electronics," *Energy Environ. Sci.*, vol. 6, no. 6, p. 1744, May 2013.

[29] T. C. Hou, Y. Yang, H. Zhang, J. Chen, L. J. Chen, and Z. Lin Wang, "Triboelectric nanogenerator built inside shoe insole for harvesting walking energy," *Nano Energy*, vol. 2, no. 5, pp. 856–862, 2013.

[30] J. Zhong, Q. Zhong, F. Fan, Y. Zhang, S. Wang, B. Hu, Z. L. Wang, and J. Zhou, "Finger typing driven triboelectric nanogenerator and its use for instantaneously lighting up LEDs," *Nano Energy*, vol. 2, no. 4, pp. 491–497, Jul. 2013.

[31] K. Y. Lee, M. K. Gupta, and S.-W. Kim, "Transparent flexible stretchable piezoelectric and triboelectric nanogenerators for powering portable electronics," *Nano Energy*, Nov. 2014.

[32] W. Seung, M. K. Gupta, K. Y. Lee, K.-S. Shin, J.-H. Lee, T. Y. Kim, S. Kim, J. Lin, J. H. Kim, and S.-W. Kim, "Nanopatterned Textile-Based Wearable Triboelectric Nanogenerator.," *ACS Nano*, vol. 9, no. 4, pp. 3501–3509, Feb. 2015.

[33] F.-R. Fan, Z.-Q. Tian, and Z. Lin Wang, "Flexible triboelectric generator," *Nano Energy*, vol. 1, no. 2, pp. 328–334, Mar. 2012.

[34] B. Saravanakumar, K. Thiyagarajan, N. R. Alluri, S. SoYoon, K. Taehyun, Z.-H. Lin, and S.-J. Kim, "Fabrication of an eco-friendly composite nanogenerator for self-powered photosensor applications," *Carbon N. Y.*, vol. 84, pp. 56–65, Apr. 2015.

[35] N. R. Alluri, B. Saravanakumar, and S.-J. Kim, "Flexible, Hybrid Piezoelectric Film (BaTi(1-x)Zr(x)O3)/PVDF Nanogenerator as a Self-Powered Fluid Velocity Sensor.," *ACS Appl. Mater. Interfaces*, vol. 7, no. 18, pp. 9831–40, May 2015.

[36] J. Yang, J. Chen, Y. Su, Q. Jing, Z. Li, F. Yi, X. Wen, Z. Wang, and Z. L. Wang, "Eardrum-Inspired Active Sensors for Self-Powered Cardiovascular System Characterization and Throat-Attached Anti-Interference Voice Recognition," *Adv. Mater.*, vol. 27, no. 8, pp. 1316–1326, 2015.

[37] Q. Liang, X. Yan, X. Liao, S. Cao, S. Lu, X. Zheng, and Y. Zhang, "Integrated active sensor system for real time vibration monitoring.," *Sci. Rep.*, vol. 5, p. 16063, Jan. 2015.

[38] J. Yang, J. Chen, Y. Su, Q. Jing, Z. Li, F. Yi, X. Wen, Z. Wang, and Z. L. Wang, "Eardrum-Inspired Active Sensors for Self-Powered Cardiovascular System Characterization and Throat-Attached Anti-Interference Voice Recognition," *Adv. Mater.*, vol. 27, no. 8, pp. 1316–1326, 2015.

[39] F. Saurenbach, D. Wollmann, B. D. Terris, and A. F. Diaz, "Force microscopy of ion-containing polymer surfaces: morphology and charge structure," *Langmuir*, vol. 8, no. 4, pp. 1199–1203, Apr. 1992.

[40] B. Meng, W. Tang, Z. Too, X. Zhang, M. Han, W. Liu, and H. Zhang, "A transparent single-friction-surface triboelectric generator and self-powered touch sensor," *Energy Environ. Sci.*, vol. 6, no. 11, p. 3235, Oct. 2013.

[41] Y. Mao, D. Geng, E. Liang, and X. Wang, "Single-electrode triboelectric nanogenerator for scavenging friction energy from rolling tires," *Nano Energy*, vol. 15, pp. 227–234, Jul.

2015.

[42] J. Chen, G. Zhu, W. Yang, Q. Jing, P. Bai, Y. Yang, T.-C. Hou, and Z. L. Wang, "Harmonic-resonator-based triboelectric nanogenerator as a sustainable power source and a self-powered active vibration sensor.," *Adv. Mater.*, vol. 25, no. 42, pp. 6094–9, Nov. 2013.

[43] X.-S. Zhang, M.-D. Han, B. Meng, and H.-X. Zhang, "High performance triboelectric nanogenerators based on large-scale mass-fabrication technologies," *Nano Energy*, vol. 11, pp. 304–322, Jan. 2015.

[44] G. Zhu, P. Bai, J. Chen, and Z. Lin Wang, "Power-generating shoe insole based on triboelectric nanogenerators for self-powered consumer electronics," *Nano Energy*, vol. 2, no. 5, pp. 688–692, 2013.

[45] Q. Liang, X. Yan, Y. Gu, K. Zhang, M. Liang, S. Lu, X. Zheng, and Y. Zhang, "Highly transparent triboelectric nanogenerator for harvesting water-related energy reinforced by antireflection coating.," *Sci. Rep.*, vol. 5, p. 9080, Jan. 2015.

[46] K. C. Aw and S. V. Praneeth, "Low frequency vibration energy harvesting from human motion using IPMC cantilever with electromagnectic transduction," *8th Annu. IEEE Int. Conf. Nano/Micro Eng. Mol. Syst.*, vol. 1, pp. 645–648, 2013.

CHAPTER-4

Smart Mobile Pouch as a Biomechanical Energy Harvester towards Self-Powered Smart Wireless Power Transfer Applications

Graphical overview
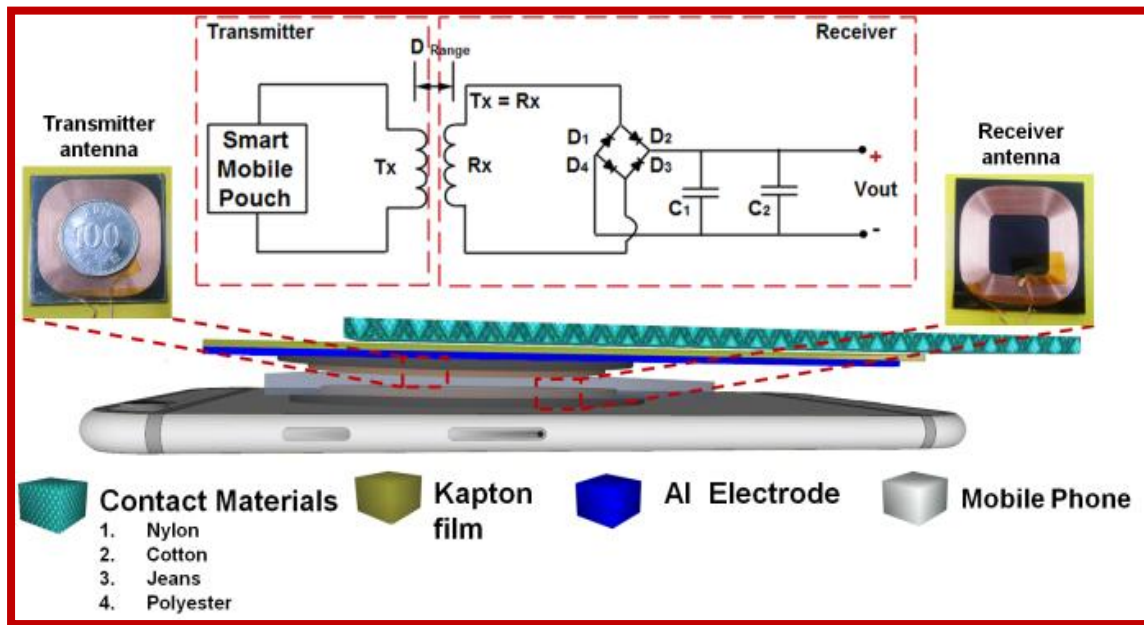
Highlights

➢ A Smart Mobile Pouch Triboelectric Nanogenerator (SMP-TENG) is introduced as a promising eco-friendly approach for scavenging biomechanical energy for powering next generation intelligent devices and smart phones

➢ The SMP-TENG is capable of harvesting energy in two operational modes: lateral sliding and vertical contact and separation

➢ A wireless power transmission setup integrated with SMP-TENG is demonstrated.

➢ This upgrades the traditional energy harvesting device into a self-powered wireless power transfer SMP-TENG

➢ The SMP-TENG opens a wide range of opportunities in the field of self-powered devices and low maintenance energy harvesting systems for portable and wearable electronic gadgets

4.1. Introduction

The invention of smart phones was a milestone technological development that heralded significant changes in mobile phones. New generation smart phones are well-equipped to fulfill a wide range of functions, such as video calling, internet access, real time health monitoring and mobile banking. However, smart phones require more power for uninterrupted functioning for a longer period of time compared to previous phones, and researchers across a range of fields, such as energy harvesting and energy storage, are working to find a solution. Many innovations have exhibited unique characteristics such as reliability, durability, cost effectiveness and eco friendliness;[1]–[3] however, satisfying real-time requirements still presents a significant challenge.

A number of electricity generation mechanisms, such as piezoelectric nanogeneration,[4], [5], [3], [6]–[8] as well as thermoelectric[9], [10] and photoelectric effects,[11]–[13] have been investigated; however, triboelectric nanogeneration (TENG)[14]–[19] is currently the technology attracting most attention for next-generation energy harvesting. Z. L. Wang discussed the potential of energy harvesting from various sources such as human activity,[20], [21] wind,[22] vibration[23] and water,[24] and the potential for self-powered application in day-to-day activities.[1] Other studies, such as those by S. W. Kim,[25] H. Zhang and[14] Y. Zhang[26],have described valuable innovations in TENG and self-powered devices. Our research on TENG is based on the coupled effects of electrostatic induction and contact electrification for harvesting biomechanical energy by utilizing worn fabrics as a contact material. By effectively integrating a TENG with an electronic device, the power source issues in wearable electronic[27], [28] gadgets could be solved, and this may also present a promising next generation technology for intelligent devices and smart phones.

Herein, we present an innovative product for scavenging biomechanical energy via eco-friendly fabrics worn in daily life, using a smart mobile pouch triboelectric nanogenerator (SMP-TENG). In the proposed SMP-TENG, the generation of electricity occurs during interactions between freestanding fabrics and a Kapton film during human movement. To study the energy harvesting process of the SMP-TENG in detail, its output performance during lateral sliding motion with various fabrics is analyzed and then tested under vertical contact and separation motion. The SMP-TENG can also act as a self-powered emergency flashlight and self-powered pedometer during normal human motion. Finally, the potential of the SMP-TENG as a self-powered wireless power transmitter for wirelessly recharging a Li-ion battery is demonstrated. This study describes a promising technology for biomechanical energy harvesting and self-powered applications.

4.2. Experimental methods

4.2.1. Surface modification of Kapton film

The Kapton film (25 μm) was cleaned with ethanol, isopropyl alcohol and deionized water, then blown dry with compressed nitrogen gas to remove dust particles. To enhance the contact electrification, a surface treatment was performed on the cleaned Kapton film using homemade DBD plasma with a power of 100 W for 5 min in an O_2/Ar atmosphere at flow rates of 10 sccm and 15 sccm, respectively.

4.2.2. Fabrication of IDT (Interdigitated electrode)

The primary design of the SMP-TENG is shown schematically in Figure 1a. An interdigitated structure electrode was shaped on a PET sheet with dimensions of 50×2 mm. The

제주대학교 중앙도서관
JEJU NATIONAL UNIVERSITY LIBRARY

electrodes were separated with a 2 mm gap using a laser cutter. The patterned IDT electrode was cleaned with ethanol and deionized water, consecutively, and then blown dry with compressed nitrogen gas. A Pt layer was deposited (for increased adhesion) using a DC sputter and an Al layer was deposited on the substrate using a thermal evaporator.

4.2.3. Fabrication of the SMP-TENG

The surface-treated Kapton film (50 × 50 mm) was tailored and surfaces without roughness were precisely adhered to the pre-patterned IDT electrode (50 × 1 mm). Two copper electrodes (Nilaco, 0.1 mm) were attached to the IDT electrode using silver paste and dried at 50 ℃ for 30 min. The device was attached to a mobile pouch for support. The total effective area of the SMP-TENG device was 16 cm^2.

4.2.4. Fabrication of self-powered wireless power transmission SMP-TENG

The self-powered wireless power transmission SMP-TENG consists of two parts: the transmitter and the receiver. For the transmitter, a commercially purchased wireless power transmission antenna (SWC424KB120-100) with 30 turns was embedded within the SMP-TENG. For the receiver section, a commercially purchased antenna (SWC424KB120-100) with 30 turns was connected to a bridge rectifier circuit to obtain a DC output voltage.

4.3.   Measurement systems

Surface morphology analyses of the plasma-treated Kapton film and other cloth materials were performed using an FE-SEM (Zeiss Supra 55VP; Carl Zeiss AG, Oberkochen, Germany). To measure the electrical output of the SMP-TENG, an external sliding motion and force was applied using a commercial linear mechanical motor. Before electrical measurements, all contact

materials were heat-treated (in a hot air oven) at 80 ℃ for 30 min to remove humidity. The output voltage signal of the SMP-TENG was measured using an electrometer (Keithley 6514; Keithley Instruments, Cleveland, OH, USA) and an SR 570 low noise current amplifier (Stanford Research Systems, Sunnyvale, CA< USA) was used to measure the short-circuit current. For real time data acquisition control and analysis, a software platform was constructed based on LabVIEW. All electrical measurements, including wireless power transmission, were conducted inside a grounded homemade Faraday cage. A self-powered wireless power transmission circuit (transmitter and receiver) was designed and constructed on a breadboard for the studies and real-time demonstrations.

4.4. Results and discussion

4.4.1. SMP-TENG design

The architecture of the SMP-TENG is composed of a 50×50 mm dielectric barrier discharge (DBD) plasma-treated Kapton film and IDT structured Al electrodes with a working area of 16 cm^2. The SMP-TENG was attached to a smart phone for physical support, as illustrated schematically in **Figure 4.1 (a)** and **Figure 4.1 (b)** shows a digital photograph of the SMP-TENG attached to a dummy mobile phone with an area of 25 cm^2.
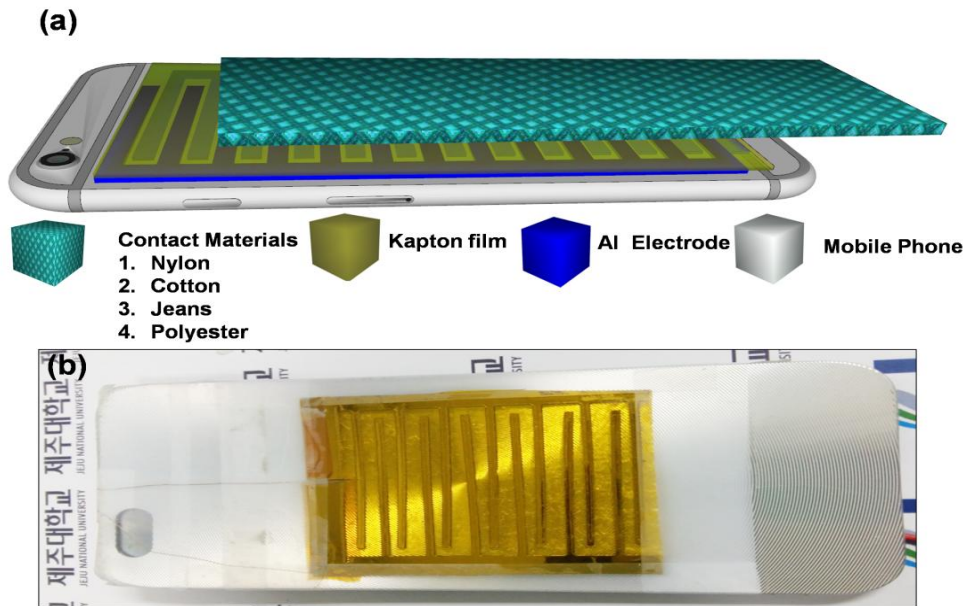
Figure 4.1 (a) Schematic illustration showing the structural design of the Smart Mobile Pouch Triboelectric Nanogenerator (SMP-TENG) during sliding motion. (b) Photograph shows a fabricated SMP-TENG used as a mobile pouch.

4.4.2. Morphology analysis of negative and positively charged layers

Here, **Figure 4.2 (a, b)** shows a field emission-scanning electron microscope (FE-SEM) image of the plasma-untreated and treated Kapton film, respectively. Were plasma treated Kapton film containing irregular nanostructures, which contributes for higher charge generation. Also, the surface structures of other contact materials are important for the charge generation. **Figure 4.2 (c-f)** shows the FE-SEM image of nylon, jeans, cotton and polyester, respectively.
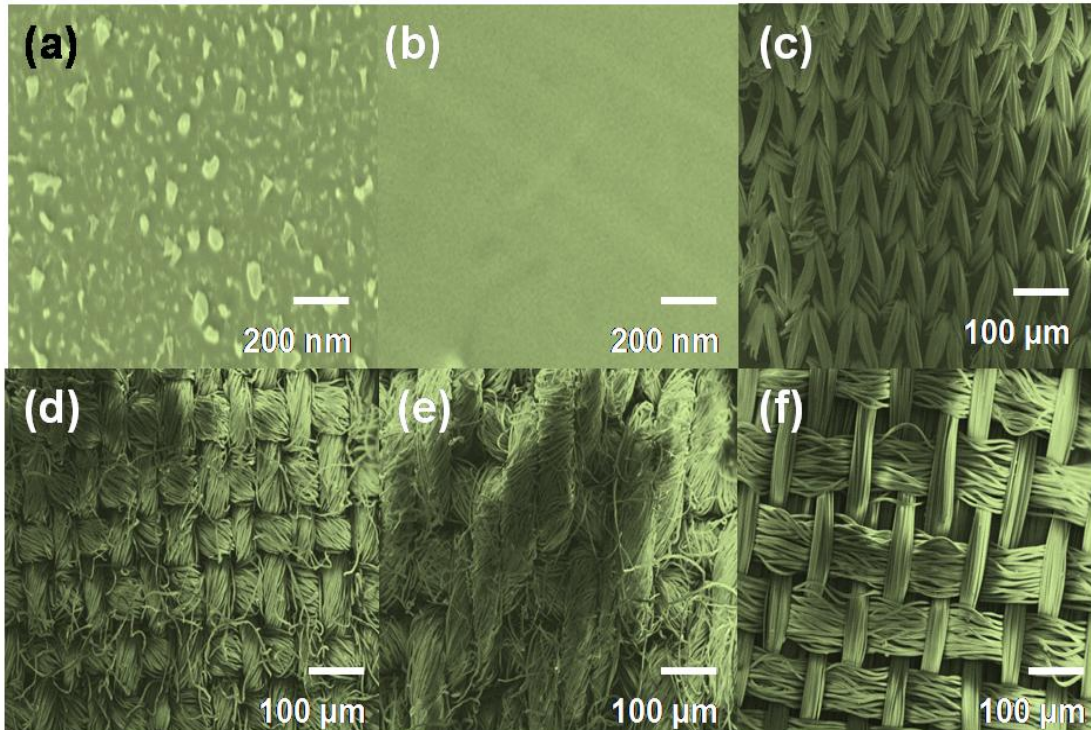
Figure 4.2 (a and b) FE-SEM images of triboelectric active layer: DBD plasma treated and untreated Kapton film. (c-f) Top view FE-SEM image of positively charged triboelectric contact materials: nylon, cotton, denim and polyester cloth.

4.4.3. Sliding mode SMP-TENG

4.4.3.1 Working mechanism

To understand the energy harvesting mechanism of the SMP-TENG, the sliding mode behavior of the device was investigated first. Here, daily wearable cloth materials such as nylon, jeans, cotton and polyester were used as freestanding contact materials for generation of triboelectric charge. **Figure 4.1.3**shows the working mechanism of the SMP-TENG during lateral sliding on the contact materials (50 × 50 mm) of the device, which acts as the freestanding triboelectric layer. The mechanism of the SMP-TENG is based on coupling between electrostatic induction and triboelectrification,[25], [26], [29]–[31] which contributes to a flow of electrons between the IDT electrodes. Initially, the freestanding fabric is in contact with the Al electrode A as shown in **Figure. 4.3 (a)**, where the Al electrode B is a pair of IDT electrodes.
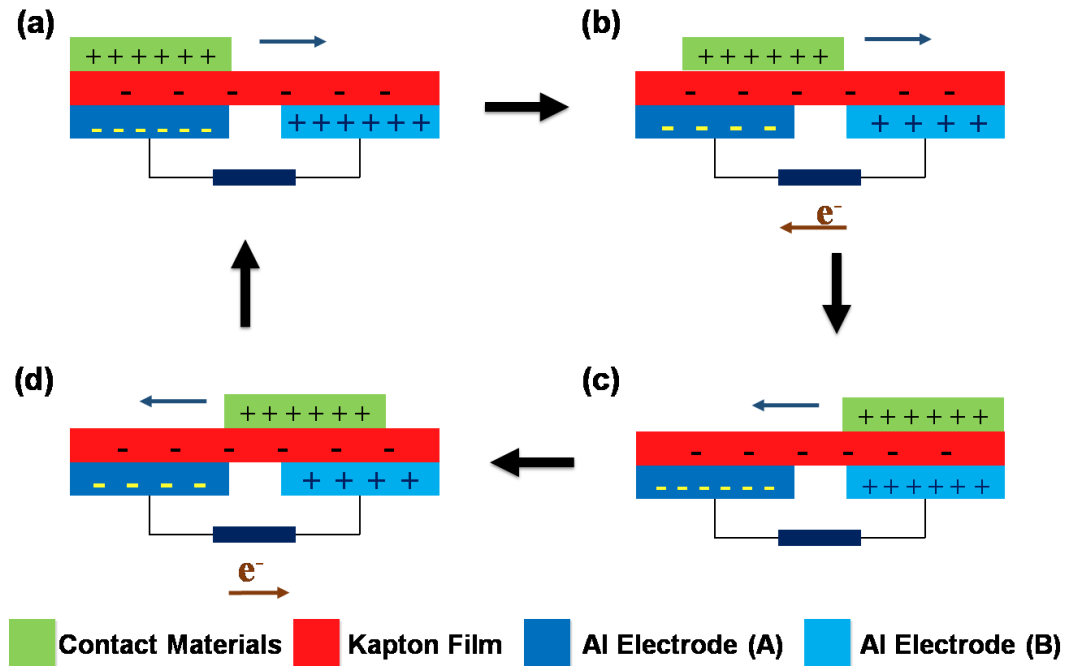
Figure 4.3 Schematic diagram of a dielectric-to-dielectric SMP-TENG energy harvesting mechanism during sliding mode operation. (a) Initial stage, (b) forward sliding, (c) equilibrium state, and (d) reverse sliding.

Under the influence of the external force, the contact material starts to slide towards Al electrode B. Because the freestanding fabric is more triboelectrically positive than the Kapton film, electrons will be transferred from the freestanding fabric to the surface of the Kapton film. During the sliding motion, electrons will flow from Al electrode A to Al electrode B, as shown in **Figure 4.3 (b)**. When the fabric reaches Al electrode B, the flow of electrons stops; this process contributes to the first half-cycle of the SMP-TENG, as shown in **Figure 4.3(c)**. The second half-cycle is obtained during the reverse sliding motion of the fabric from Al electrode B to Al electrode A, and electrons flow in the opposite direction, as shown in **Figure 4.3(d)**.

4.4.3.2. Electrical analysis of SMP-TENG

To quantify the typical electrical performance of the SMP-TENG, a linear motor (LinMot, Inc., Elkhorn, WI, USA) was used to provide a controlled lateral sliding motion to the

제주대학교 중앙도서관
JEJU NATIONAL UNIVERSITY LIBRARY

freestanding fabric. Initially, an SMP-TENG with seven pairs of IDT electrodes was studied. **Figure 4.4 (a–b)** illustrates the electrical response of the SMP-TENG with nylon as the freestanding fabric. The peak open circuit voltage (V_{oc}) was 150 V and the peak short circuit current (I_{sc}) was 305 μA. An enlarged view of the V_{oc} and I_{sc} signals is shown in the center inset of **Figure 4.4 (a–b)**. To identify the energy harvesting efficiency of the SMP-TENG with a range of freestanding fabrics, the experiment was repeated with four different fabric materials: polyester, jeans, cotton and nylon. **Figure 4.4 (c–d) shows** the measured values of V_{oc} and I_{sc} for different freestanding fabrics; an increment in the electrical response can clearly be seen when the fabric was changed from polyester to nylon. This behavior results from different levels of triboelectric charge of the contact materials.[32]
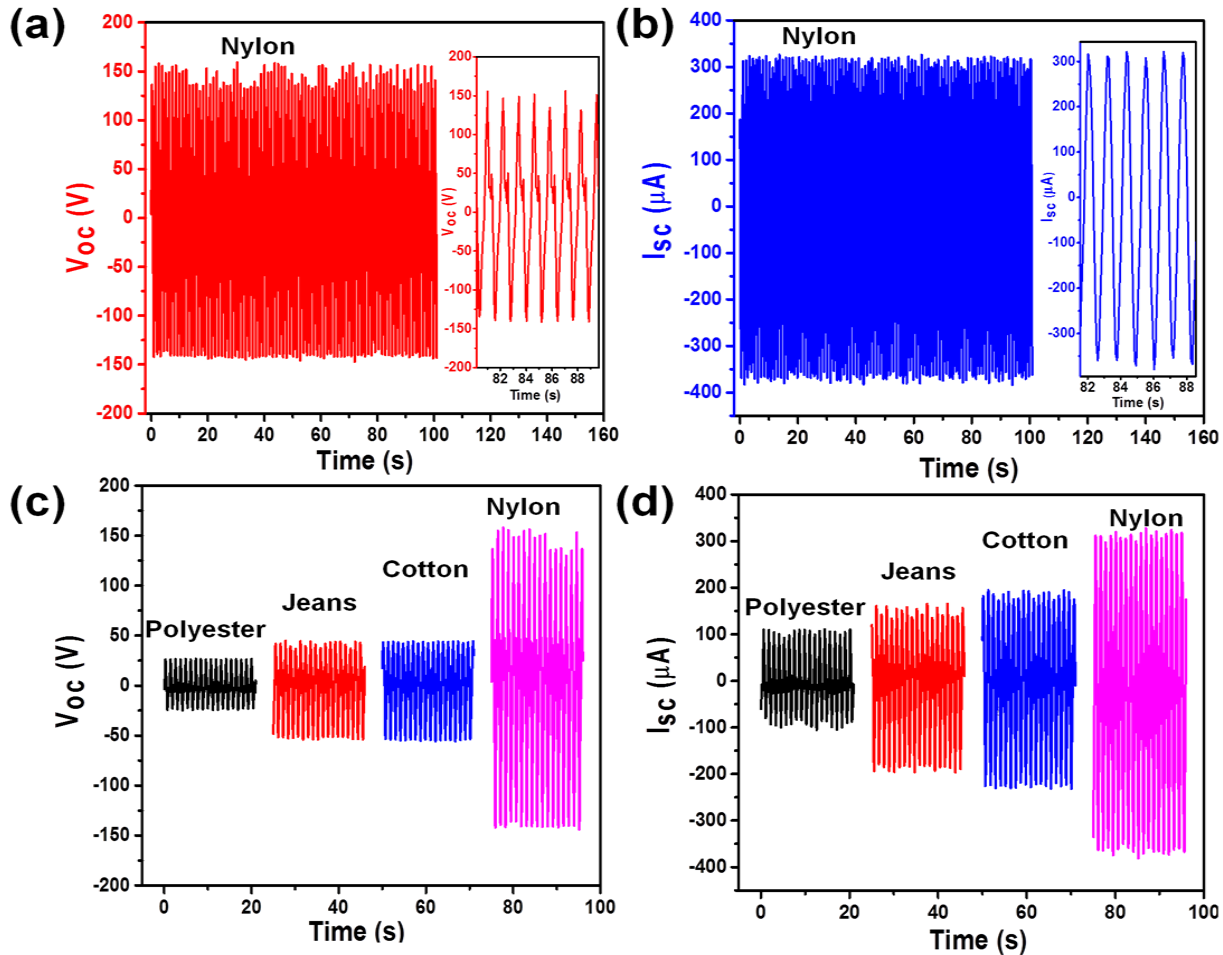
Figure 4.4 (a–b) Typical electrical output performance of the SMP-TENG from sliding the contact materials on the Kapton film. (a) Open-circuit voltage and (b) short-circuit current of the SMP-TENG with nylon as a sliding material at a sliding velocity of 1 m/s. (c–d) Electrical response of the SMP-TENG with different freestanding fabrics (contact materials) at a sliding velocity of 1 m/s.

Similarly, the influence of freestanding fabric and sliding velocity on I_{sc} are presented in **Figure 4.5 (a)**. The current amplitude increased with a change in both sliding material and sliding velocity. The I_{sc} induced by the nylon fabric at a velocity of 1 m/s was 305 μA. This experiment confirms the ability of the SMP-TENG to harvest energy from freestanding fabrics at different sliding velocities. To systematically identify the effect of the IDT electrodes, the number of IDT electrode pairs was varied between one and seven sets. **Figure 4.5 (b)** shows I_{sc} for the SMP-TENG with different numbers of electrodes pairs, with nylon as a sliding material at

65

a sliding velocity of 1 m/s. I_{sc} gradually increased with increasing numbers of electrode pairs, showing that an IDT electrode-structured SMP-TENG can provide more efficient energy harvesting. To identify the optimum load resistance, instantaneous peak power and power density for the SMP-TENG, we performed an experiment with different external load resistances. **Figure 4.5 (c)** shows the output V_{oc} for different load resistances; V_{oc} increased and then saturated with increasing load resistance. The instantaneous peak power reached 0.021 mW and a maximum power density of 0.13 mW/m^2 was obtained across a matched load resistance of 500 MΩ. A diode bridge rectifier circuit was used to investigate the total accumulative induced charge with respect to the sliding velocity, with nylon as freestanding fabric. Figure 3d shows the rate of charge accumulation, which was found to be directly proportional to the sliding velocity. The greater number of sliding movements (forwards and backwards) associated with a higher velocity provides rapid triboelectric charge generation, and hence results in higher charge accumulation. The electrical output obtained from different sliding velocities was used to charge a 47 μF capacitor, as shown in **Figure 4.5 (d)**. It can be seen that the time required for the capacitor to charge to 3 V decreases with increasing sliding velocity. This faster charging performance is due to the higher rate of charge accumulation.
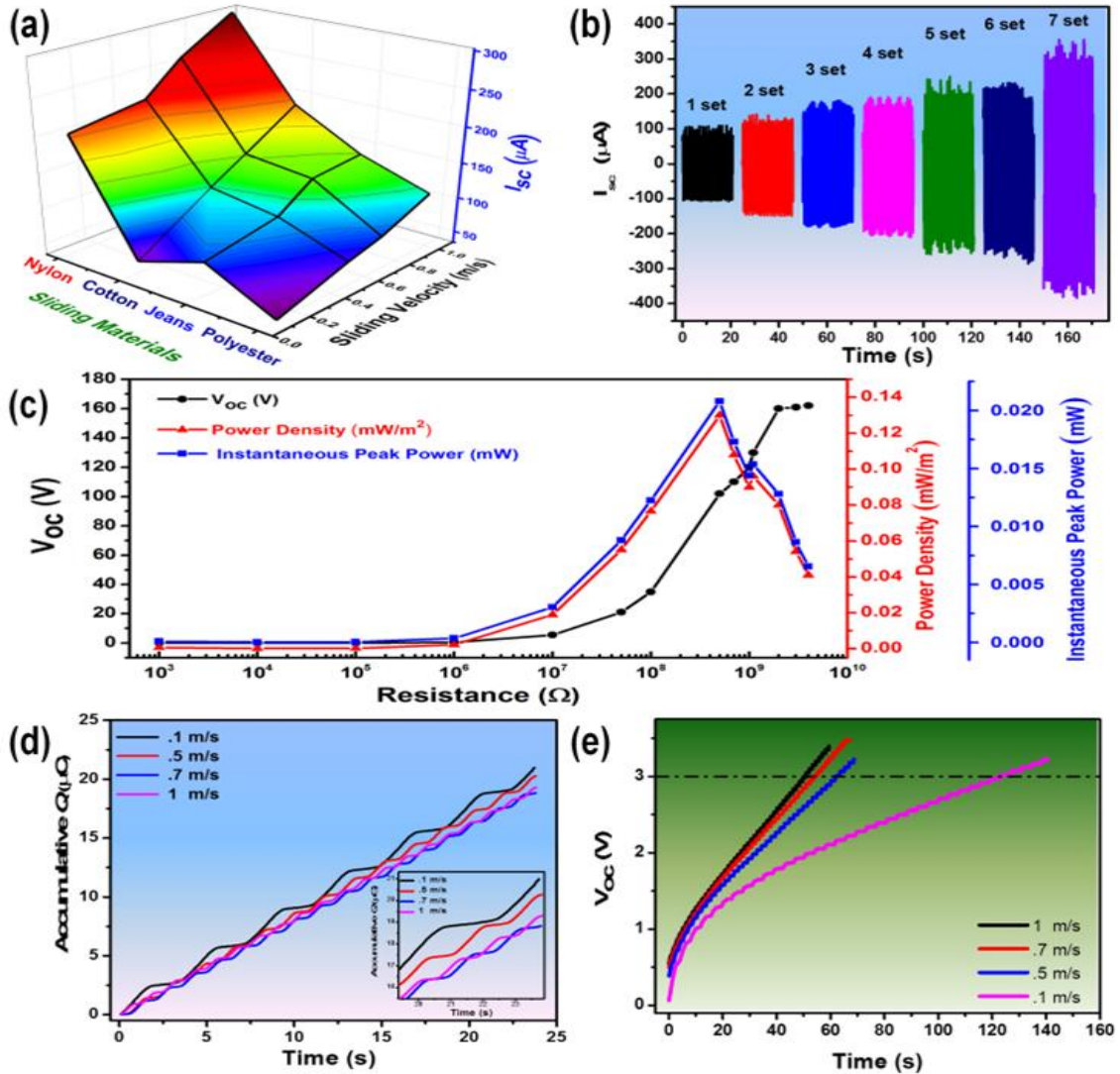
Figure 4.5 (a) Influence of freestanding fabric and sliding velocity on the short-circuit current. (b) The short-circuit current of the SMP-TENG with different numbers of electrode pairs, with nylon as a sliding material at a sliding velocity of 1 m/s. (c) The relationship between the output voltage (black), the instantaneous peak power (blue) and the power density on the external load resistance (red). (d) Accumulative induced charge generated by the SMP-TENG with nylon as a sliding material at different sliding velocities. (e) The measured voltage curve of a 10 μF capacitor charged using the SMP-TENG, with nylon as a sliding material at different sliding velocities.

A stability test was performed for 1500 cycles using nylon cloth as a contact material; the V_{oc} and I_{sc} were measured and shown in **Figure 4.6 (a-b)**. The inset shows an enlarged view of the electrical response at the end of the stability test and (inset) the FE-SEM image of the Kapton film after the stability test. The electrical response of the SMP-TENG remained steady after prolonged operation
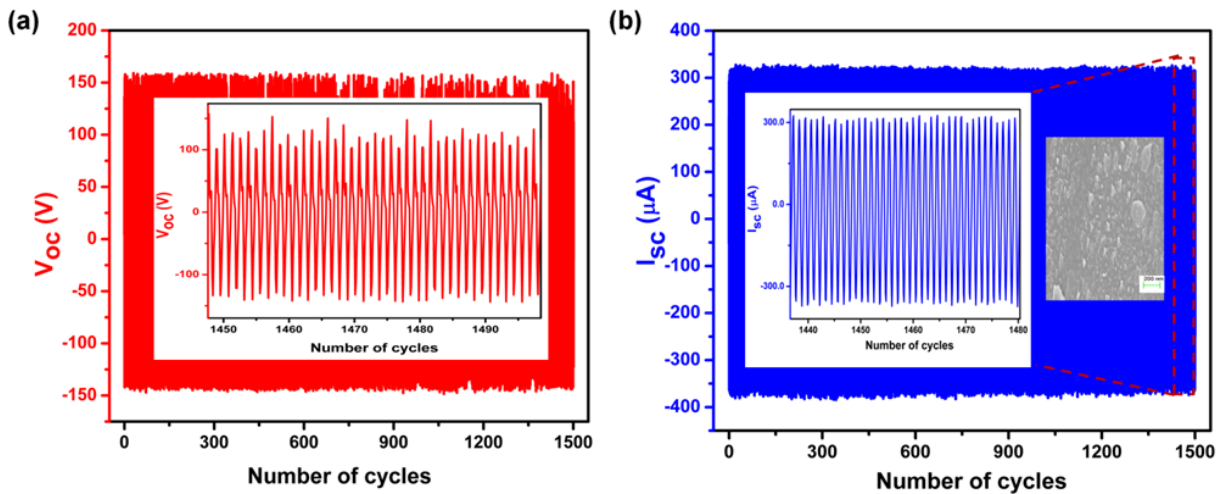
Figure 4.6 Stability test of SMP-TENG (a) Open circuit voltage and (b) Short circuit current. The inset shows an enlarged view of the electrical response at the end of the stability test and (inset) the FE-SEM image of the SMP-TENG after the stability test.

4.4.4.   Contact and separation mode SMP-TENG

4.4.4.1 Working mechanism

Here, **Figure 4.7** depicts the working mechanism of the SMP-TENG during the vertical contact and separation mode. Initially, the nylon fabric is in contact with the Kapton film, as shown in **Figure 4.7 (a)**. When the nylon fabric moves away from the SMP-TENG, the surface separates and a potential difference is generated between them. This causes a flow of electrons from Al electrode A to Al electrode B through an external load, as shown in **Figure 4.7 (b)**, and electrostatic equilibrium is achieved, as shown in **Figure 4.7 (c)**. This process contributes to the

first half-cycle of the SMP-TENG. The second half-cycle is obtained as the nylon fabric moves towards the surface of the SMP-TENG, where electrons flow in the opposite direction, from Al electrode B to Al electrode A through an external circuit, as shown in **Figure 4.7 (d)**. To measure the electrical response systematically, the SMP-TENG was anchored and the nylon fabric was fixed on the moving head of a programmable linear motor.
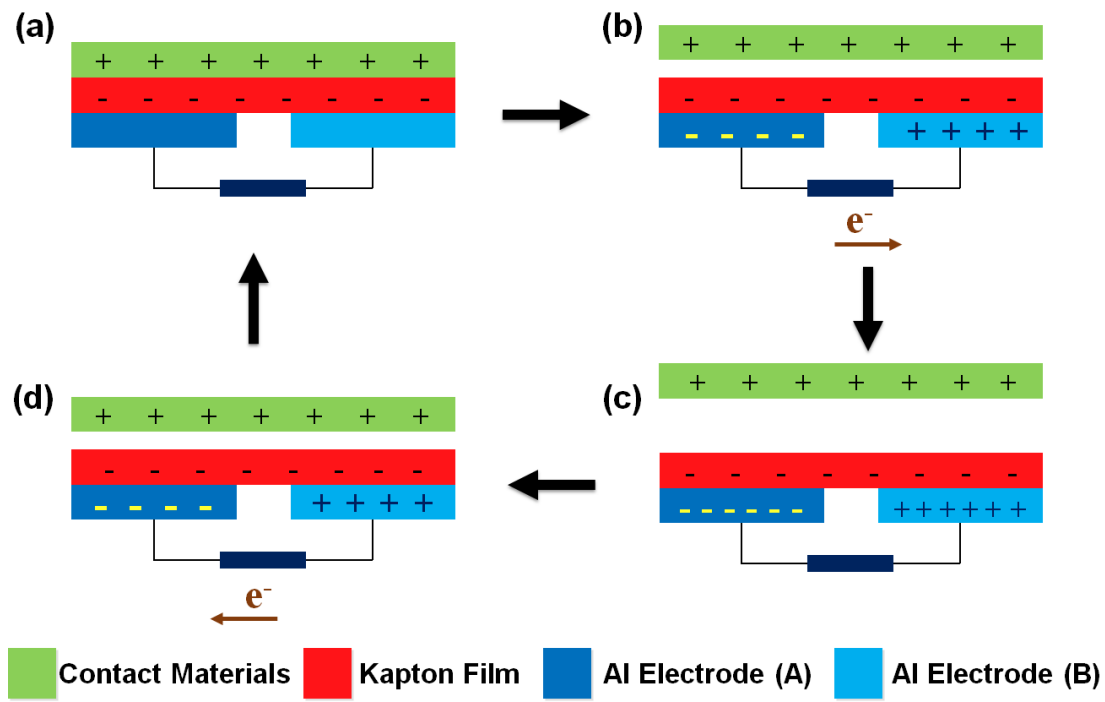
Figure 4.7 Schematic diagram of a dielectric-to-dielectric SMP-TENG energy harvesting mechanism during contact and separation motion. (a) Initial stage, (b) releasing, (c) equilibrium state, and (d) pressing.

4.4.4.2 Electrical analysis of SMP-TENG

Figure 4.8 (a, b) shows the electrical output of the SMP-TENG during vertical contact and separation with the freestanding fabric. In this scenario, the measured V_{oc} peak value was 40

69

V and the peak I_{sc} was 175 μA. An enlarged view of the V_{oc} and I_{sc} signals is shown in the right

inset of **Figure 4.8 (a, b)**. The peak value of I_{sc} increased with increasing contact force, from 130

μA at 10 N to 175 μA at 70 N, as shown in **Figure 4.8 (c)**. A stability test was performed for 200

cycles using nylon cloth as a contact material; the V_{oc} and I_{sc} were measured and shown in

Figure 4.8 (d). It was found that the electrical response of the SMP-TENG remained stable after

prolonged operation, with negligible variation in the electrical output signal.
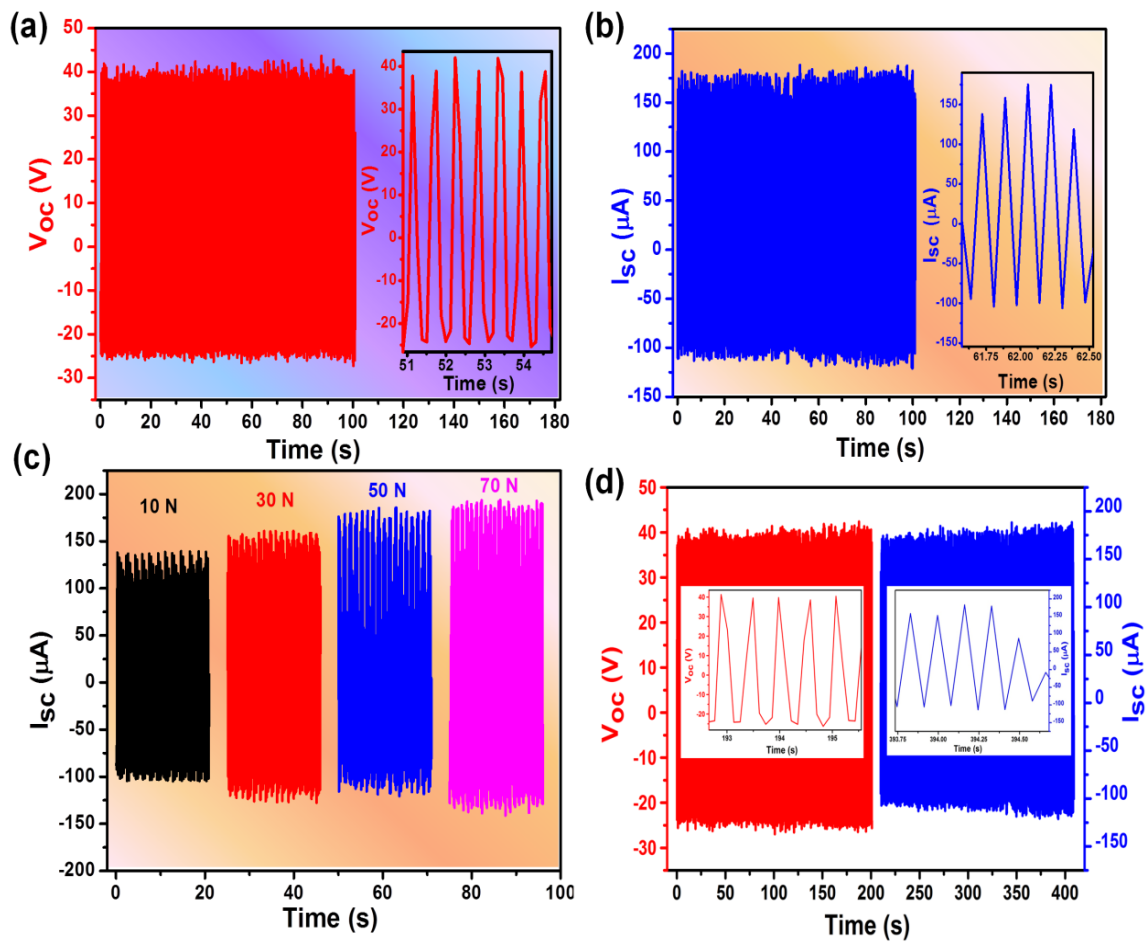
Figure 4.8 Typical electrical output performance of the SMP-TENG by contact and separation of contact materials on the Kapton film. (a) The open-circuit voltage and (b) short-circuit current of the SMP-TENG with nylon as a contact material. (c) The short-circuit current of the SMP-TENG with nylon as a contact material at various contact and separation forces. (d) Cyclic stability test of the SMP-TENG V_{oc} (red) and short circuit current (I_{sc}) (blue) with nylon as a contact material.

70

To verify the real-time human motion energy harvesting efficiency of the SMP-TENG, we conducted a practical experiment to convert various human motions (walking, running and sitting) into electricity (were a bridge rectifier diode was used to convert AC signal to DC signal) as shown in **Figure 4.9** and Video S1. To confirm low frequency human motion energy harvesting, the electrical signal obtained was Fourier transformed, and it can be seen in the inset of **Figure 4.9** that the frequency of the electrical signal was less than 5 Hz.
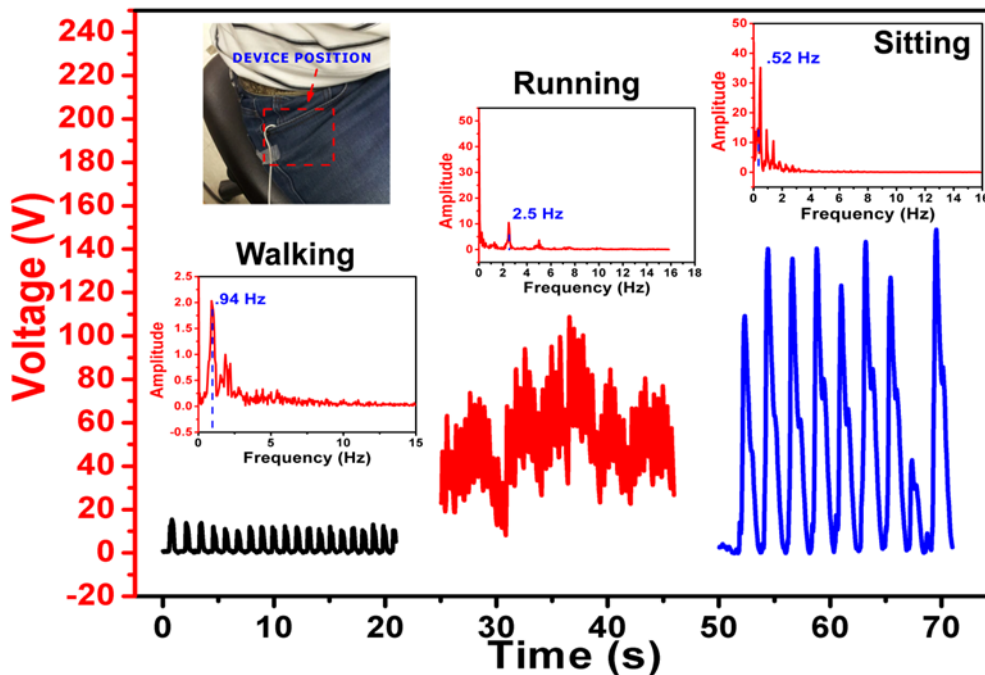
Figure 4.9 Energy harvesting using SMP-TENG during a range of human motions. (Inset) The frequency domain after Fourier transformed of the harvested electrical signal during human motions.

4.4.5. SMP-TENG for Self-powered applications

4.4.5.1. Self-powered emergency flash light

As the flash light in the mobile phone consumes more battery, while used as a torch light. Here we introduce a new self-powered application, which can be used in the emergency scenario. This self-powered emergency flash light was designed using SMP-TENG. A detailed circuit

71

diagram is shown in **Figure 4.10**, was constructed with a diode bridge rectifier (DF06G), capacitor (C_1= 20nF), a press switch and a green LED array (50 LEDs). During the human motion an electrical signal is generated, this charge is stored in a capacitor (C_1). With respect to the human motion the charge stored in the capacitor and the time taken to charge varies, at once the switch is pressed the stored charge lit up the LED array which is connected to the circuit. Also with respect to the stored charge the intensity of the flash light varies. This integrated facility with the SMP-TENG will reduce the conception of mobile battery and extend the operation time of mobile phones.
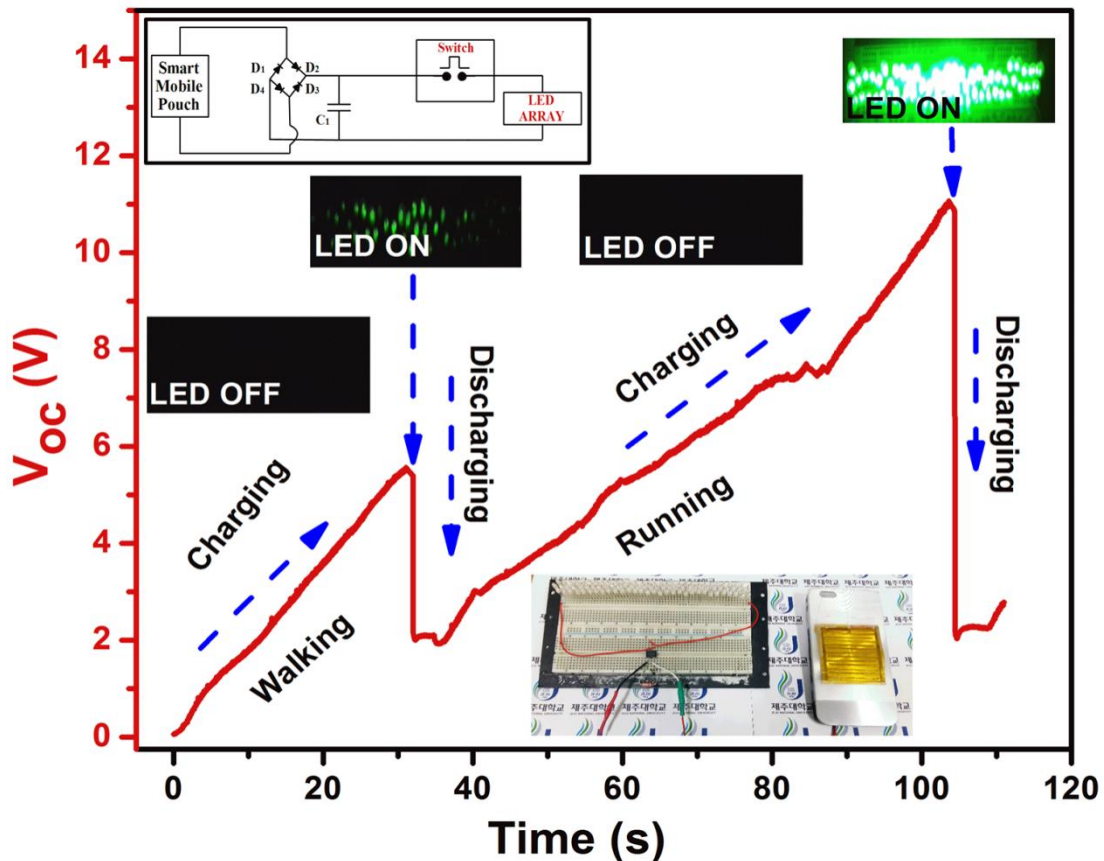
Figure 4.10 Self-powered emergency flash light, powered during human motion. (Inset left) A circuit connection designed for self-powered emergency flash light and (inset right) photograph of SMP-TENG with self-powered emergency flash light setup.

4.4.5.2. Self-powered pedometer

Here, we propose an interesting application of SMP-TENG as a self-powered pedometer. It's an addition multi-feature of SMP-TENG, this demonstration shows the working of a self-powered pedometer to calculate the number of steps, speed of the motion and distance travelled. **Figure 4.11 (a)** presents the electrical signals obtained during walking motion, the cyclic peaks was acquired for each step of motion. **Figure 4.11 (a)** presents the voltage peaks for 131 steps obtained in 135 seconds and **Figure 4.11 (b)** shows the enlarged view of 19 voltage peaks to demonstrate the calculation From the voltage signal we can calculate the distance travelled and speed of the motion using the following equation.

$$\text{Distance travelled} = \text{Walking steps} \times \text{Step length} \qquad (4.1)$$

$$\text{Distance travelled} = 131 \times .52 \text{ m}$$

$$= 68.2 \text{ m}$$

$$\text{Speed of motion} = \frac{\text{Distance Covered}}{\text{Time taken}} \qquad (4.2)$$

$$\text{Speed of motion} = \frac{68.2 \text{ m}}{135 \text{ sec}}$$

$$= .5 \text{ m/s}$$

Equation (4.1) denotes the distance travelled by the person and equation (4.2) denotes the speed of the motion. Apart, for a constant time period (10 s) we obtained various numbers of steps as presented in **Figure 4.11 (c)**. Based on the equation (4.1) and (4.2) these data helps to find the distance travelled and speed of the motion for various numbers of steps at a constant time. The bar graph **Figure 4.11 (d)** presents the distance travelled and speed of the motion for 8,

12 and 16 steps. This demonstration clearly shows the potential of SMP-TENG as a self-powered pedometer.
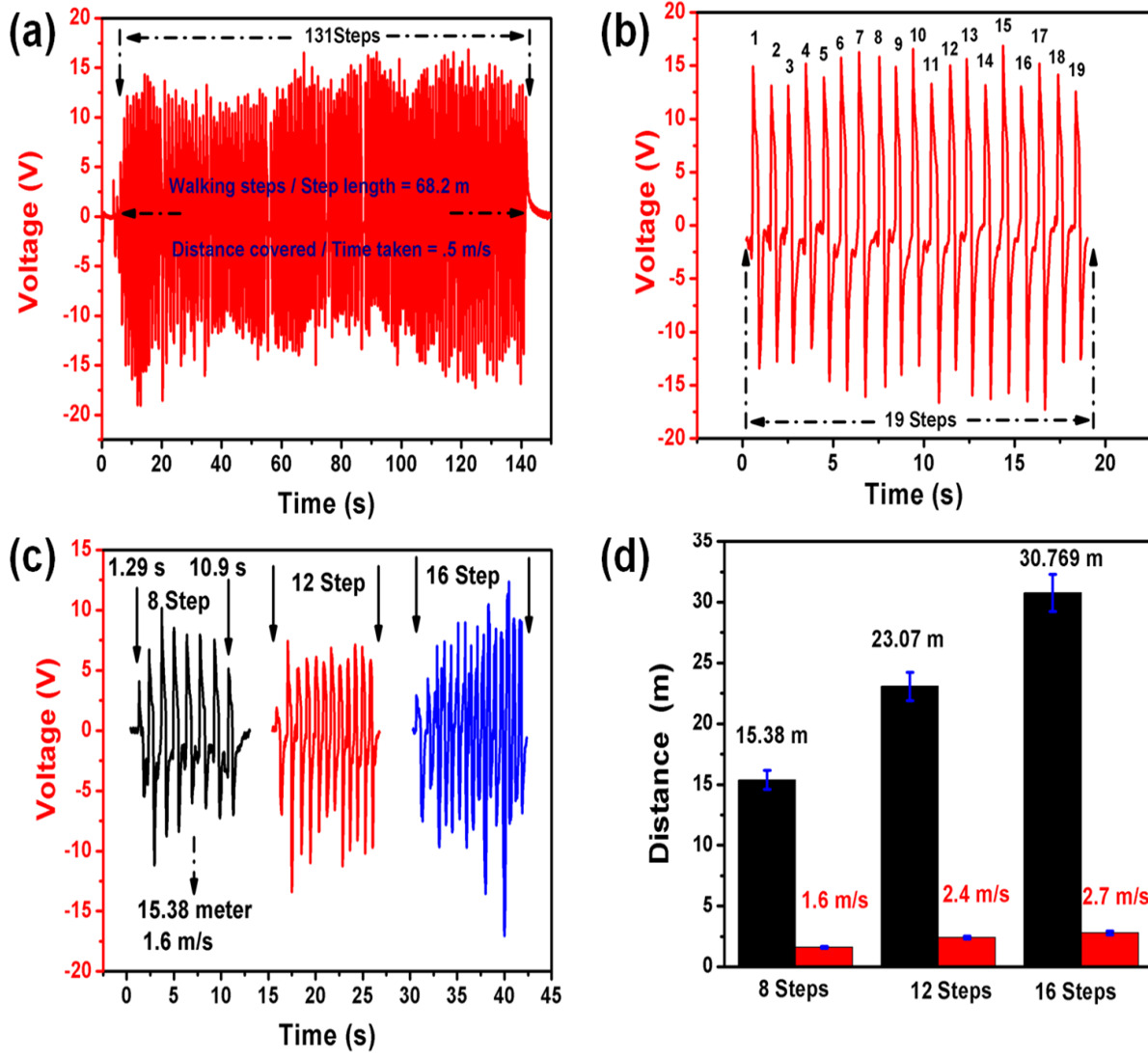
Figure 4.11 (a) The self-powered pedometer measurement of SMP-TENG for walking motion 131 steps. (b) Enlarged view of 19 voltage peaks to demonstrate the calculation. (c) Voltage peaks obtained for different walking speed for 10 sec. (d) Self-powered pedometer act as a, distance travelled and speed of motion measurement with respect to number of steps.

4.4.5.3. Self-powered wireless power transfer SMP-TENG

The recent requirement for wireless power transfer in gadgets such as mobile phones, MP3 players and other portable devices motivated us to design and develop a self-powered wireless power transfer SMP-TENG. Here, energy is transferred by electromagnetic induction from the transmitter to the receiver via inductive coupling; this technique works over a short range with low directivity, and at operational frequencies in the range of Hz to MHz. Because this is a near-field wireless power transmission technique, electrical energy is transferred between two coils separated by a short distance. **Figure 4.12 (a)** shows a schematic illustration of an SMP-TENG with a wireless power transmitter and receiver setup. The self-powered wireless power transfer SMP-TENG can be divided into two parts. The transmitter section consists of a transmitter antenna connected to the SMP-TENG that transfers power electromagnetically via a transmitter coil to the receiver section. The reception section consists of a receiver antenna connected to a bridge rectifier, to convert the induced AC voltage to a DC voltage, and of capacitors that act as a filter to reduce ripple voltage. The center inset of **Figure 4.12 (a)** shows the circuit diagram of the wireless power transfer setup and a digital photograph of the transmitter (left) and receiver antennae (right).
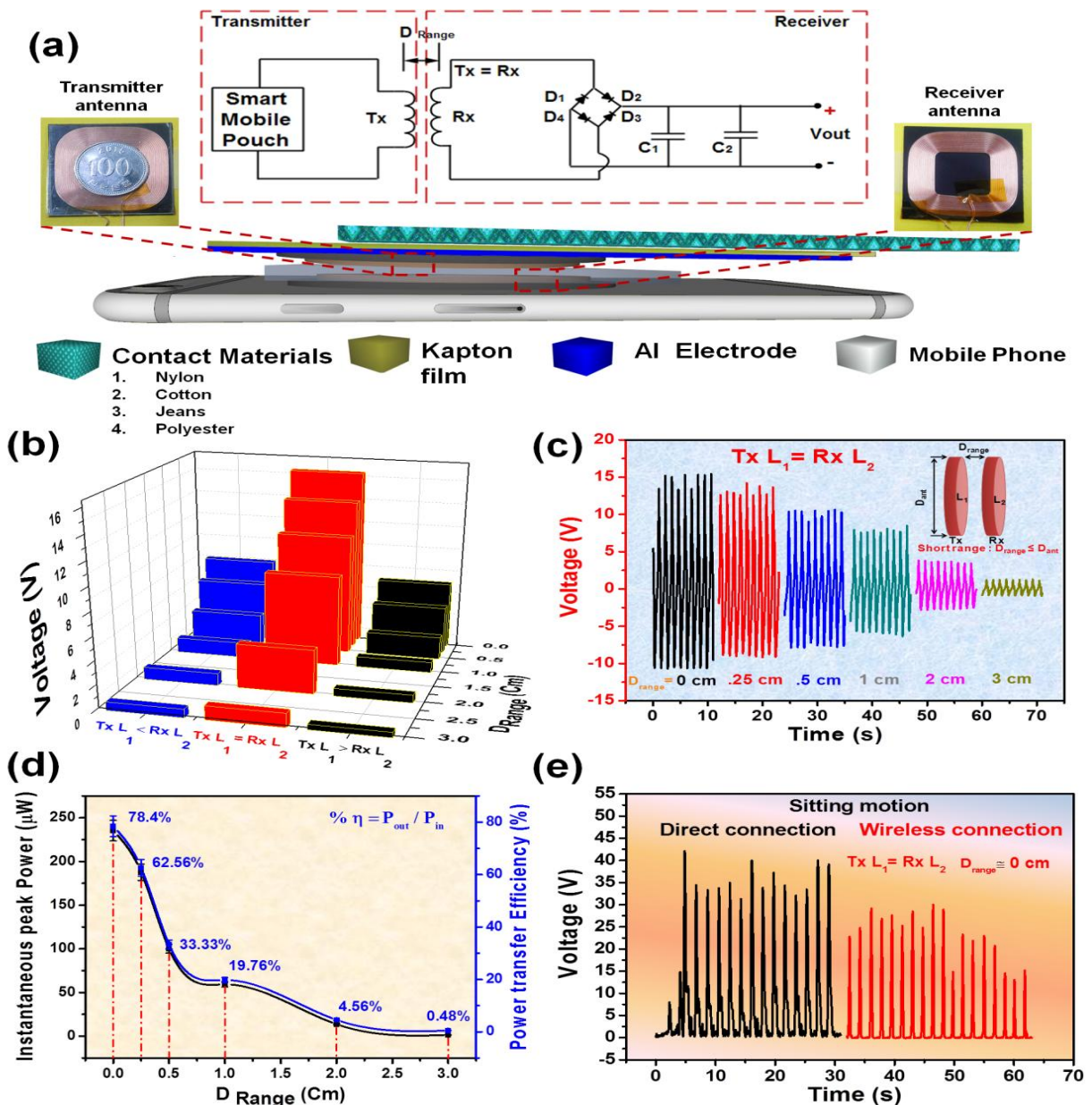
Figure 4.12 (a) Schematic structure of the SMP-TENG with a wireless power transmitter and receiver setup. (Inset, left) Digital photograph of the transmitter antenna (coin for scale comparison), (inset, center) the circuit diagram of the self-powered wireless power transmitter and receiver setup and (inset, right) digital photograph of the receiver antenna. (b) Wireless received open circuit voltage (V_{oc}) with respect to the number of turns of the transmitter and receiver antenna at various distances between the transmitter and receiver antennae (D_{Range}), with nylon as a contact material, during cyclic contact and separation motion. (c) Wireless received V_{oc} when Tx L_1 = Rx L_2 at various D_{Range} values. (d) Relationship between the instantaneous peak power (black) and the power transfer efficiency (blue), and D_{Range}. (e) Bio-mechanical energy harvesting (sitting) comparison between direct connection and wireless connection.

The power transfer efficiency depends significantly on the number of coil turns and the distance between the transmitter and receiver antennae. Transmitter (TxL_1) and receiver (RxL_2) antennae with different turn ratios (10 : 30, 30 : 30 and 30 : 10) were connected at various distances ($D_{range} \approx 0$, .25, .5, 1, 2 and 3 cm), as shown in **Figure 4.12 (b)**. To study wireless power transfer performance quantitatively, the electrical signal obtained from the SMP-TENG during contact and separation mode was applied as the input to the TxL_1. During the practical experiment, we found that the voltage received at RxL_2 was very high for $TxL_1 = RxL_2$ compared to when $TxL_1 < RxL_2$ and $TxL_1 > RxL_2$. This high power transfer efficiency when $TxL_1 = RxL_2$ is due to strong coupling between coils of the same turn ratio. When the distance between the two antennae increased, the voltage received decreased, because a greater separation between the coils means that more of the magnetic field from TxL_1 misses RxL_2. This separation lowers the coupling coefficient "k", resulting in loss of power transfer efficiency, which decreases to almost zero at larger separations.[33]–[35] The peak voltages obtained when $TxL_1 = RxL_2$ at various antennae separations are shown in **Figure 4.12 (c)**. Here, the maximum voltage was obtained when $D_{range} \approx 0$ cm, where the peak value reached 15 V. **Figure 4.12 (d)** shows the instantaneous peak power and power transfer efficiency when $TxL_1 = RxL_2$ at various distances between the two antennae. When the distance between TxL_1 and RxL_2 was increased ($\approx 0 - 3$ cm) the power transfer efficiency gradually decreased from 78.4 % to 0.48 %. Hence, the distance between TxL_1 and RxL_2 was maintained at less than 0.25 cm in subsequent experiments, to obtain the maximum power transfer efficiency. **Figure 4.12 (e)**. Comparing the two, it can be seen that a drop in received voltage occurs due to wireless power transfer over a small distance between TxL_1 and RxL_2. The results indicate, however, that harvested energy can be effectively

77

transferred wirelessly for real-time applications, such as mobile battery charging and driving low power electronic devices.
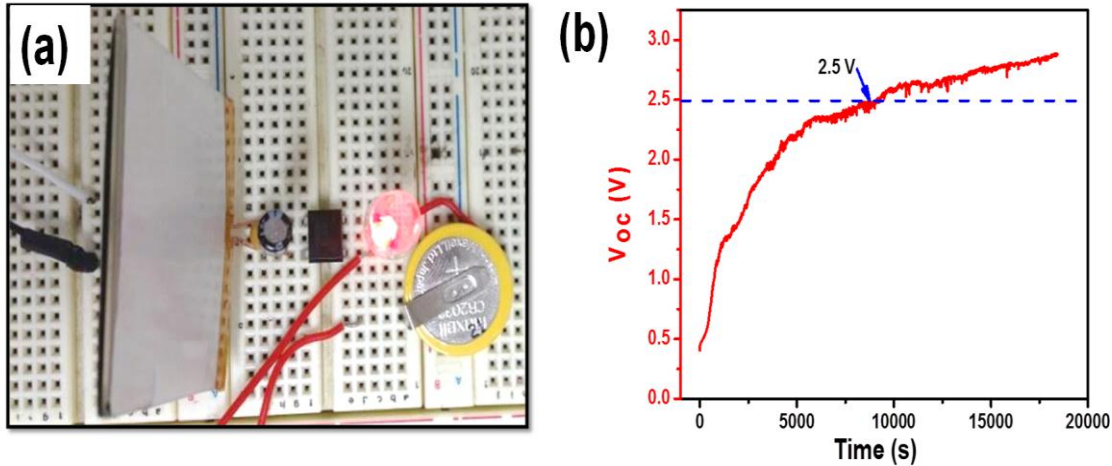
Figure 4.13 (a) Photograph of wireless power transmission and reception setup to charge a Li-ion battery. (b) Wireless charging of Li-ion battery.

From the above observations, it is clear that the self-powered wireless power transfer SMP-TENG can be utilized as a power source for charging Li-ion batteries. To investigate their utility in this application, we integrated a Li-ion battery charging circuit with the self-powered wireless power transfer SMP-TENG. Figure S7e shows a photograph of the wireless power transmission and reception setup for charging a Li-ion battery, and Figure S7f shows the charging performance when the Li-ion battery was charged to 2.5 V. These demonstrations prove that the self-powered wireless power transfer SMP-TENG is suitable for energy harvesting from a wide range of human motions and cloth materials.

4.5. Conclusion

In this work, we have successfully developed and demonstrated an innovative approach to electrical energy harvesting utilizing everyday worn fabrics. The SMP-TENG can generate electricity from lateral sliding and vertical contact and separation with freestanding fabrics, and

78

can serve as a self-powered emergency flashlight and self-powered pedometer. We have also introduced a wireless power transmission setup integrated with the SMP-TENG. This upgrades the traditional energy harvesting device into a self-powered wireless power transfer SMP-TENG that can be used to charge a Li-ion battery and light LEDs. Other competitive features, including a simple fabrication process, low fabrication cost and good electrical performance, indicate that this represents significant progress in the field of self-powered devices. This study opens up a new approach in the field of commercializing TENG in future smart phones.

4.6. References

[1]   Z. L. Wang, "Triboelectric nanogenerators as new energy technology and self-powered sensors - principles, problems and perspectives.," *Faraday Discuss.*, vol. 176, pp. 447–58, Jan. 2014.

[2]   Z. L. Wang and W. Wu, "Nanotechnology-enabled energy harvesting for self-powered micro-/nanosystems.," *Angew. Chem. Int. Ed. Engl.*, vol. 51, no. 47, pp. 11700–21, Nov. 2012.

[3]   R. Yang, Y. Qin, L. Dai, and Z. L. Wang, "Power generation with laterally packaged piezoelectric fine wires.," *Nat. Nanotechnol.*, vol. 4, no. 1, pp. 34–9, Jan. 2009.

[4]   N. R. Alluri, B. Saravanakumar, and S.-J. Kim, "Flexible, Hybrid Piezoelectric Film (BaTi(1-x)Zr(x)O3)/PVDF Nanogenerator as a Self-Powered Fluid Velocity Sensor.," *ACS Appl. Mater. Interfaces*, vol. 7, no. 18, pp. 9831–40, May 2015.

[5]   K. Y. Lee, M. K. Gupta, and S.-W. Kim, "Transparent flexible stretchable piezoelectric and triboelectric nanogenerators for powering portable electronics," *Nano Energy*, Nov.

2014.

[6]   B. Saravanakumar, S. Soyoon, and S.-J. Kim, "Self-powered pH sensor based on a flexible organic-inorganic hybrid composite nanogenerator.," *ACS Appl. Mater. Interfaces*, vol. 6, no. 16, pp. 13716–23, Aug. 2014.

[7]   B. Saravanakumar, K. Thiyagarajan, N. R. Alluri, S. SoYoon, K. Taehyun, Z.-H. Lin, and S.-J. Kim, "Fabrication of an eco-friendly composite nanogenerator for self-powered photosensor applications," *Carbon N. Y.*, vol. 84, pp. 56–65, Apr. 2015.

[8]   A. Ramadoss, B. Saravanakumar, S. W. Lee, Y.-S. Kim, S. J. Kim, and Z. L. Wang, "Piezoelectric-driven self-charging supercapacitor power cell.," *ACS Nano*, vol. 9, no. 4, pp. 4337–45, Apr. 2015.

[9]   R. Venkatasubramanian, E. Siivola, T. Colpitts, and B. O'Quinn, "Thin-film thermoelectric devices with high room-temperature figures of merit.," *Nature*, vol. 413, no. 6856, pp. 597–602, Oct. 2001.

[10]   L. E. Bell, "Cooling, heating, generating power, and recovering waste heat with thermoelectric systems.," *Science*, vol. 321, no. 5895, pp. 1457–61, Sep. 2008.

[11]   M. Grätzel, "Photoelectrochemical cells.," *Nature*, vol. 414, no. 6861, pp. 338–44, Nov. 2001.

[12]   S. K. Balasingam, M. Lee, M. G. Kang, Y. Jun, J. C. Hummelen, A. Marchioro, S. J. Moon, R. Humphry-Baker, J. H. Yum, J. E. Moser, M. Grätzel, N. G. Park, C. A. Bignozzi, and M. Grätzel, "Improvement of dye-sensitized solar cells toward the broader light harvesting of the solar spectrum," *Chem. Commun.*, vol. 49, no. 15, pp. 1471–1487,

2013.

[13]   S. K. Balasingam, M. G. Kang, Y. Jun, T. Nagai, H. Arakawa, T. Ma, K. C. Ho, R. Fu, S. Tan, T. Ma, and T. Sato, "Metal substrate based electrodes for flexible dye-sensitized solar cells: fabrication methods, progress and challenges," *Chem. Commun.*, vol. 49, no. 98, p. 11457, 2013.

[14]   B. Meng, W. Tang, Z. Too, X. Zhang, M. Han, W. Liu, and H. Zhang, "A transparent single-friction-surface triboelectric generator and self-powered touch sensor," *Energy Environ. Sci.*, vol. 6, no. 11, p. 3235, Oct. 2013.

[15]   J. Chun, J. W. Kim, W. Jung, C.-Y. Kang, S.-W. Kim, Z. L. Wang, and J. M. Baik, "Mesoporous pores impregnated with Au nanoparticles as effective dielectrics for enhancing triboelectric nanogenerator performance in harsh environments," *Energy Environ. Sci.*, vol. 8, no. 10, pp. 3006–3012, Oct. 2015.

[16]   Q. Liang, X. Yan, Y. Gu, K. Zhang, M. Liang, S. Lu, X. Zheng, and Y. Zhang, "Highly transparent triboelectric nanogenerator for harvesting water-related energy reinforced by antireflection coating.," *Sci. Rep.*, vol. 5, p. 9080, Jan. 2015.

[17]   P. Bai, G. Zhu, Z. H. Lin, Q. Jing, J. Chen, G. Zhang, J. Ma, and Z. L. Wang, "Integrated multilayered triboelectric nanogenerator for harvesting biomechanical energy from human motions," *ACS Nano*, vol. 7, no. 4, pp. 3713–3719, 2013.

[18]   A. Chandrasekhar, N. R. Alluri, V. Vivekananthan, Y. Purusothaman, and S.-J. Kim, "Sustainable Freestanding Biomechanical Energy Harvesting Smart Back Pack as a Portable-Wearable Power Source," *J. Mater. Chem. C*, 2017.

[19]   A. Chandrasekhar, N. R. Alluri, S. Balasubramaniam, S. Selvarajan, and S.-J. Kim, "Microcrystalline cellulose ingrained polydimethylsiloxane triboelectric nanogenerator as a self-powered locomotion detector," *J. Mater. Chem. C*, 2017.

[20]   W. Seung, M. K. Gupta, K. Y. Lee, K.-S. Shin, J.-H. Lee, T. Y. Kim, S. Kim, J. Lin, J. H. Kim, and S.-W. Kim, "Nanopatterned Textile-Based Wearable Triboelectric Nanogenerator.," *ACS Nano*, vol. 9, no. 4, pp. 3501–3509, Feb. 2015.

[21]   T.-C. Hou, Y. Yang, H. Zhang, J. Chen, L.-J. Chen, and Z. Lin Wang, "Triboelectric nanogenerator built inside shoe insole for harvesting walking energy," *Nano Energy*, vol. 2, no. 5, pp. 856–862, Sep. 2013.

[22]   R. Zhang, L. Lin, Q. Jing, W. Wu, Y. Zhang, Z. Jiao, L. Yan, R. P. S. Han, and Z. L. Wang, "Nanogenerator as an active sensor for vortex capture and ambient wind-velocity detection," *Energy Environ. Sci.*, vol. 5, no. 9, p. 8528, Aug. 2012.

[23]   S. Wang, S. Niu, J. Yang, L. Lin, Z. L. Wang, and W. E. T. Al, "of Vibration Amplitude Using a Contact-Mode Freestanding Triboelectric Nanogenerator," no. Xx, 2014.

[24]   Z.-H. Lin, G. Cheng, X. Li, P.-K. Yang, X. Wen, and Z. Lin Wang, "A multi-layered interdigitative-electrodes-based triboelectric nanogenerator for harvesting hydropower," *Nano Energy*, vol. 15, pp. 256–265, 2015.

[25]   K. Y. Lee, J. Chun, J.-H. Lee, K. N. Kim, N.-R. Kang, J.-Y. Kim, M. H. Kim, K.-S. Shin, M. K. Gupta, J. M. Baik, and S.-W. Kim, "Hydrophobic sponge structure-based triboelectric nanogenerator.," *Adv. Mater.*, vol. 26, no. 29, pp. 5037–42, Aug. 2014.

[26]   Q. Liang, X. Yan, X. Liao, S. Cao, S. Lu, X. Zheng, and Y. Zhang, "Integrated active

sensor system for real time vibration monitoring.," *Sci. Rep.*, vol. 5, p. 16063, Jan. 2015.

[27]   Y. Fu, X. Cai, H. Wu, Z. Lv, S. Hou, M. Peng, X. Yu, and D. Zou, "Fiber supercapacitors utilizing pen ink for flexible/wearable energy storage.," *Adv. Mater.*, vol. 24, no. 42, pp. 5713–8, Nov. 2012.

[28]   L. Kou, T. Huang, B. Zheng, Y. Han, X. Zhao, K. Gopalsamy, H. Sun, and C. Gao, "Coaxial wet-spun yarn supercapacitors for high-energy density and safe wearable electronics.," *Nat. Commun.*, vol. 5, p. 3754, Jan. 2014.

[29]   Q. Liang, X. Yan, X. Liao, S. Cao, X. Zheng, H. Si, S. Lu, and Y. Zhang, "Multi-unit hydroelectric generator based on contact electrification and its service behavior," *Nano Energy*, vol. 16, pp. 329–338, Sep. 2015.

[30]   Y. Mao, D. Geng, E. Liang, and X. Wang, "Single-electrode triboelectric nanogenerator for scavenging friction energy from rolling tires," *Nano Energy*, vol. 15, pp. 227–234, Jul. 2015.

[31]   J. H. Lee, R. Hinchet, S. K. Kim, S. Kim, and S.-W. Kim, "Shape memory polymer-based self-healing triboelectric nanogenerator," *Energy Environ. Sci.*, vol. 8, no. 12, pp. 3605–3613, Nov. 2015.

[32]   Z. L. Wang, "Triboelectric nanogenerators as new energy technology for self-powered systems and as active mechanical and chemical sensors.," *ACS Nano*, vol. 7, no. 11, pp. 9533–57, Nov. 2013.

[33]   C. M. Zierhofer and E. S. Hochmair, "Geometric approach for coupling enhancement of magnetically coupled coils.," *IEEE Trans. Biomed. Eng.*, vol. 43, no. 7, pp. 708–14, Jul.

1996.

[34] Z. Duan, Y.-X. Guo, and D.-L. Kwong, "Rectangular coils optimization for wireless power transmission," *Radio Sci.*, vol. 47, no. 3, p. n/a-n/a, Jun. 2012.

[35] M. Fareq, M. Fitra, M. Irwanto, H. S. Syafruddin, N. Gomesh, S. Farrah, and M. Rozailan, "Solar wireless power transfer using inductive coupling for mobile phone charger," in *2014 IEEE 8th International Power Engineering and Optimization Conference (PEOCO2014)*, 2014, pp. 473–476.

CHAPTER - 5

Microcrystalline Cellulose Ingrained Polydimethylsiloxane Triboelectric Nanogenerator as a Self-Powered Locomotion Detector

Graphical overview
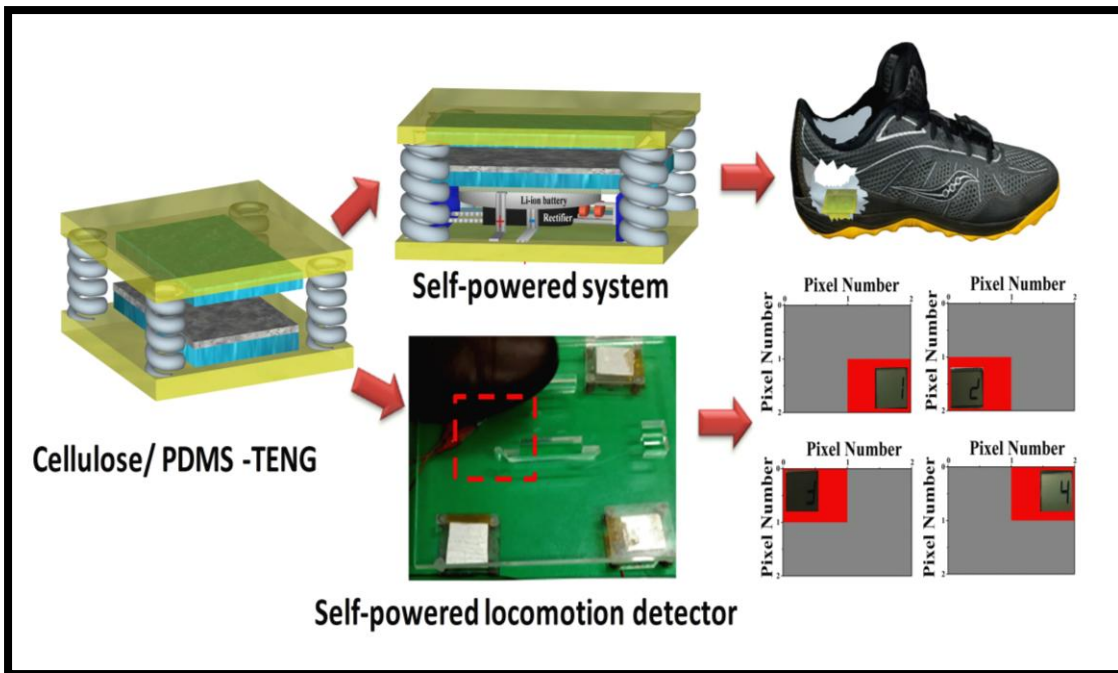
Highlights

- ➤ Scavenging of ambient dissipated mechanical energy addresses the limitations of conventional batteries by providing an auxiliary voltaic power source, and thus has significant potential for self-powered and wearable electronics

- ➤ Here, Cellulose/polydimethylsiloxane (PDMS) triboelectric nanogenerator (C-TENG) based on the contact and separation mode between a cellulose/PDMS composite film and an aluminium electrode

- ➤ The device fabricated with a composite film of 5 wt% generates an open circuit voltage of 28 V and a short circuit current of 2.8 µA with an instantaneous peak power of 576 µW

- ➤ The C-TENG was systematically studied and demonstrated to be a feasible power source that can commute instantaneous operation of LEDs and act as a self-powered locomotion detector for security applications

- ➤ The C-TENG can also be used as a wearable power source with an in-built lithium ion battery charging circuit during a range of human motion

5.1. Introduction

Rapid development in the field of triboelectric nanogenerators has led to a revolution in scavenging different mechanical energy sources. A number of methods of electricity generation, such as piezoelectricity,[1]–[6] and thermoelectric[7], [8] and photoelectric effects,[9] have been investigated; however, triboelectric nanogenerators (TENGs)[10]–[14] are a recent technology attracting attention as a next-generation energy harvesting system. Many attractive features, such as eco-friendliness and simple and reliable technology, have led to a research focus on smart energy harvesting using TENGs.

Z. L. Wang discussed the potential of energy harvesting from various sources such as human activity,[15], [16] wind,[17] vibration[18] and water[19]. Other studies, such as those by S. W. Kim,[20] H. Zhang and[10] Y. Zhang[21], have described valuable innovations in TENG and self-powered devices. Several recent investigations on biocompatible and biodegradable materials have led to increased demand in the field of eco-friendly energy harvesting. Hence, this study is based on the coupled effects of contact electrification and electrostatic induction for scavenging biomechanical energy by utilizing eco-friendly contact materials.

Here, we present an innovative design for harvesting biomechanical energy via a bio-compatible composite material called cellulose/ polydimethylsiloxane (PDMS). Both cellulose and PDMS are bio-compatible, electricity generation occurs during vertical contact and separation of these layers between the cellulose/PDMS film and an aluminum electrode. A cellulose/PDMS triboelectric nanogenerator device (C-TENG) fabricated with a composite film of 5 wt% generates an open circuit voltage of 28 V and a short circuit current of 2.8 μA with a peak power of 576 μW at a mechanical force of 32.16 N. Finally, the potential of the device as a

self-powered locomotion detector for identifying human motion and as a self-powered charging unit for recharging a Li-ion battery is demonstrated. Owing to its compact size and portability, this study opens up a new approach in the field of commercializing TENGs for future wearable applications.

5.2. Experimental methods

5.2 .1. Fabrication process of cellulose/PDMS film

Commercial PDMS (Sylgard 184; Dow Corning Corporation, Midland, MI, USA) was used as an epoxy resin. Microcrystalline cellulose (cellulose powder; Sigma Aldrich, St. Louis, MO, USA) was dispersed to form a polymer film, using a gel-casting technique. A schematic figure illustrating the fabrication of the cellulose/PDMS film is shown in **Figure 5.1**. Initially, the PDMS monomer and its corresponding cross-linker were mixed thoroughly at a mass ratio of 10:1 as shown in **Figure 5.1 (a)**. Then, cellulose powder was slowly added to the PDMS solution at different weight percentages (1, 3, 5 wt%) and stirred for 20 min by simple mechanical agitation as shown in **Figure 5.1 (b)**. The solution was then transferred to a Petri dish, which was initially attached with a layer of sandpaper to create irregular surface roughness as shown in **Figure 5.1 (c)**. After 10 min of degassing with the aid of a vacuum pump, the sandpaper template was cured at 70°C for 40 min and next, semi-solidified cellulose/PDMS was removed from the oven and an aluminum film was attached onto the smooth surface as shown in **Figure 5.1 (d, e)**. The film was cured again for 30 min and the cellulose/PDMS film was then peeled off the sandpaper template as shown in **Figure 5.1 (f)**. Digital photographs of the pure PDMS and cellulose/PDMS films of different weight ratios with surface roughness are shown in as shown in **Figure 5.1 (g)**

제주대학교 중앙도서관
JEJU NATIONAL UNIVERSITY LIBRARY
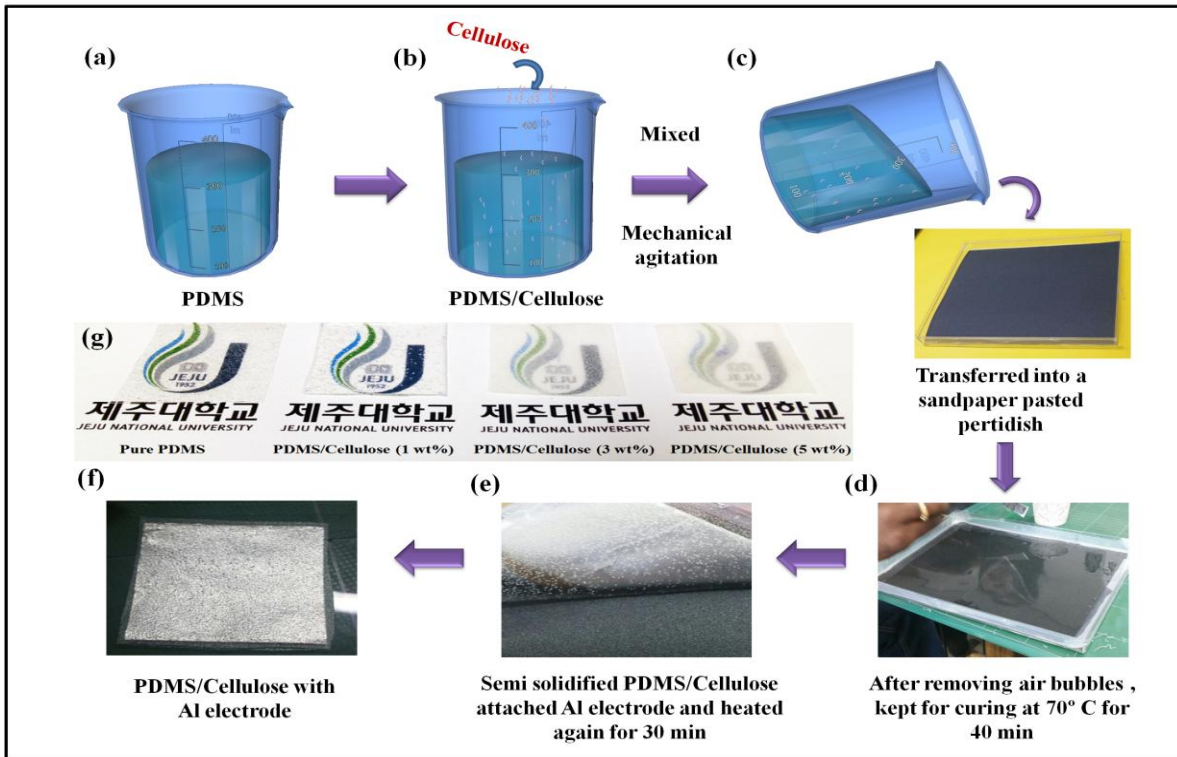
Figure 5.1 Cellulose/PDMS film fabrication. (a) PDMS monomer and its corresponding cross-linker, (b) cellulose powder added to the PDMS solution at different weight percentages. (c) Transferred to a Petri dish, (d) degassing with the aid of a vacuum pump, (e) semi-solidified cellulose/PDMS and attach electrode, (f) fully cured PDMS film and (g) cellulose/PDMS films of different weight ratios.

5.2 .2. Fabrication of the C-TENG

To fabricate the C-TENG, an acrylic sheet was selected as a supporting substrate due to its excellent mechanical strength, low cost and light weight. A laser cutter was used to cut the acrylic sheet into two pieces with dimensions of $50 \times 50 \times 3$ mm as shown in **Figure 5.2 (a)**.

제주대학교 중앙도서관
JEJU NATIONAL UNIVERSITY LIBRARY
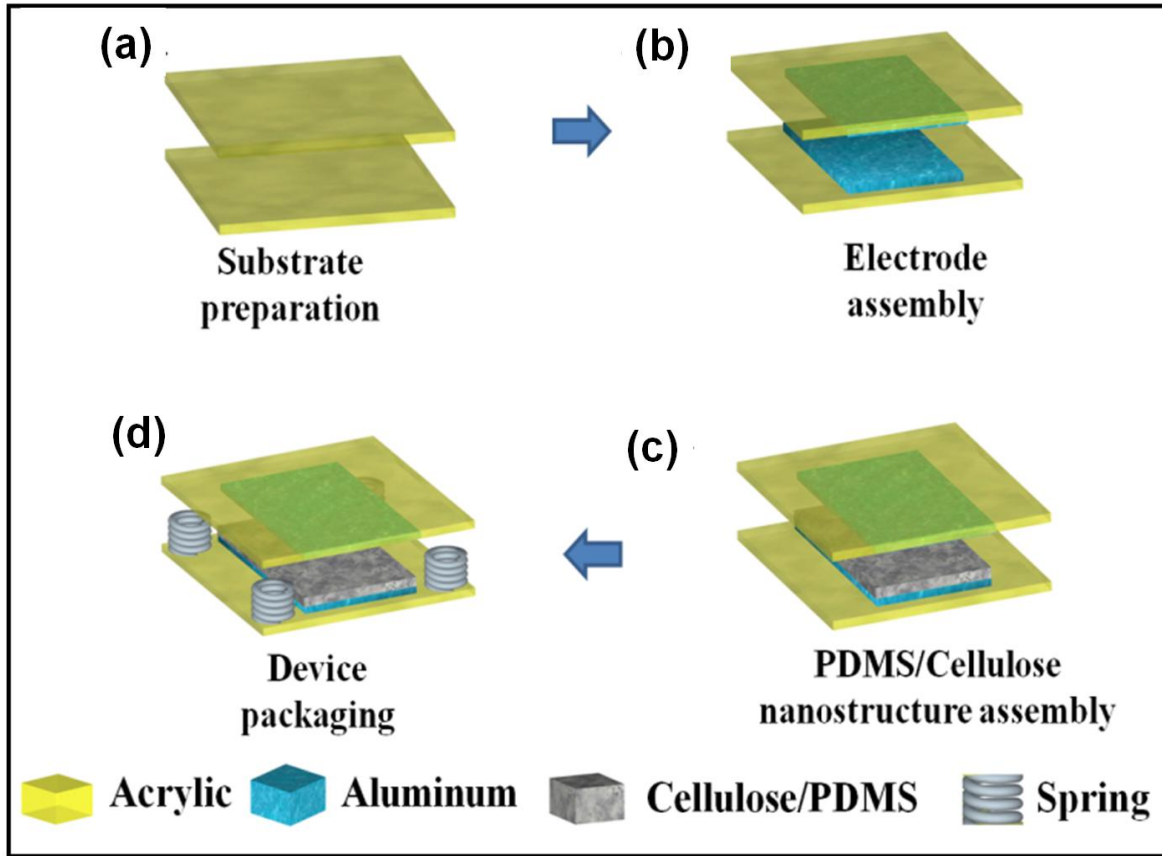
Figure 5.2 (a) Laser cut acrylic sheet, (b) electrode assembly, (c) assembling PDMS/Cellulose film and (d) device packing.

A layer of aluminum film of dimensions 30×30 mm was attached to the acrylic substrate as the electrode. Cellulose/PDMS film of dimensions of 30×30 mm was assembled on the bottom acrylic substrate as shown in **Figure 5.2 (b, c)**. To connect the top and bottom substrates, four springs were docked with a gap of 10 mm between the two plates as shown in **Figure 5.2 (d)**.

5.3. Measurement system

A JEOL JSM-6700F field emission-scanning electron microscope (FE-SEM) was used for morphological analysis of surface-modified cellulose/PDMS films. For quantitative measurement of the electrical outputs of the C-TENG, an external force was applied using a

linear motor (E1100), and a custom-made Faraday's cage was installed to cover the device during measurement. The output current and voltage of the device were measured using a picoammeter (Keithley 6485) and a nanovoltmeter (Keithley 2182A), respectively. A logical circuit was designed and constructed on a breadboard for real-time analysis and demonstrations of self-powered applications.

5.4. Results and discussion

5.4.1. C-TENG design

The 3D schematic representation of the cellulose TENG has a multilayer architecture as shown in **Figure 5.3 (a)**. The fabrication process of the C-TENG comprises an acrylic sheet as a supporting substrate, Al film as an electrode for electrical measurements and a layer of cellulose/PDMS film adhered to the bottom. **Figure 5.3 (b)** presents a digital photograph of the C-TENG.
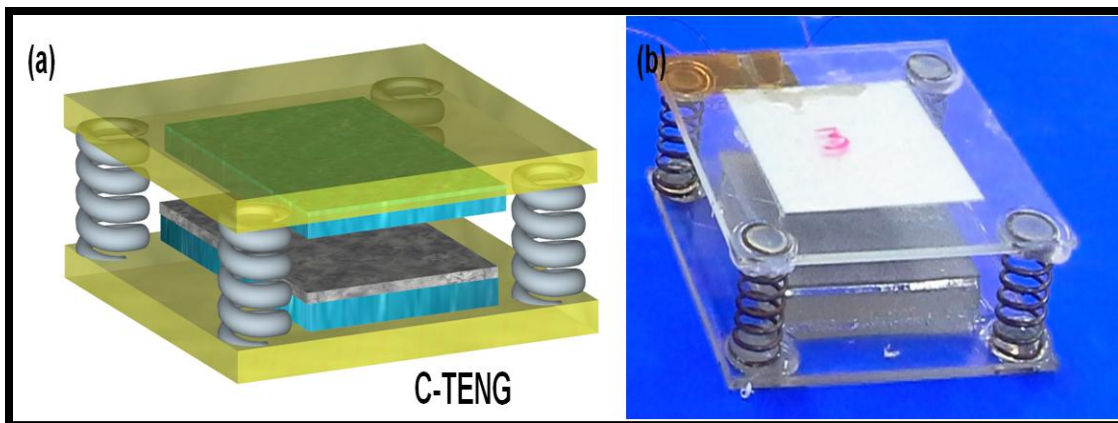
Figure 5.3 (a) 3D schematic illustration of the C-TENG and (b) Photograph of a fabricated C-TENG, with dimensions of $50 \times 50 \times 30$ mm.

5.4.2. Structural characterization

A 3D illustration of the chemical structure of cellulose is shown in Figure 1(b). A chain of multiple hydroxyl groups with the glucose from one chain structure hydrogen-bonding with oxygen atoms on the same, holding the chains firmly together, can be seen, leading to the formation of micro-fibrils. The vibrational properties of PDMS and cellulose/PDMS were analyzed using 514-nm-wavelength excited Raman spectroscopy. Figure 1(c) shows the Raman spectrum for the pure PDMS[22] and cellulose/PDMS.[23] The spectrum (in red) confirms the presence and formation of cellulose/PDMS, and the inset shows an enlarged view.
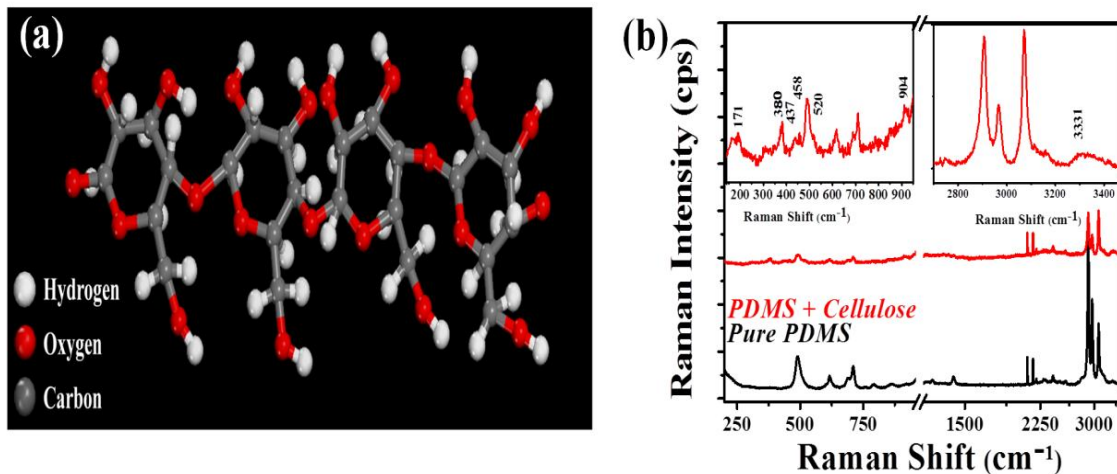
Figure 5.4 (a) 3D illustration of the chemical structure of cellulose. (b) Raman spectroscopic results for pure PDMS and cellulose/PDMS film.

5.4.3. Morphology analysis of negative charged layer

A top view field emission scanning electron microscope (FE-SEM) image of the cellulose/PDMS with surface roughness and its 3D view are shown in **Figure 5.5 (a ,b)**, demonstrating an average height of about 191 μm. FE-SEM image justifies the incorporation of cellulose in PDMS matrix and also the irregular structures on the surface of the PDMS.

92
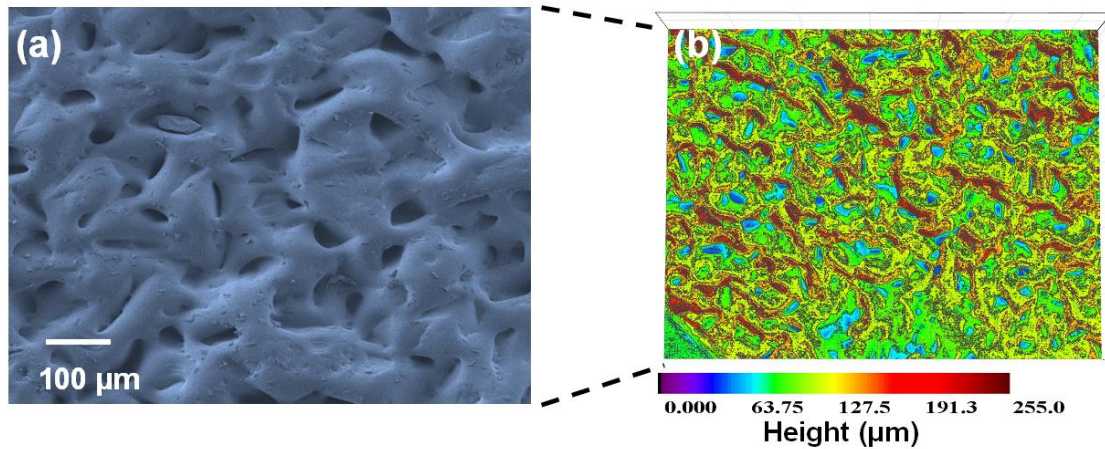
Figure 5.5 (a) Top view FE-SEM image of cellulose/PDMS and (b) 3D view.

5.4.4. Working mechanism of C-TENG

The working mechanism of the C-TENG is based on contact electrification[11], [24] between the irregular micro-structured cellulose/PDMS film as the bottom substrate and Al film as the top substrate. Cellulose/PDMS and Al film were chosen due to their triboelectric charge difference and ability to attract and retain electrons. A detailed description of the triboelectric effect between these films is shown in **Figure 5.6**. Initial position of the upper Al electrode and cellulose/PDMS surface with Al electrodes separated by air-gap is shown in **Figure 5.6 (a)**. An external force causes interaction between the upper electrode and the cellulose/PDMS surface, inducing positive triboelectric charges on the upper Al electrode and negative triboelectric charges on the cellulose/PDMS surface and release of the external force causes electrons to flow from the upper Al electrode to the bottom electrode through an external circuit is shown in **Figure 5.6 (b, c)**. In the equilibrium state, where the charge carriers are distributed on both sides of the layers and electrons are driven back owing to the applied external force, reducing the inductive charge on the Al electrode **Figure 5.6 (d, e)**.

제주대학교 중앙도서관
JEJU NATIONAL UNIVERSITY LIBRARY

(a) Initial state

(b) Pressing

(e) Pressing

(c) Releasing

(d) Equilibrium State
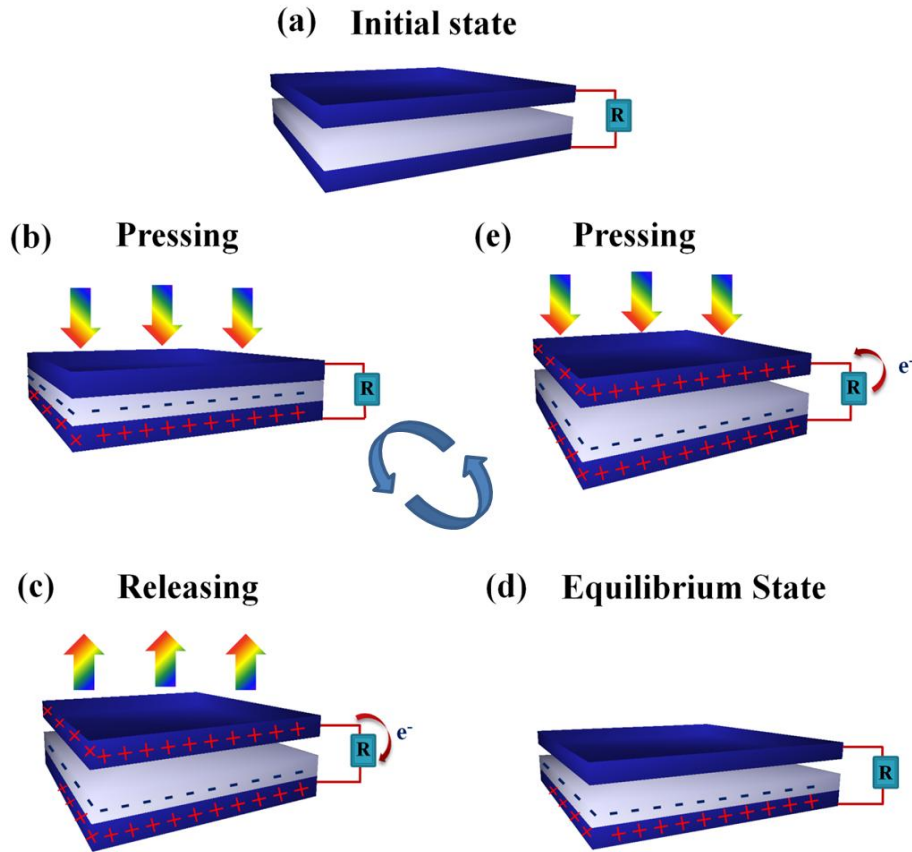
Figure 5.6 (a) Initial stage of the upper layer, (b) an external applied force causes the interaction, (c) release of the external force causes electrons to flow, (d) equilibrium state, and (e) electrons are driven back.

5.4.5. Electrical analysis of SS-TENG

First, the electrical response of the C-TENG with an external cyclic compressive force of around 32.16 N was investigated, which was applied onto the upper substrate of the device, so that the upper plate was pushed periodically into contact with the bottom substrate. All devices had a working area of 9 cm^2 (3 × 3 cm). Comparisons of the open circuit voltage (V_{oc}) and short circuit current (I_{sc}) between the pure PDMS and cellulose/PDMS (1, 3, 5 wt%) are shown in **Figure 5.7 (a-b)**, respectively. The peak output voltage and current for pure PDMS were about 9 V and 0.8 µA, respectively, while the device fabricated with 5 wt% cellulose/PDMS showed

electrical outputs of about 28 V and 2.8 μA. To optimize effective energy harvesting, we varied the concentration of cellulose in the PDMS matrix. The addition of a large amount of cellulose (>7 wt%) caused agglomeration and restricted the formation of a uniform film. An optimal cellulose ratio of 5 wt% was chosen for further studies, and devices for measurement were fabricated using this ratio. **Figure 5.7 (c-d)** shows the measured V_{oc} and I_{sc} values of the C-TENG. The value of V_{oc} reached 28 V and the corresponding value of I_{sc} reached 2.8 μA during the cyclic contact and separation process. Several V_{oc} and I_{sc} cycles are shown in an enlarged view in **Figure 5.7 (c-d)**.
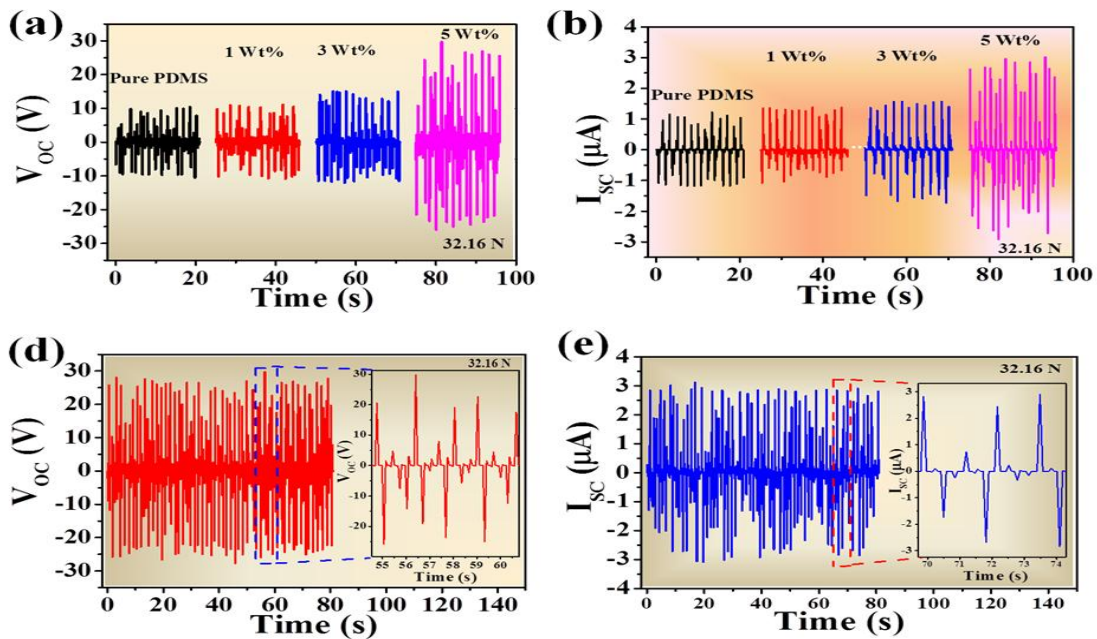
Figure 5.7 Electrical measurement results for a C-TENG with a working area of 6 cm². (a) Voltage and (b) current profiles using pure PDMS and 1, 3 and 5 wt% cellulose/PDMS at an external force of 32.16 N. (c) Output voltage and (d) current using 5 wt% cellulose/PDMS as the contact electrification material at an external force of 32.16 N. Insets of (c) and (d): enlarged view of a few cycles of voltage and current.

95

It is essential to obtain the optimum output power from the fabricated device for real-time application. To obtain the maximum output power, we performed a load matching investigation with a wide range of load resistors (100 Ω to 5 GΩ). For values of external load resistance up to 10 MΩ, the average output peak current showed no decrement. This illustrates that the C-TENG is applicable as a steady current source.[25], [26] With increasing external load resistance, the current amplitude decreased owing to ohmic loss; at the same time, V_{oc} across the load resistor increased, as shown in **Figure 5.8 (a)**.
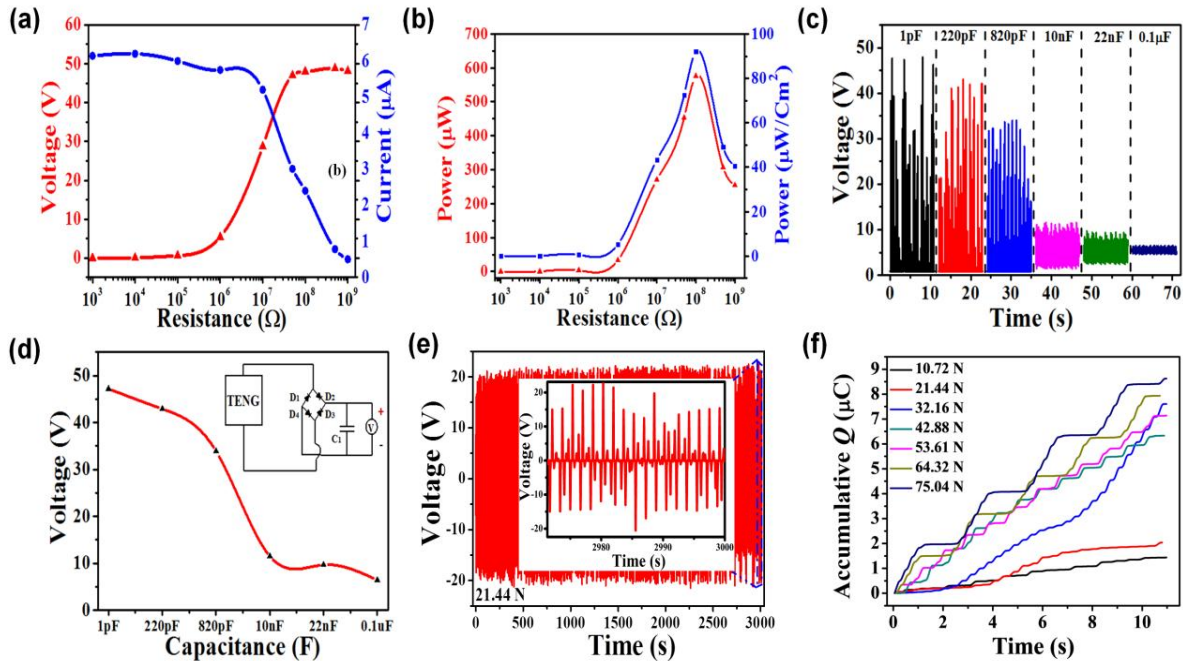
Figure 5.8 Electrical performance of C-TENG as an energy harvester for an external force. (a) Output voltage and current for an external load matching test with 5 wt% C-TENG and (b) its corresponding output power and power density. (c-d) Charging process of capacitors, six different load capacitances from 1 pF to 0.1 μF. (d) Inset shows the circuit diagram used for charging the capacitor. (e) The output voltage of the C-TENG with an external force for 3000 sec as an endurance test. The inset shows an enlarged view of the output voltage signal at the end of the endurance test. (f) The accumulative charge developed by the C-TENG under different external forces from 10.72 to 75.04 N.

The instantaneous peak power of the C-TENG was maximized at an external load resistance of 100 MΩ, corresponding to peak power of 576 μW and power density of 64 μW/cm^2

(measured under a cycled compressive force of 32.16 N at a frequency of 1 Hz), as shown in **Figure 5.8 (b)**. To demonstrate the charging process of the capacitor, six different load capacitances from 1 pF to 0.1 µF were measured under a cycled compressive force of 32.16 N at a frequency of 1 Hz, as shown in **Figure 5.8 (c, d)**. The maximum storing voltage decreased with increasing load capacitance and an increase in load capacitance (0.1 µF) results in a saturation voltage of 6.5 V. The right inset of **Figure 5.8 (d)** shows the circuit diagram of the full wave bridge rectifier with a load capacitor. An endurance test was performed by repeatedly pressing and releasing the C-TENG with a cycled compressive force for 3600 cycles. The electrical results indicate the reliability of the C-TENG even over prolonged cycles of operation, with negligible changes in V_{oc}, as shown in **Figure 5.8 (e)**. The inset shows an enlarged view of the output voltage signal during the final stage of the endurance test.

The charge output can be derived from the differentiated electrical output of the C-TENG. The alternating electrons flowing across the electrodes can be rectified using a bridge rectification circuit, which leads to accumulative induced charges, as shown in **Figure 5.8 (f)**. Under an external force of 75 N, the C-TENG generated a charge output of 8.5 µC in 10 seconds with 2 µC per cycle. During a small external force, the irregular surface roughness caused by the cellulose/PDMS hinders full contact between the upper electrode, leaving some regions untouched. The charge accumulation increased with increasing external force, due to increasing contact area at larger forces reducing voids or gaps due to the irregular surface roughness.[11], [16], [25], [27]

5.4.6. Low power electronics driving analysis

To demonstrate that the device can drive low-power electronic devices efficiently, the generated AC signal was converted to a unidirectional pulse using a full-wave bridge rectifier

(DF06G). The rectified pulsating DC output directly lit up an array of 120 green and blue LEDs (60 green and 60 blue of 3.0–3.4 V, 20 mA max) and 40 (25 red and 25 white 3.0–3.4 V, 20 mA max) assembled in series on a breadboard, when an external mechanical force of 32.16 N was applied on the upper plate of the C-TENG. **Figure 5.9 (a-d)** shows the instantaneous lighting of an array LEDs assembled in series on a breadboard, this study clearly shows that the C-TENG can be used as a direct power source for low-power electronic devices.
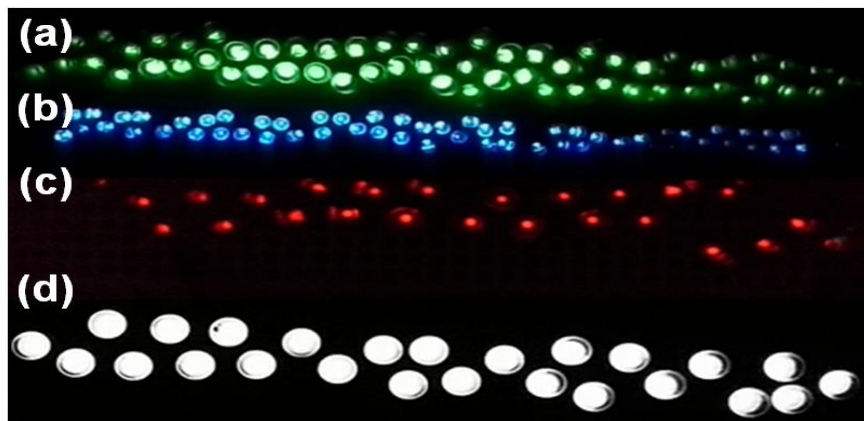
Figure 5.9 The instantaneous lighting of an array LEDs. (a) green, (b) blue, (c) red, and (d) white LEDs assembled in series.

5.4.7. C-TENG for Self-powered applications

5.4.7.1. Self-powered locomotion detector

Here, a self-powered locomotion detector is proposed that can be used in a home security system to identify the location of a moving object on the floor, based on electrical output signals obtained through contact and separation of two triboelectric materials.[28] As a simple construction, four individual C-TENG devices were assembled on the ground in a square pattern at equal distances, and covered with a hard transparent acrylic sheet. When a human stepped on

the first device, electrical output energy was generated across the C-TENG. This output was connected to a logic-circuit to drive a monochrome LCD displaying the location of the moving object, as shown in Figure 5(a). Here, we designed a simple logical circuit using commercially available capacitors (C_1 = 10 nF, C_2 = 47 pF) connected across a full wave bridge rectifier (DF06G) output. The logical circuit and operation of the multi-unit C-TENG as a self-powered device for displaying the location of a moving object location were demonstrated experimentally.

When a person moves on the C-TENG devices along the path: $1 \rightarrow 2$, $2 \rightarrow 3$, $3 \rightarrow 4$, the V_{oc} of each device rises to the peak value (20 V) and then falls, as shown in Figure 5(b). The evolution of the peak value of V_{oc} occurs when the person steps on the centre of a C-TENG (the evolution of the lower peak is due to the rectification of the AC signal obtained from the C-TENG). A map of the moving object was plotted to identify the exact location of the object, as shown in Figure 5(c). A digital photograph of the monochrome LCD displaying the location code (device code) is shown as an inset for each location. The above demonstration clearly indicates that the C-TENG can be used as a self-powered locomotion detector for home security applications.
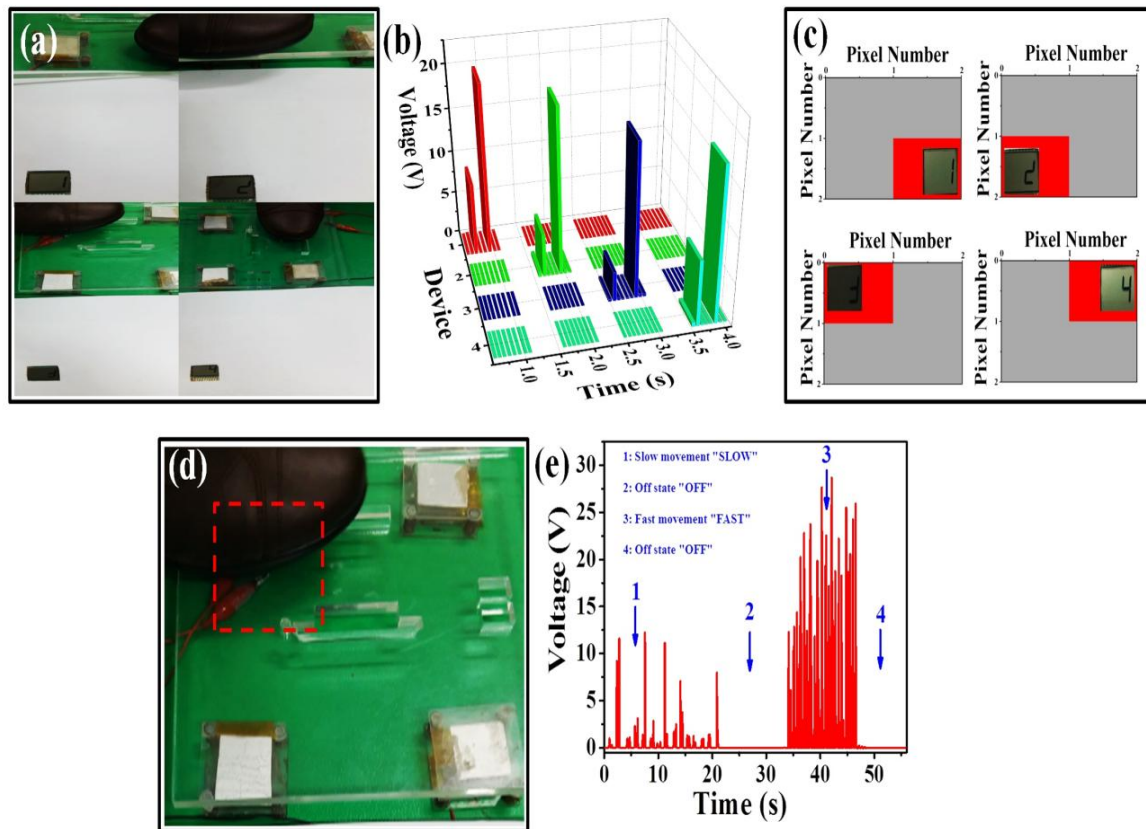
Figure 5.10 Application of the C-TENG as a self-powered locomotion detector and floor energy harvester. (a) Illustration of self-powered locomotion detector identifying the moving object location and displaying the object location code in an LCD display. (b) Measured open circuit voltage of the C-TENG when a human moves as follows: 1 → 2, 2 → 3, 3 → 4. (c) Mapping figure obtained from the open circuit voltage of the C-TENG when a human moves as follows: 1 → 2, 2 → 3, 3 → 4. (d) Photograph of the C-TENG as a floor energy harvester. (e) Open circuit voltage obtained during human motion.

The main purpose of the C-TENG device is to scavenge mechanical energy; in this regard, we investigated energy harvesting from a single device during human motion. A digital photograph of a human stepping on a C-TENG is shown in **Figure 5.10 (d)**. When the person stepped up and down slowly (denoted by "SLOW"), V_{oc} was generated; during the rest state ("OFF"), there was no V_{oc} generation, and during the fast stepping movement ("FAST"), there was generation of a V_{oc} signal with an increase in V_{oc}, as shown in **Figure 5.10 (e)**. Here, a

100

change in the amplitude of the V_{oc} signal with respect to the speed of human motion was observed. This demonstration shows that the C-TENG is fully capable of deployment as a floor energy harvester for converting human motion into high-end electrical energy.

5.4.7.2.   C-TENG based self-powered system

To develop the C-TENG as a commercial self-powered system and considering future uses in portable and wearable applications, we fabricated an inbuilt charging unit with a simple charging circuit. **Figure 5.11 (a, b)** shows a schematic and photograph (inset) of the top view of the charging unit and a cross-sectional view of the C-TENG as a self-powered system. The design of the C-TENG with the inbuilt charging unit had dimensions of $50 \times 50 \times 30$ mm. The charging unit consists of three parts: a full wave bridge rectifier, capacitors and a Li-ion battery, and the C-TENG were used as a power source, as shown in **Figure 5.11 (c)**. The size of the C-TENG was less than 100 mm and it could be easily embedded inside the heel of a shoe for real-time application, as shown in the schematic diagram in the inset of **Figure 5.11 (c)**. This can be used to harvest energy during physical activity such as running, walking or jumping. A linear motor for periodic motion was used to examine the electrical properties of the self-powered charging unit. A commercial Li-ion battery (Maxell CR 2032) was charged using the C-TENG from 1.85 to 2.8 V within 2500 sec (at 32.16 N external force), as shown in **Figure 5.11 (d)**.
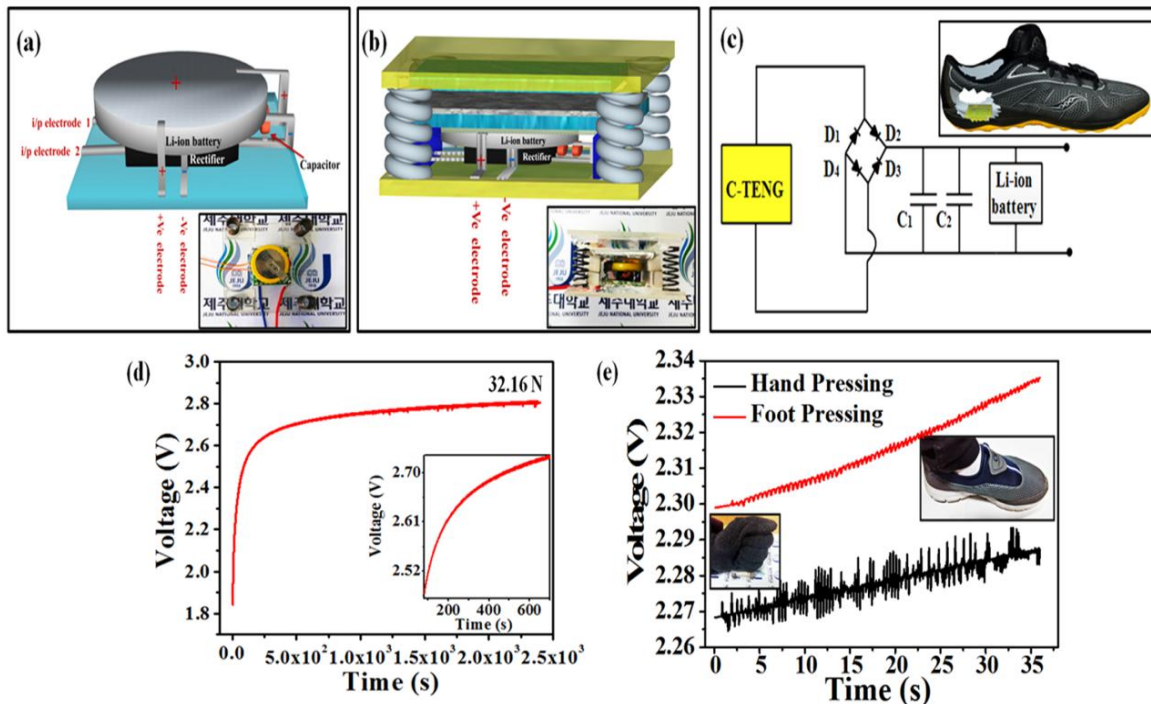
Figure 5.11. Niche application of C-TENG as a self powered system. (a,b) Schematic diagram and photograph of inbuilt rectifier and Li-ion battery of the C-TENG. (c) Circuit diagram used for charging Li-ion battery, inset shows the schematic representation of C-TENG embedded inside a shoe. (d) Charging curves of the Li-ion battery embedded inside the C-TENG, inset shows the enlarged view of charging curve. (e) The C-TENG used for harvesting the human motion energy and charging the Li-ion battery.

This experiment validates the potential of the C-TENG for charging a Li-ion battery by scavenging mechanical energy. To corroborate the battery charging effectiveness with human activity, the C-TENG was continuously pressed by hand and foot, as shown in the inset of Figure 6(e). For a charging time of 30 s, both hand and foot press motions resulted in charging of the Li-ion battery, as shown in Figure 6(e). These results demonstrate the unique properties of the C-TENG as a self-powered system, which can be used over a wide range of biomechanical energy harvesting applications as a portable and anchored device. Furthermore, this approach creates an opening for commercialization of TENG products.

5.5.   Conclusion

A C-TENG device was fabricated for harvesting mechanical and biomechanical energy to drive low-power wearable electronics continually during human motion. The proposed C-TENG was developed using eco-friendly materials that are clean and safe for wearable and portable applications. Electricity was generated from vertical contact and separation between a cellulose/PDMS film and an aluminum electrode, and the C-TENG can be used as a self-powered locomotion detector or a self-powered charging unit. Other competitive features, including a simple fabrication process, low fabrication cost and good electrical performance, indicate that this represents significant progress in the field of self-powered devices. This study opens up a new approach in the field of commercializing TENGs for future wearable applications.

5.6.   References

[1]   N. R. Alluri, B. Saravanakumar, and S.-J. Kim, "Flexible, Hybrid Piezoelectric Film (BaTi(1-x)Zr(x)O3)/PVDF Nanogenerator as a Self-Powered Fluid Velocity Sensor.," *ACS Appl. Mater. Interfaces*, vol. 7, no. 18, pp. 9831–40, May 2015.

[2]   K. Y. Lee, M. K. Gupta, and S.-W. Kim, "Transparent flexible stretchable piezoelectric and triboelectric nanogenerators for powering portable electronics," *Nano Energy*, Nov. 2014.

[3]   R. Yang, Y. Qin, L. Dai, and Z. L. Wang, "Power generation with laterally packaged piezoelectric fine wires.," *Nat. Nanotechnol.*, vol. 4, no. 1, pp. 34–9, Jan. 2009.

[4]   B. Saravanakumar, S. Soyoon, and S.-J. Kim, "Self-powered pH sensor based on a flexible organic-inorganic hybrid composite nanogenerator.," *ACS Appl. Mater. Interfaces*, vol. 6, no. 16, pp. 13716–23, Aug. 2014.

[5]   B. Saravanakumar, K. Thiyagarajan, N. R. Alluri, S. SoYoon, K. Taehyun, Z.-H. Lin, and S.-J. Kim, "Fabrication of an eco-friendly composite nanogenerator for self-powered photosensor applications," *Carbon N. Y.*, vol. 84, pp. 56–65, Apr. 2015.

[6]   A. Ramadoss, B. Saravanakumar, S. W. Lee, Y.-S. Kim, S. J. Kim, and Z. L. Wang, "Piezoelectric-driven self-charging supercapacitor power cell.," *ACS Nano*, vol. 9, no. 4, pp. 4337–45, Apr. 2015.

[7]   R. Venkatasubramanian, E. Siivola, T. Colpitts, and B. O'Quinn, "Thin-film thermoelectric devices with high room-temperature figures of merit.," *Nature*, vol. 413, no. 6856, pp. 597–602, Oct. 2001.

[8]   L. E. Bell, "Cooling, heating, generating power, and recovering waste heat with thermoelectric systems.," *Science*, vol. 321, no. 5895, pp. 1457–61, Sep. 2008.

[9]   M. Grätzel, "Photoelectrochemical cells.," *Nature*, vol. 414, no. 6861, pp. 338–44, Nov. 2001.

[10]   B. Meng, W. Tang, Z. Too, X. Zhang, M. Han, W. Liu, and H. Zhang, "A transparent single-friction-surface triboelectric generator and self-powered touch sensor," *Energy Environ. Sci.*, vol. 6, no. 11, p. 3235, Oct. 2013.

104

[11] J. Chun, J. W. Kim, W. Jung, C.-Y. Kang, S.-W. Kim, Z. L. Wang, and J. M. Baik, "Mesoporous pores impregnated with Au nanoparticles as effective dielectrics for enhancing triboelectric nanogenerator performance in harsh environments," *Energy Environ. Sci.*, vol. 8, no. 10, pp. 3006–3012, Oct. 2015.

[12] Q. Liang, X. Yan, Y. Gu, K. Zhang, M. Liang, S. Lu, X. Zheng, and Y. Zhang, "Highly transparent triboelectric nanogenerator for harvesting water-related energy reinforced by antireflection coating.," *Sci. Rep.*, vol. 5, p. 9080, Jan. 2015.

[13] P. Bai, G. Zhu, Z. H. Lin, Q. Jing, J. Chen, G. Zhang, J. Ma, and Z. L. Wang, "Integrated multilayered triboelectric nanogenerator for harvesting biomechanical energy from human motions," *ACS Nano*, vol. 7, no. 4, pp. 3713–3719, 2013.

[14] A. Chandrasekhar, N. R. Alluri, V. Vivekananthan, Y. Purusothaman, and S.-J. Kim, "Sustainable Freestanding Biomechanical Energy Harvesting Smart Back Pack as a Portable-Wearable Power Source," *J. Mater. Chem. C*, 2017.

[15] W. Seung, M. K. Gupta, K. Y. Lee, K.-S. Shin, J.-H. Lee, T. Y. Kim, S. Kim, J. Lin, J. H. Kim, and S.-W. Kim, "Nanopatterned Textile-Based Wearable Triboelectric Nanogenerator.," *ACS Nano*, vol. 9, no. 4, pp. 3501–3509, Feb. 2015.

[16] T.-C. Hou, Y. Yang, H. Zhang, J. Chen, L.-J. Chen, and Z. Lin Wang, "Triboelectric nanogenerator built inside shoe insole for harvesting walking energy," *Nano Energy*, vol. 2, no. 5, pp. 856–862, Sep. 2013.

[17] R. Zhang, L. Lin, Q. Jing, W. Wu, Y. Zhang, Z. Jiao, L. Yan, R. P. S. Han, and Z.

L. Wang, "Nanogenerator as an active sensor for vortex capture and ambient wind-velocity detection," *Energy Environ. Sci.*, vol. 5, no. 9, p. 8528, Aug. 2012.

[18] S. Wang, S. Niu, J. Yang, L. Lin, Z. L. Wang, and W. E. T. Al, "of Vibration Amplitude Using a Contact-Mode Freestanding Triboelectric Nanogenerator," no. Xx, 2014.

[19] Z.-H. Lin, G. Cheng, X. Li, P.-K. Yang, X. Wen, and Z. Lin Wang, "A multi-layered interdigitative-electrodes-based triboelectric nanogenerator for harvesting hydropower," *Nano Energy*, vol. 15, pp. 256–265, 2015.

[20] K. Y. Lee, J. Chun, J.-H. Lee, K. N. Kim, N.-R. Kang, J.-Y. Kim, M. H. Kim, K.-S. Shin, M. K. Gupta, J. M. Baik, and S.-W. Kim, "Hydrophobic sponge structure-based triboelectric nanogenerator.," *Adv. Mater.*, vol. 26, no. 29, pp. 5037–42, Aug. 2014.

[21] Q. Liang, X. Yan, X. Liao, S. Cao, S. Lu, X. Zheng, and Y. Zhang, "Integrated active sensor system for real time vibration monitoring.," *Sci. Rep.*, vol. 5, p. 16063, Jan. 2015.

[22] Sung Chul Bae, † Hyunjung Lee, ‡ and Zhiqun Lin, and S. Granick*, "Chemical Imaging in a Surface Forces Apparatus: Confocal Raman Spectroscopy of Confined Poly(dimethylsiloxane)," 2005.

[23] M. Szymańska-Chargot, J. Cybulska, and A. Zdunek, "Sensing the Structural Differences in Cellulose from Apple and Bacterial Cell Wall Materials by Raman

and FT-IR Spectroscopy," *Sensors*, vol. 11, no. 12, pp. 5543–5560, May 2011.

[24] J. Chen, J. Yang, Z. Li, X. Fan, Y. Zi, Q. Jing, H. Guo, Z. Wen, K. C. Pradel, S. Niu, and Z. L. Wang, "Networks of triboelectric nanogenerators for harvesting water wave energy: a potential approach toward blue energy.," *ACS Nano*, vol. 9, no. 3, pp. 3324–31, Mar. 2015.

[25] G. Zhu, P. Bai, J. Chen, and Z. Lin Wang, "Power-generating shoe insole based on triboelectric nanogenerators for self-powered consumer electronics," *Nano Energy*, vol. 2, no. 5, pp. 688–692, Sep. 2013.

[26] G. Zhu, P. Bai, J. Chen, and Z. Lin Wang, "Power-generating shoe insole based on triboelectric nanogenerators for self-powered consumer electronics," *Nano Energy*, vol. 2, no. 5, pp. 688–692, 2013.

[27] P. Yang, Z. Lin, Z. L. Wang, K. C. Pradel, L. Lin, X. Li, X. Wen, J. He, M. Science, U. States, E. Engineering, M. Sciences, S. Arabia, B. Engineering, and C. Academy, "Paper-Based Origami Triboelectric," no. Xx, 2015.

[28] F.-R. Fan, L. Lin, G. Zhu, W. Wu, R. Zhang, and Z. L. Wang, "Transparent triboelectric nanogenerators and self-powered pressure sensors based on micropatterned plastic films.," *Nano Lett.*, vol. 12, no. 6, pp. 3109–14, Jun. 2012.

CHAPTER- 6
Sustainable Freestanding Biomechanical Energy Harvesting Smart Back Pack as a Portable-Wearable Power Source

Graphical overview
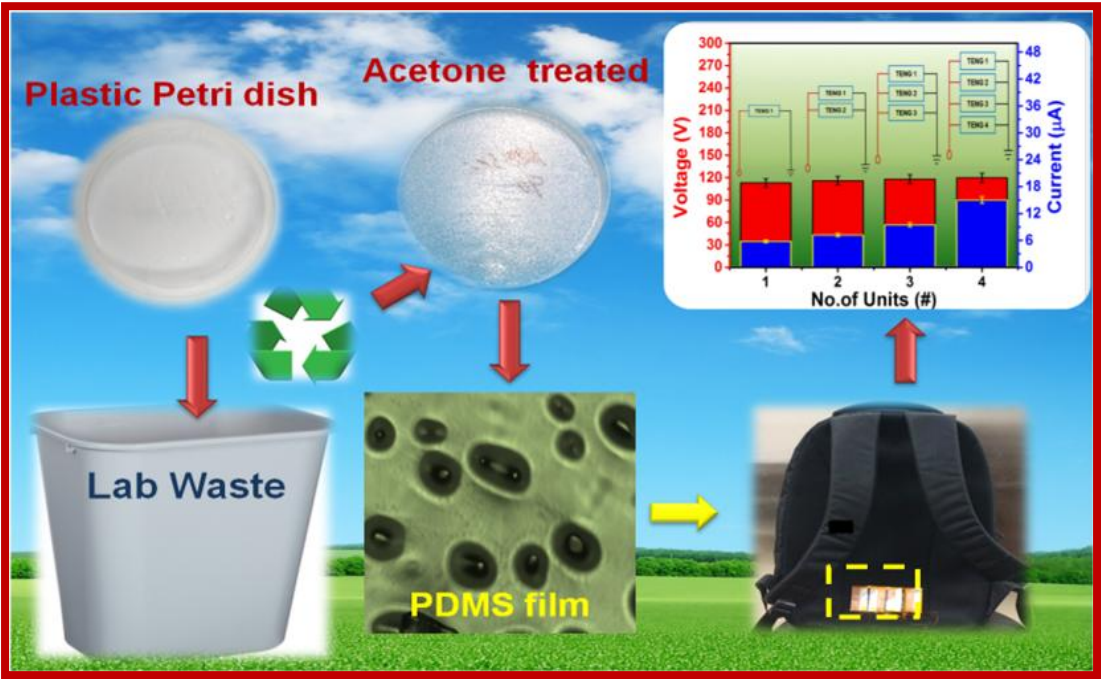
Highlights

➢ Wearable gadgets have attracted consumer attention, resulting in an abundance of research on the development of self-powered devices

➢ An innovative, cost-effective and eco-friendly freestanding smart backpack-triboelectric nanogenerator (SBP-TENG) is presented for scavenging bio-mechanical energy

➢ A new approach to creating irregular surfaces on polydimethylsiloxane (PDMS) film is demonstrated by recycling a plastic petri dish discarded after laboratory usage

➢ The SBP-TENG relies on contact and separation electrification between the PDMS film and the contact materials (wool, paper, cotton, denim and polyethylene)

➢ This study confirms that the SBP-TENG is an excellent technology for scavenging bio-mechanical energy, capable of driving a variety of low-power electronic devices such as Global Positioning System (GPS) systems, wearable sensors and flash lights

6.1. Introduction

The rapid development of wearable gadgets and smart devices has prompted a focus on energy harvesting techniques to power portable devices, such as smart watches, Global Positioning System (GPS) sensors and wearable cameras. Energy scavenging from human motion has attracted research interest due to its feasibility in the field of wearable electronics using soft elastomeric materials.[1]–[3] A number of electricity generation mechanisms, such as the photoelectric effect,[4] the piezoelectric effect[5]–[8] and the thermoelectric effect[9], [10] have been studied. Recently, triboelectric nanogenerators (TENGs)[11]–[16] have been developed based on the coupling of electrostatic induction[17], [18] and contact electrification,[19]–[21] and this is a promising technology for high energy conversion efficiency and cost-effective fabrication.[14], [21]

Professor Z. L. Wang first discovered the potential of TENGs for energy harvesting from various sources, such as wind,[22] water,[23] vibration[24] and human motion,[25] and their application as self-powered devices.[25] Other researchers, such as H. Zhang,[17] Y. Zhang[18], Z.H. Lin[26], [27] and S. W. Kim[28], [29], have developed innovative approaches in the TENG field. The invention of plastics was a turning point in societal development; however, this also leads to a rapid increase in environmental pollution caused by plastic products. Although high energy conversion nanogenerators have been developed, device fabrication should also focus on an eco-friendly approach that reduces the use of plastic and provides opportunities for waste plastic recycling during TENG production.

In this work, a sustainable smart backpack-triboelectric nanogenerator (SBP-TENG) is proposed as a platform for scavenging bio-mechanical energy using different contact materials. Here, a plastic petri dish discarded after laboratory use was recycled and its surface-modified

using acetone to create an irregular microstructure. This petri dish acted as a template for creating an irregular microstructure on PDMS film. In the proposed SBP-TENG, the generation of charge occurs during interactions between the surface-modified polydimethylsiloxane (PDMS) film and freestanding contact materials during various human motions. To study the energy harvesting performance of SBP-TENG quantitatively, its electrical output during contact and separation motion with different contact materials was analyzed. The SBP-TENG can also act as a real-time energy harvester by utilizing different human motions (walking, running and bending). Hence, a detailed investigation of human motion and the weight of the bag was performed to demonstrate the potential of the SBP-TENG as a bio-mechanical energy harvester. A multi-unit SBP-TENG was also investigated for scavenging bio-mechanical energy (with four SBP-TENG units fixed on the back side of a bag). In addition, the potential of the SBP-TENG as a self-powered emergency LED flashing light for use in emergency situations was also demonstrated. This study demonstrates a promising approach for portable, wearable and eco-friendly energy harvesting from human motion and its use in self-powered electronic applications.

6.2. Experimental methods

6.2.1. Surface treatment on the plastic petri dish

The base of the SBP-TENG was developed by recycling the plastic petri dish discarded from the laboratory. The petri dish was made of ABS polymer, which is a common thermoplastic polymer. ABS polymers are resistant to aqueous acids, alcohols, and concentrated hydrochloric acids but soluble in acetone, ketones, ethylene dichloride and esters. Hence, instead of disposing of the petri dish after a single use, its surface was modified using acetone as an etchant, and it

was used as a template to create irregular microstructures on a PDMS film. **Figure 6.1 (a)** shows a schematic representation of the surface-modification process on a plastic petri dish using acetone as an etchant. Initially, the petri dish was cleaned with ethanol and deionised water and then blow-dried with compressed nitrogen gas. Then, the petri dish was dipped into an acetone filled beaker and removed after a period of time (10, 30, 60, 90, 120 s); the etching rate was varied by use of different times, and resulted in irregular microstructures on the surface of petri dish. This surface-modified Petri dish was used as a template to create irregular surface roughness on the PDMS film. **Figure 6.1 (b)** shows the fabrication process of the PDMS film using a surface-modified petri dish. Initially, the PDMS monomer and its cross-linker were mixed (ratio of 10:1) and stirred using a magnetic stirrer for 20 min. Then the solution was degassed for 15 min with the aid of a vacuum pump and spin coated (500 rpm for 30 s) to a surface-modified petri dish. After spin coating, the petri dish was cured at 70º C for 40 min and removed from the oven, forming a PDMS layer. After cooling for 20 min at room temperature, the PDMS film was peeled off the petri dish, as shown in Figure **6.1 (b) (vi)**. The lower surface of the PDMS film retained the irregular microstructure from the petri dish.
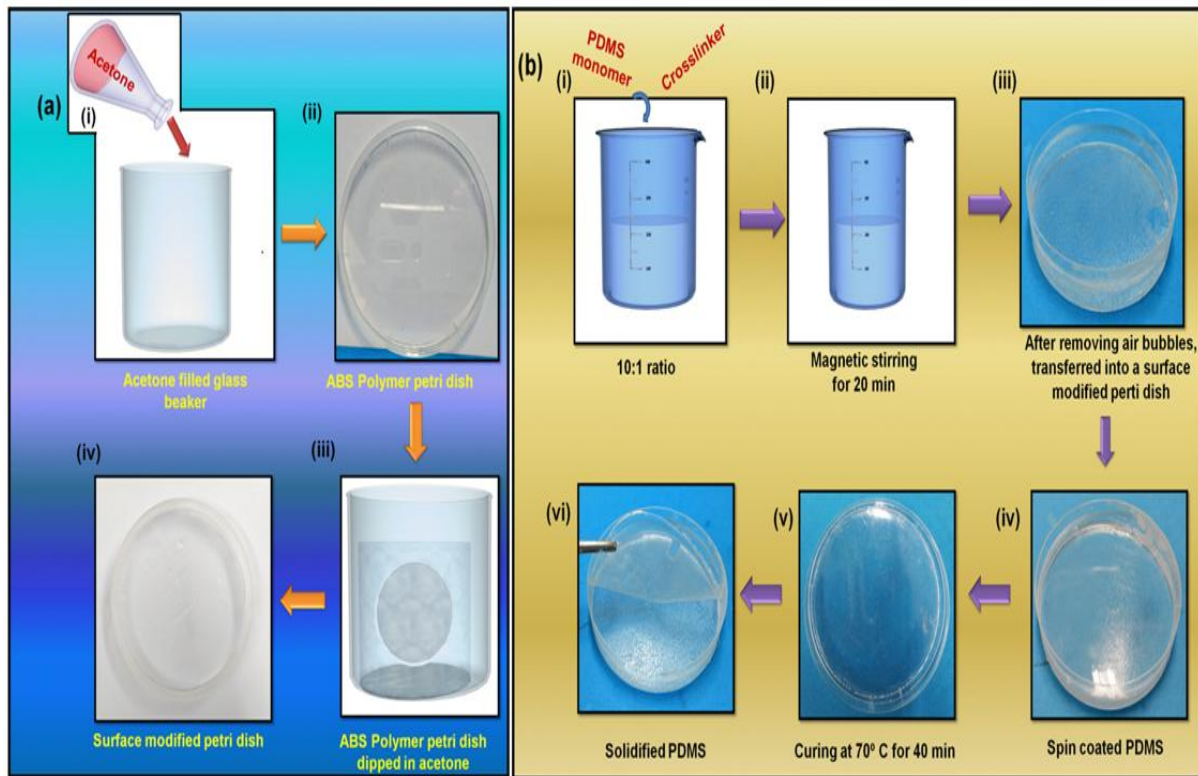
Figure 6.1 (a) Schematic illustration of the surface-modification process on a plastic petri dish using acetone as an etching medium and (b) fabrication process of the polydimethylsiloxane (PDMS) film using surface-modified petri dish.

6.2.2. SBP-TENG fabrication

The SBP-TENG requires two steps for electricity generation: electrostatic induction and contact electrification.[11], [30] The influence of external bio-mechanical energy, for vertical contact and separation between the SBP-TENG and contact materials, contributes to energy conversion. The basic unit of the SBP-TENG has a flat sheet-like structure, with PDMS film (with irregular microstructures) on top. Figure 2(a) shows a 3D schematic illustration of the SBP-TENG with a multilayer architecture.
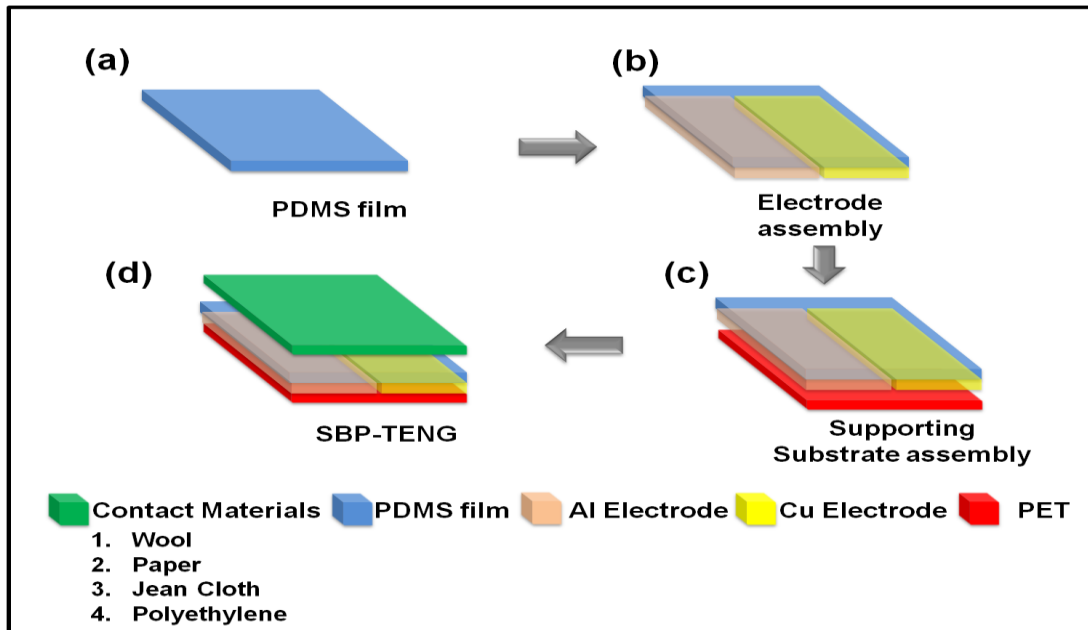
Figure 6.2 Graphical fabrication process of smart backpack-triboelectric nanogenerator (SBP-TENG) mainly composed of (a) PDMS film, (b) copper and aluminum electrodes, (c) its assembly process and, (d) packing.

The PDMS film was attached on top of aluminum (Al; 12 mm × 50 mm) and (Cu; 12 mm × 50 mm) electrodes with a fine air gap between the two electrodes, and a polyethylene terephthalate sheet was attached as a supporting substrate.

6.3. Measurement systems

Surface morphology analysis for the surface-modified PDMS and other cloth materials was performed using an FE-SEM (Supra 55VP; Carl Zeiss, Oberkochen, Germany). Further, to measure the electrical output of the SBP-TENG, an external motion was applied using a commercial linear motor (LinMot, Inc., Zurich, Switzerland). The output voltage signal and short circuit current of the SBP-TENG were measured using an electrometer (model 6514; Keithley Instruments Inc., Cleveland, OH, USA) and a SR 570 low noise current amplifier (Stanford Research Systems, Sunnyvale, CA, USA). All contact materials were heat-treated (in a hot air

oven) at 70 ºC for 30 min to remove humidity before carrying out the electrical measurements. The electrical measurements were conducted inside a grounded homemade Faraday cage. For real-time data acquisition control and analysis, a software platform was constructed based on LabVIEW.

6.4. Results and discussion

6.4.1. SBP-TENG design

The architecture of the SBP-TENG is composed of a PDMS film (25 mm × 50 mm) and two electrodes, made of aluminium (Al; 12 mm × 50 mm) and copper (Cu; 12 mm × 50 mm) were attached, with a small gap between the electrodes. Finally, a PET sheet was attached as a supporting layer for the SBP-TENG as illustrated schematically in **Figure 6.1 (a)** and **Figure 6.1 (b)** shows a digital photograph of the SBP-TENG.
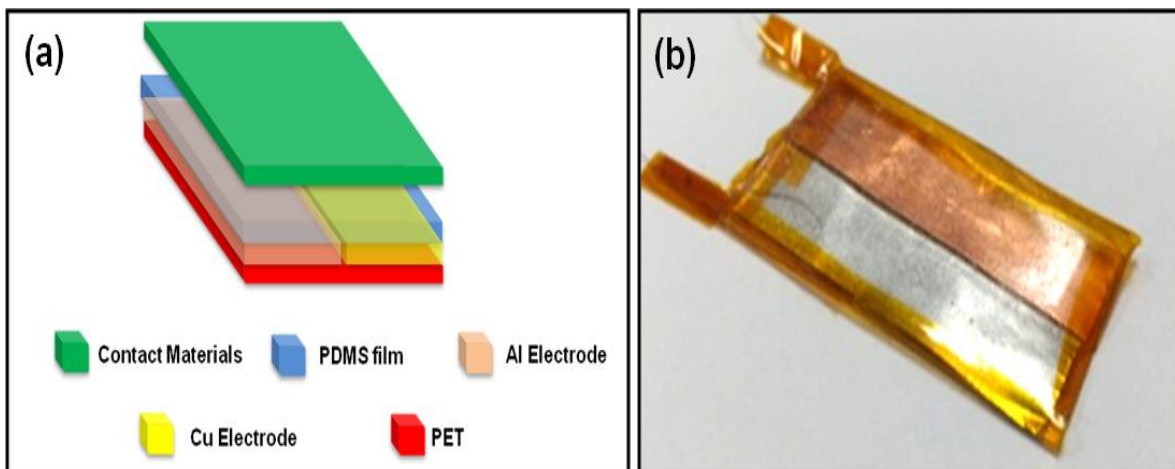
Figure 6.3 (a) Schematic illustration showing the structural design of the Smart Back Pack Triboelectric Nanogenerator (SBP-TENG) and (b) Photograph shows a fabricated SBP-TENG.

6.4.2. Morphology analysis of negative and positively charged layers

A top view field emission scanning electron microscope (FE-SEM) image of the PDMS film from various templates is shown in **Figure 6.4 (a-f)**. The etching rate increased with increasing dipping time, which contributed to the formation of irregular microstructures on the petri dish. The longest dipping time was 180 s, which modified the physical structure of the petri dish; hence, the dipping time was limited thereafter to 120 s.
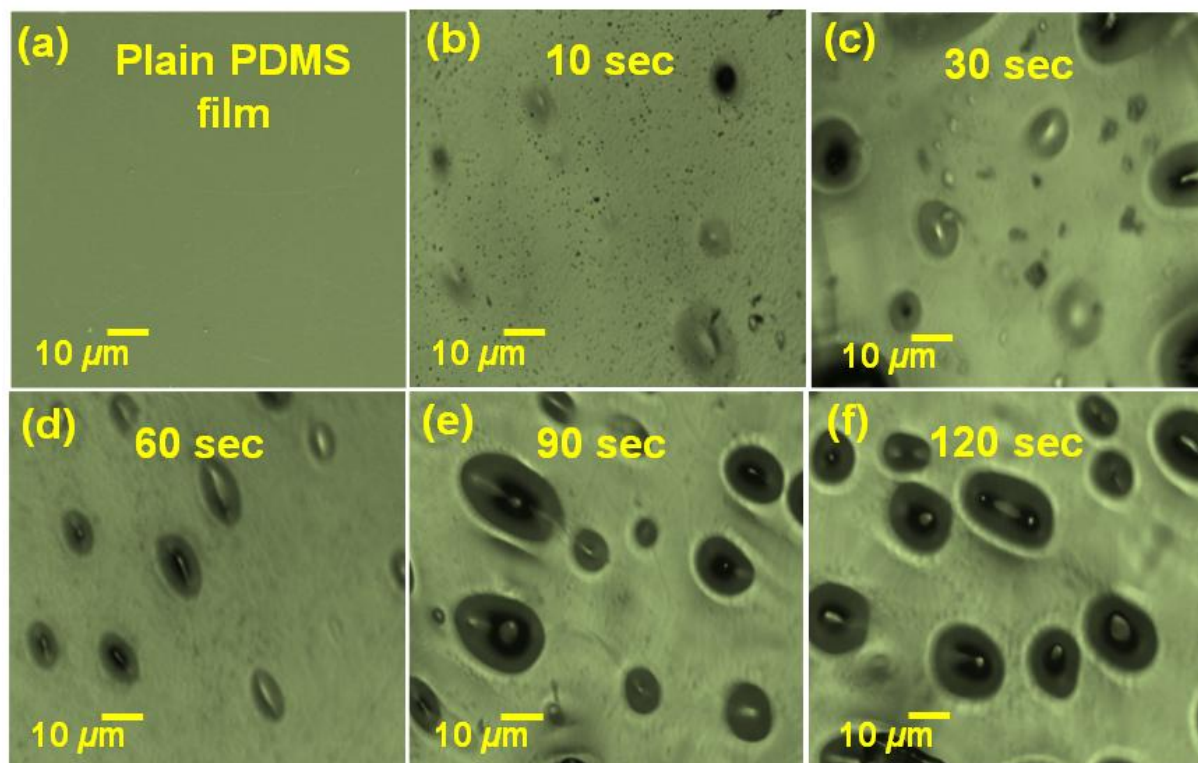
Figure 6.4 (a-f) Top view field emission scanning electron microscope image of surface-modified PDMS film from different moulds (10–120 s).

제주대학교 중앙도서관
JEJU NATIONAL UNIVERSITY LIBRARY

Also, the surface structures of other contact materials are important for the charge generation. **Figure 6.5 (a-e)** shows the FE-SEM image of polyethylene, jeans, cotton, paper and wool, respectively.
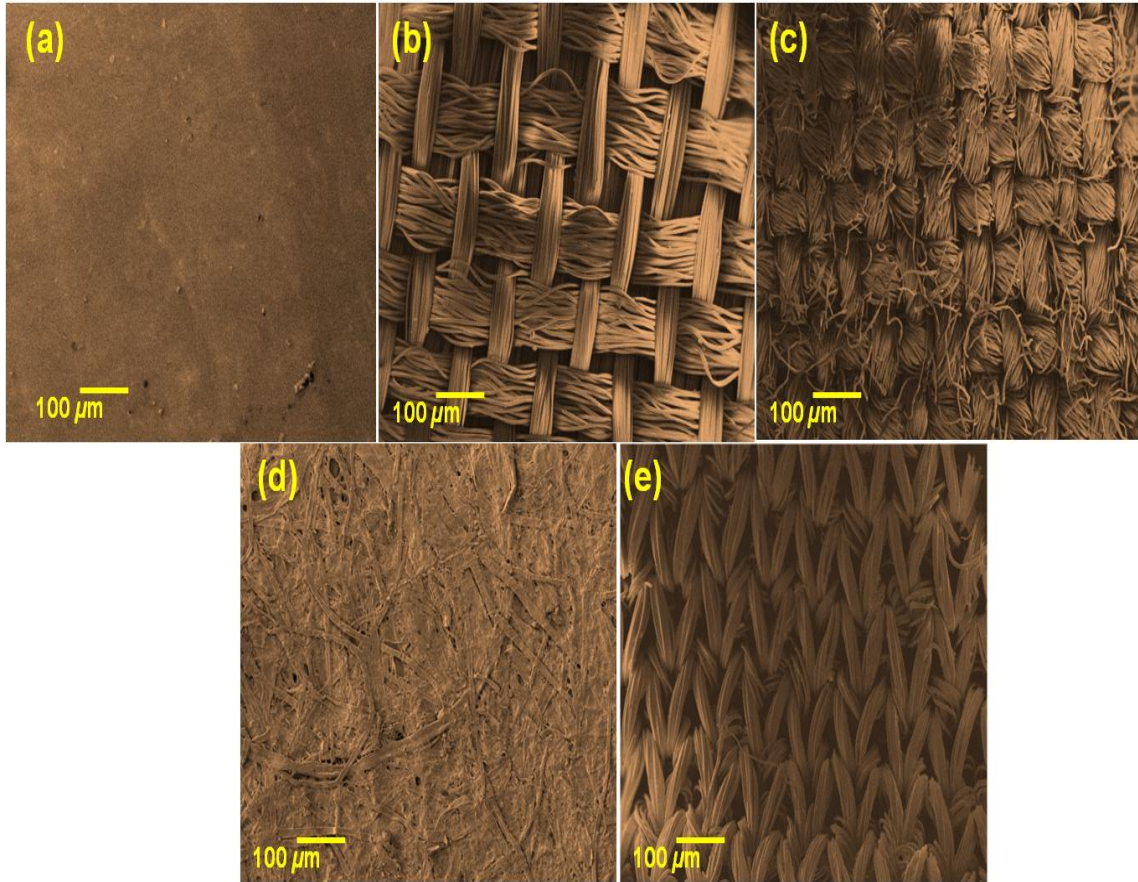
Figure 6.5 (a-e) Top view FE-SEM image of positively charged triboelectric contact materials: polyethylene, jeans, cotton, paper and wool.

6.4.3. Working mechanism

Figure 6.6 shows the working mechanism of the SBP-TENG during the interaction of contact materials on the surface of the PDMS film. Initially, the contact material is in contact with the PDMS film, as shown in **Figure 6.6 (a)**. Subsequently, due to the external motion, the surface separates (contact material moves away from the SBP-TENG) and a potential difference is created between them.

117
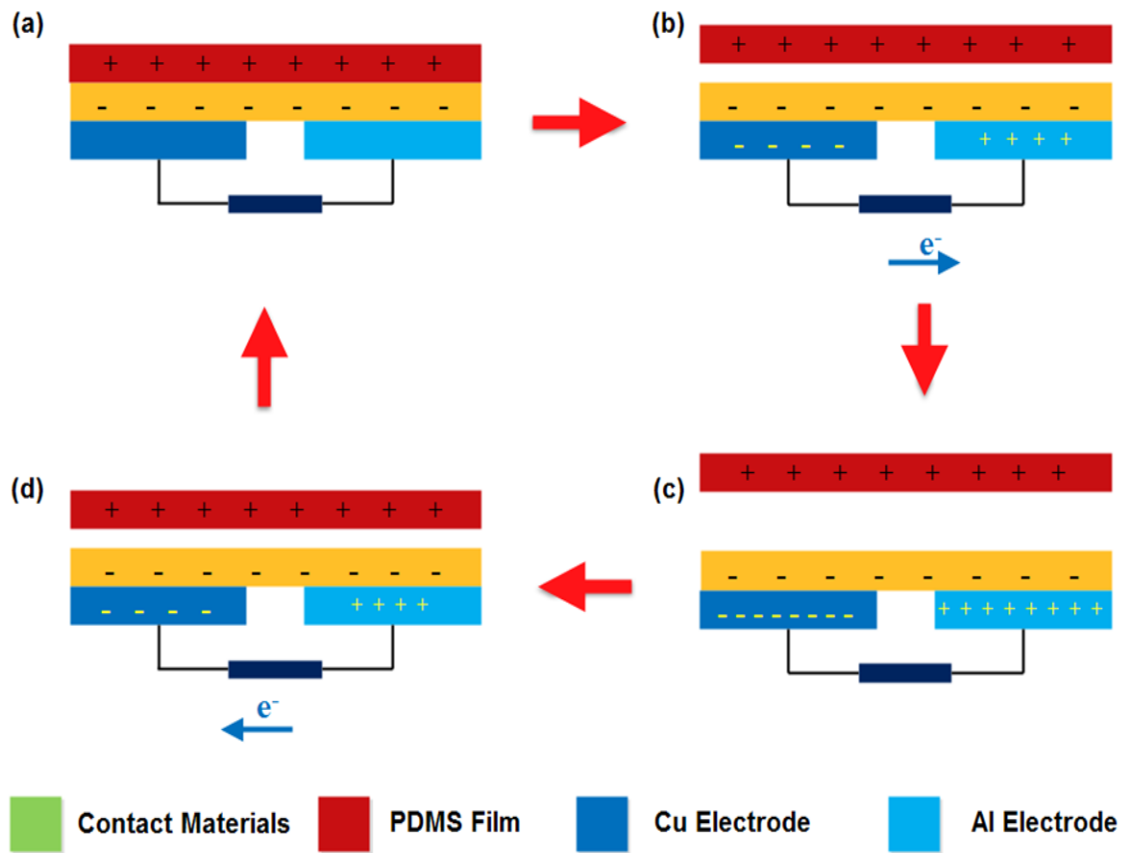
Figure 6.6 Schematic diagram of a SBP-TENG energy harvesting mechanism during contact and separation motion. (a) Initial stage, (b) releasing, (c) equilibrium state, and (d) pressing.

This process causes a flow of electrons from the Al electrode to the Cu electrode through an external circuit, as shown in **Figure 6.6 (b)** and finally reaches an electrostatic equilibrium state, as shown in **Figure 6.6 (c)**. This process contributes to the positive half-cycle of the AC signal; the negative half cycle is achieved as the contact material approaches the surface of the PDMS film, which induces a flow of electrons in the reverse direction, as shown in **Figure 6.6 (d)**.

6.4.4. Electrical analysis of SBP-TENG

The SBP-TENG acts as a freestanding mode energy harvester that is capable of energy harvesting by utilizing a series of contact materials. To quantitatively measure the electrical performance of the SBP-TENG, a linear motor (velocity: 1 m/s) was used to provide a controlled

118

contact and separation motion between the SBP-TENG and the contact materials. Initially, we investigated the electrical response of the SBP-TENG, fabricated using the PDMS film peeled from the petri dish treated and with acetone at different dipping times. **Figure 6.7 (a, b)** shows the voltage and I_{sc} values, respectively; the devices show an improvement of about 136 V and 5.7 μA for the PDMS film peeled from the 120 s acetone-treated petri dish compared to the plain PDMS film. This experiment demonstrates that surface-modified PDMS film has the potential to harvest energy.
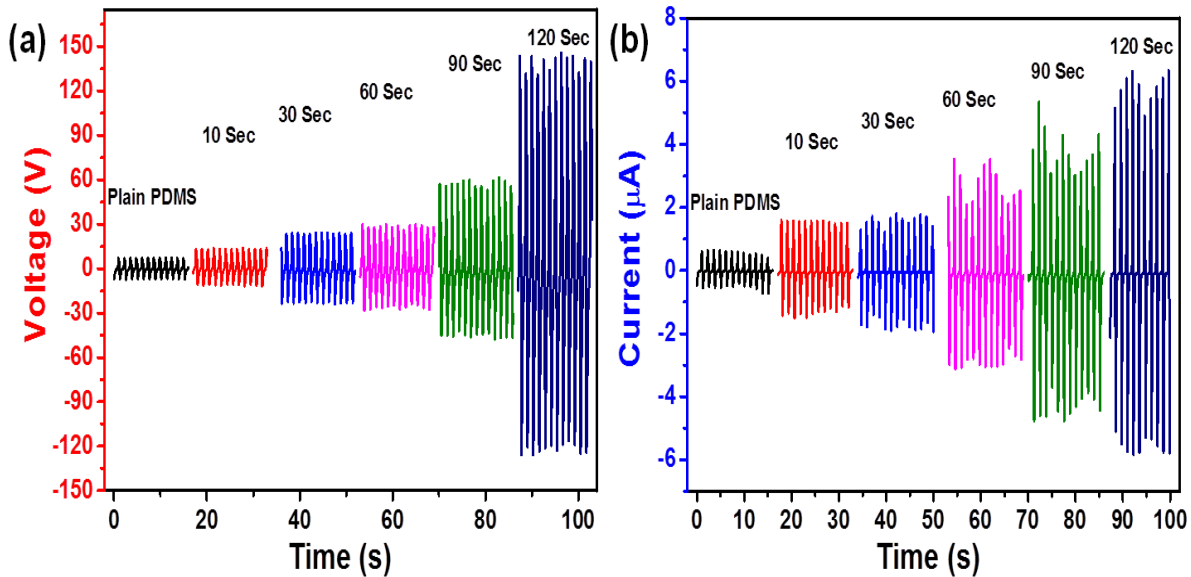
Figure 6.7 (a, b) Electrical measurement results of the SBP-TENG using plain PDMS film, with dipping times of 10, 30, 60, 90 and 120 s. The inset shows digital images of the surface-modified petri dish and solidified PDMS film.

To quantitatively measure the electrical performance of the SBP-TENG, a linear motor (velocity: 1 m/s) was used to provide a controlled contact and separation motion between the SBP-TENG and the contact materials. Initially, we selected a series of contact materials (wool, paper, cotton, jeans and polyethylene) that may interact with a bag in a real-time operation..

119

Figure 6.8 (a, b) shows the measured output voltage and short circuit current of the SBP-TENG obtained during the interaction between different contact materials. An increment in the electrical response was clearly observed when the contact materials changed from polyethylene to wool.
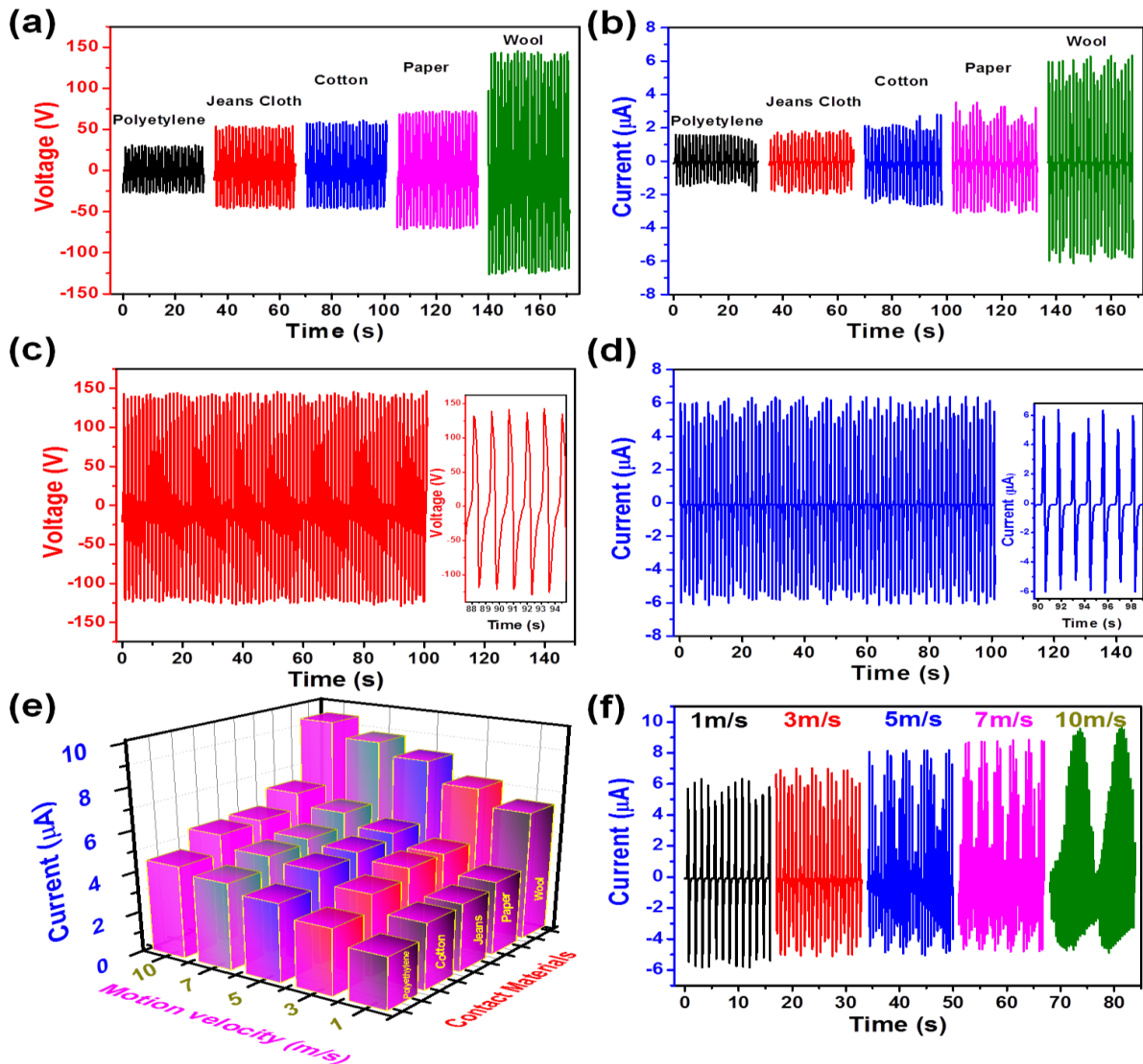
Figure 6.8 Typical electrical response of SBP-TENG: (a) voltage and (b) short-circuit current during contact and separation on the PDMS film using different freestanding contact materials. (c, d) Electrical response of SBP-TENG with wool as a contact material. (e) Influence of freestanding materials and different velocities of contact and separation motion on the short circuit current. (f) The short circuit current of the SBP-TENG with different velocities of motion, with wool as a contact material.

This behavior is because of the surface-modified PDMS that has a tendency for electron attraction, whereas the surface of the interaction materials tends to donate electrons.[1] Consequently, for further investigation, a woollen cloth was used as the contact material. **Figure 6.8 (c, d)** shows the electrical output of the SBP-TENG; the output voltage reached 142 V and its corresponding I_{sc} reached 5.9 μA. An enlarged view of the signals is shown in the left inset. The influence of contact materials and velocity of motion on I_{sc} are shown in **Figure 6.8 (e)**. An increment in the current amplitude was observed with the change in contact material and velocity of motion. The I_{sc} developed by the woollen cloth at a velocity of 10 m/s was 9.1 μA and **Figure 6.8 (f)** indicates the I_{sc} amplitude obtained while increasing the velocity of motion (1 m/s to 10 m/s) with woollen cloth as a contact material. This study confirms the potential of the SBP-TENG to harvest energy from different contact materials at different velocities of contact and separation.

Instantaneous peak power and power density are important parameters for finding the optimum load resistance for real-time application. Hence, we systematically studied the performance of the SBP-TENG under different load resistances and contact materials. **Figure 6.9 (a)** shows the output voltage obtained for different contact materials while increasing the load resistance; here, the output voltage increased and then saturated with increasing external load resistance.
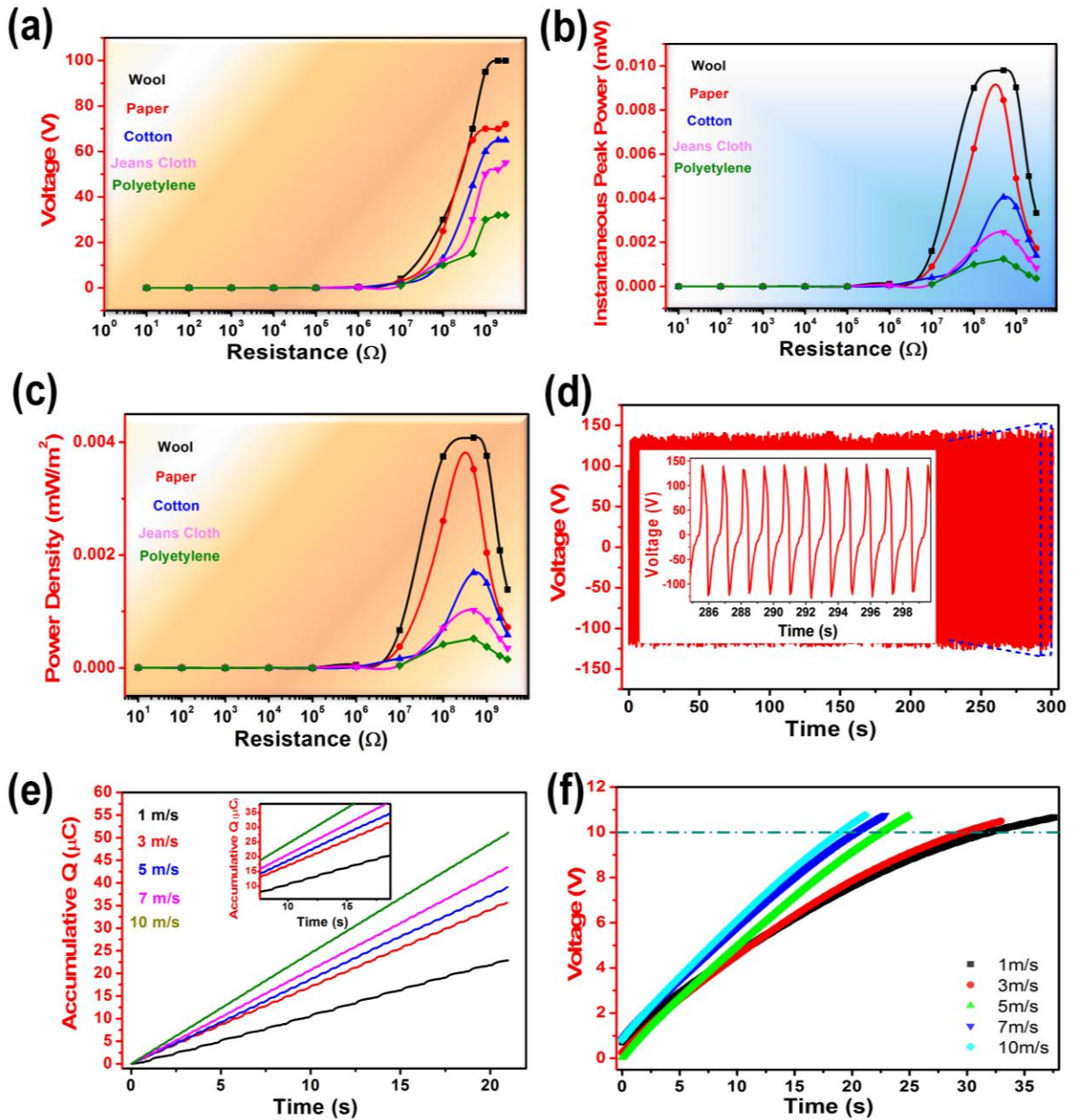
Figure 6.9 (a) Output voltage for external load resistance during interaction with different freestanding contact materials, (b) corresponding instantaneous peak power and (c) power density. (d) Output voltage of SBP-TENG during cyclic stability test (with wool as a contact material). The inset shows an enlarged view of the electrical signal at the end of the stability test. (e) Accumulative induced charge and (f) the measured voltage curve of a 1 μF capacitor charged by SBP-TENG (wool as a contact material) with different contact and separation velocities.

As a result, the instantaneous peak power reached 0.092 mW and a power density of 0.039 mW/m^2 was achieved across a 500 MΩ external load resistance using woollen cloth as a contact material, as shown in **Figure 6.9 (b, c)** (power and power density calculation equations are provided in Supporting Information). For other contact materials, the output power varied, but the maximum peak power was obtained at 500 MΩ load resistance. Since the SBP-TENG can be used for real-time energy harvesting, it is essential to confirm the durability of the device. **Figure 6.9 (d)** shows a stability test performed over 300 s using woollen cloth. This confirms that there is not much change in the surface morphology even after several thousand cycles of operation. The electrical response of the SBP-TENG was stable for a long operational period; this confirms the stability of the device. Using a diode bridge rectifier circuit (DF06G), we investigated the total accumulation of induced charge with respect to the velocity of motion, as shown in **Figure 6.9 (e)**. Here, the rate of charge accumulation was directly proportional to the velocity of motion. Since the higher velocity of motion (rapid contact and separation) provides more triboelectric charge generation, this results in higher charge accumulation. To demonstrate the charging capability of the SBP-TENG, we charged a 1 μF capacitor with different velocities of motion, as shown in **Figure 6.9 (f)**. Due to the higher rate of charge accumulation with increasing motion velocity, the time required for the capacitor to charge to 10 V decreased and resulted in faster charging.

To extrapolate the capability for real-time energy harvesting using an SBP-TENG as a portable and wearable device, a single unit was attached to the back side of a school bag. Initially, we studied different human motions (walking, running and bending) for scavenging bio-mechanical energy and found that the weight of the bag also plays a major role. **Figure 6.10 (a)** shows the output voltage and **(b)** I_{sc} with respect to different human motions with increasing bag

123

weight (1 – 5 kg); the electrical response was particularly susceptible to the weight of the bag, with larger weights showing a diminishing response. This behavior was observed because increasing the weight of the bag restricted its free motion. **Figure 6.10 (c)** shows the voltage and **(d)** I_{sc} signal obtained during different human motions To demonstrate the real-time energy harvesting and charging capability of the SBP-TENG, the rectified voltage signal was connected to a 1 μF capacitor and charged during various human motions, as shown in **Figure 6.10 (e)**. Additionally, the accumulative induced charge with respect to human motions is shown in **Figure 6.10 (f)**. This experiment demonstrates the potential of the SBP-TENG for scavenging biomechanical energy.
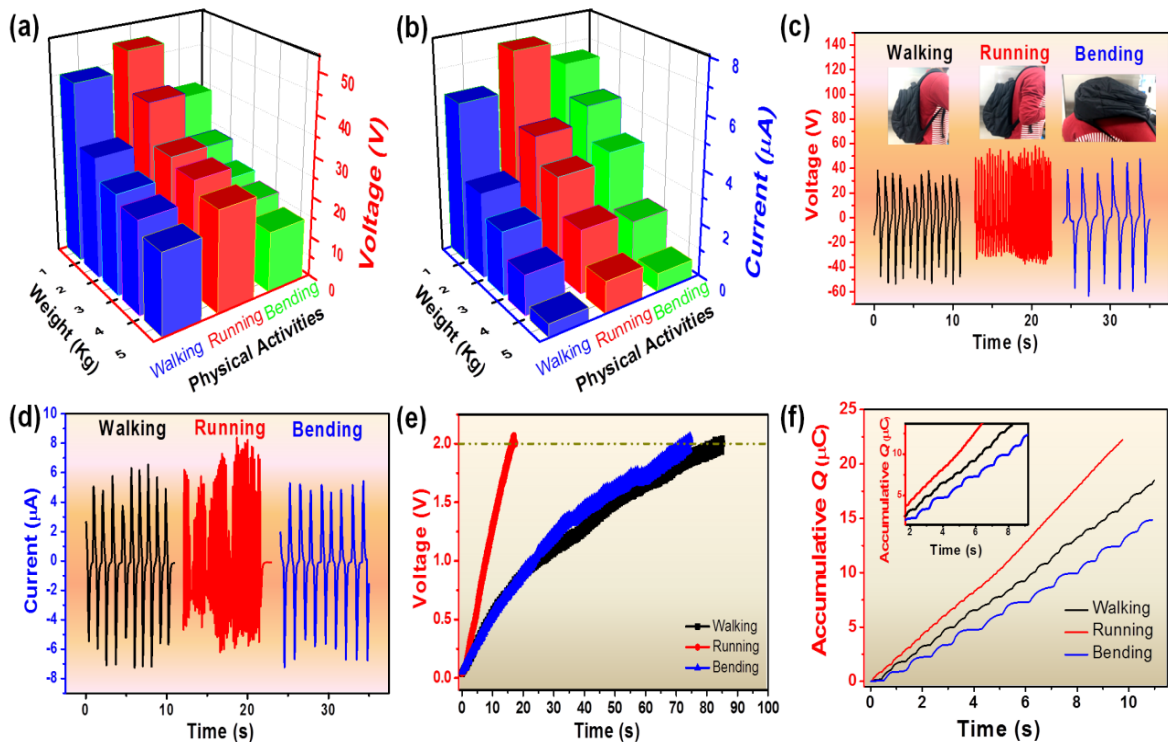
Figure 6.10. Real-time energy harvesting SBP-TENG. (a) Output voltage and (b) short-circuit current with respect to different human motions during increasing of the weight of the bag (cotton T-shirt as an interacting material). (c) Voltage and (d) short-circuit current obtained during different human motions with a 1 kg bag. (e) The measured voltage curve of a 1 μF capacitor charged by SBP-TENG and (f) accumulative induced charge generated by walking, running and bending.

124
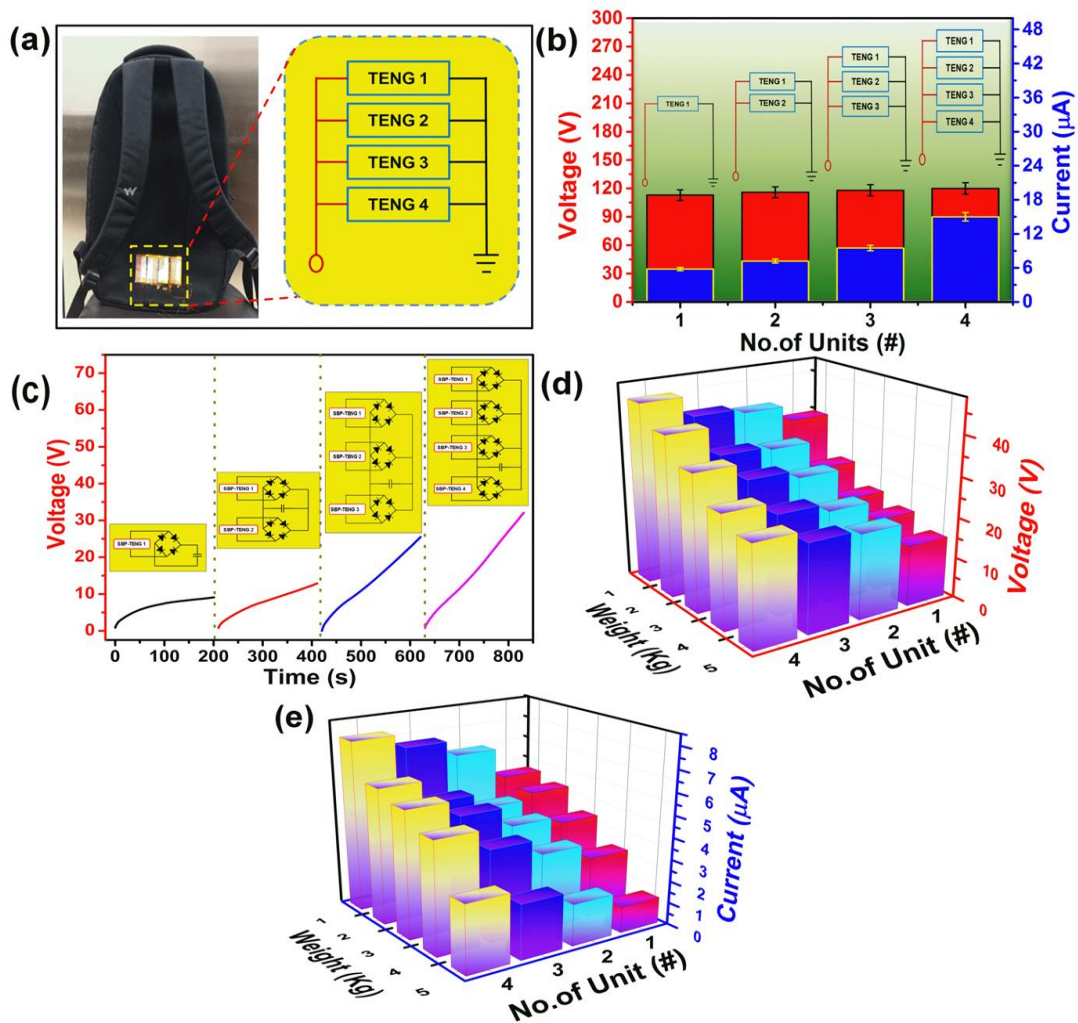
Figure 6.11 Electrical response of multi unit SBP-TENG (a) photograph of a multi unit SBP-TENG for harvesting biomechanical energy, including a schematic diagram of parallel circuit connection (Inset). (b) Output voltage (red) and short circuit current (blue) performance of multi unit SBP-TENG connected in parallel. (c) Capacitor charging curve for various SBP-TENG units. (d) Voltage and (e) short circuit current with respect to human motion (walking) with increasing bag weight (cotton T-shirt as an interacting material).

The ultimate aim of the SBP-TENG is to harvest electrical energy by utilizing human motion and contact materials; hence, to harvest more electrical power, we fabricated a multi-unit SBP-TENG and attached a school bag, as shown in the Figure 6(a); the inset circuit shows the electrical connection of the multi unit SBP-TENG (devices are connected in parallel). To enhance the energy harvesting efficiency of the SBP-TENG, four units were electrically

125

connected in parallel. Hence, the amplitude of the voltage peak was steady (120 V) and the amplitude of the current signal (5.8–15 μA) was gradually increased while increasing the unit number, as shown in Figure 6(b).

To validate the efficiency of the multi-unit SBP-TENG, the rectified voltage, according to the number of units, was connected to a 10 μF capacitor and charged for 100 s, as shown in Figure 6(c). The complete circuit is shown in the inset of Figure 6(c). The addition of more SMP-TENG units (from 1–4) resulted in faster charging of the capacitor. To demonstrate the potential of the SBP-TENG for harvesting biomechanical energy using a multi-unit SBP-TENG, the electrical signals were investigated for human motion (walking) by varying the weight of the bag with a cotton T-shirt as the contact material, and the results are shown in Figure 6(d–e). According to the addition of units, the output voltage was maintained at an average, but I_{sc} gradually increased from 5.2 μA to 7.9 μA; with respect to increasing weight, the output I_{sc} was gradually decreased and eventually maintained an output of 2.7 μA.

6.4.5. SBP-TENG for Self-powered emergency LED

Figure 6(f) demonstrates that the SBP-TENG can be utilized as a self-powered device. Here we introduce a new self-powered application that can be used in an emergency scenario. This self-powered emergency LED was designed and powered using an SBP-TENG. A detailed circuit diagram is shown in Figure S12, and the circuit was constructed with a diode bridge rectifier (DF06G), a capacitor (C_1= .1 μF), a press switch and a white LED strip (three LEDs). During contact and separation of a contact material with the SBP-TENG, an electrical signal is generated and this charge is stored in a capacitor (C_1). When the switch is pressed the capacitor stored charge discharges by lighting the LED, which is connected to the circuit. Also, with

respect to the stored charge, the intensity of the flash light varies. The inset of Figure 6(f) shows an enlarged view of the charging and discharging curve during self-powered emergency LED operation. Figure 6(g) shows a photograph of the self-powered emergency LED during the off- and on-states. This integrated facility with the SBP-TENG would simplify the consumption of external battery sources for emergency applications.

From the above discussion and the results obtained, it is clear that the SBP-TENG is suitable for scavenging energy from human motion by utilizing materials that could be used in day to day life. This energy can be used for powering electronic devices, such as portable power packs, GPS systems and security sensors. Also, in the field of triboelectric nanogeneration, the SBP-TENG is original in the fields of sustainable energy harvesting and self-powered applications.
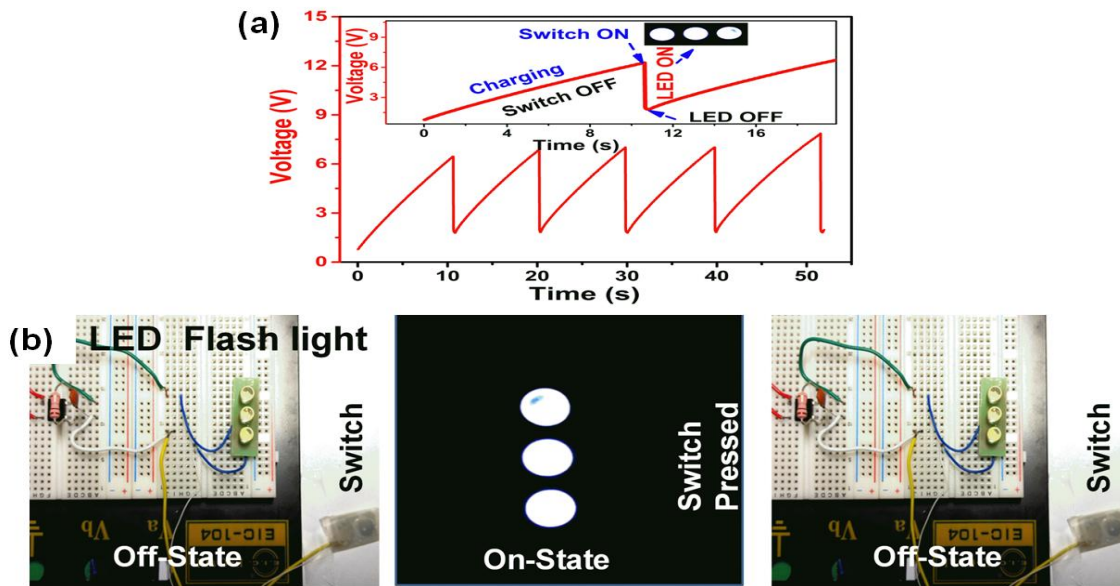
Figure 6.12 (a) Capacitor charging curve of self-powered emergency flashlight; (Inset) enlarged view of self-powered operation. (b) Photograph of the self-powered emergency flashlight during operation.

127

6.5.   Conclusion

In this work, we developed an innovative design for scavenging biomechanical energy using materials found in daily life, by reusing a plastic petri dish discarded after laboratory use to fabricate an SBP-TENG. The results clearly show that the device performs well as a sustainable freestanding TENG; the SBP-TENG can generate energy from contact and separation of the contact materials. This work upgrades a traditional school bag into a smart bag that can harvest energy with respect to the load in the bag and human motion, and can also work as a self-powered emergency LED. These experiments validate the potential of the SBP-TENG for real-time energy harvesting and as a standalone system to drive low power electronic devices for emergency scenarios. Other merits of the SBP-TENG include its simple fabrication process, robustness and excellent electrical performance. This experiment demonstrates a new approach for the production of TENGs as portable, wearable, energy harvesting and self-powered devices.

6.6.   References

[1]   Z. L. Wang, "Triboelectric nanogenerators as new energy technology for self-powered systems and as active mechanical and chemical sensors.," *ACS Nano*, vol. 7, no. 11, pp. 9533–57, Nov. 2013.

[2]   S. Wang, L. Lin, and Z. L. Wang, "Nanoscale triboelectric-effect-enabled energy conversion for sustainably powering portable electronics.," *Nano Lett.*, vol. 12, no. 12, pp. 6339–46, Dec. 2012.

[3]   X. Chen, T. Jiang, Y. Yao, L. Xu, Z. Zhao, and Z. L. Wang, "Stimulating Acrylic Elastomers by a Triboelectric Nanogenerator - Toward Self-Powered Electronic Skin and Artificial Muscle," *Adv. Funct. Mater.*, vol. 26, no. 27, pp. 4906–4913, Jul. 2016.

[4]   M. Grätzel, "Photoelectrochemical cells.," *Nature*, vol. 414, no. 6861, pp. 338–44, Nov.

2001.

[5]   B. Saravanakumar and S.-J. Kim, "Growth of 2D ZnO Nanowall for Energy Harvesting Application," *J. Phys. Chem. C*, vol. 118, no. 17, pp. 8831–8836, May 2014.

[6]   B. Saravanakumar, S. Soyoon, and S.-J. Kim, "Self-powered pH sensor based on a flexible organic-inorganic hybrid composite nanogenerator.," *ACS Appl. Mater. Interfaces*, vol. 6, no. 16, pp. 13716–23, Aug. 2014.

[7]   N. R. Alluri, B. Saravanakumar, and S. J. Kim, "Flexible-Hybrid Piezoelectric Film (BaTi(1-x)ZrxO3)-PVDF Nanogenerator as a Self-Powered Fluid Velocity Sensor.," *ACS Appl. Mater. Interfaces*, Apr. 2015.

[8]   Z. L. Wang and J. Song, "Piezoelectric nanogenerators based on zinc oxide nanowire arrays.," *Science*, vol. 312, no. 5771, pp. 242–6, Apr. 2006.

[9]   R. Venkatasubramanian, E. Siivola, T. Colpitts, and B. O'Quinn, "Thin-film thermoelectric devices with high room-temperature figures of merit.," *Nature*, vol. 413, no. 6856, pp. 597–602, Oct. 2001.

[10]   L. E. Bell, "Cooling, heating, generating power, and recovering waste heat with thermoelectric systems.," *Science*, vol. 321, no. 5895, pp. 1457–61, Sep. 2008.

[11]   A. Chandrasekhar, N. R. Alluri, B. Saravanakumar, S. Selvarajan, and S.-J. Kim, "Human Interactive Triboelectric Nanogenerator as a Self-Powered Smart Seat.," *ACS Appl. Mater. Interfaces*, vol. 8, no. 15, pp. 9692–9, Apr. 2016.

[12]   T.-C. Hou, Y. Yang, H. Zhang, J. Chen, L.-J. Chen, and Z. Lin Wang, "Triboelectric nanogenerator built inside shoe insole for harvesting walking energy," *Nano Energy*, vol. 2, no. 5, pp. 856–862, Sep. 2013.

[13]   Y. Yang, H. Zhang, Z. H. Lin, Y. S. Zhou, Q. Jing, Y. Su, J. Yang, J. Chen, C. Hu, and Z.

L. Wang, "Human skin based triboelectric nanogenerators for harvesting biomechanical energy and as self-powered active tactile sensor system," *ACS Nano*, vol. 7, no. 10, pp. 9213–9222, 2013.

[14] P. Bai, G. Zhu, Z. H. Lin, Q. Jing, J. Chen, G. Zhang, J. Ma, and Z. L. Wang, "Integrated multilayered triboelectric nanogenerator for harvesting biomechanical energy from human motions," *ACS Nano*, vol. 7, no. 4, pp. 3713–3719, 2013.

[15] W. Yang, J. Chen, X. Wen, Q. Jing, J. Yang, Y. Su, G. Zhu, W. Wu, and Z. L. Wang, "Triboelectrification based motion sensor for human-machine interfacing.," *ACS Appl. Mater. Interfaces*, vol. 6, no. 10, pp. 7479–84, May 2014.

[16] X. Chen, X. Pu, T. Jiang, A. Yu, L. Xu, and Z. L. Wang, "Tunable Optical Modulator by Coupling a Triboelectric Nanogenerator and a Dielectric Elastomer," *Adv. Funct. Mater.*, Nov. 2016.

[17] Q. Liang, X. Yan, X. Liao, S. Cao, X. Zheng, H. Si, S. Lu, and Y. Zhang, "Multi-unit hydroelectric generator based on contact electrification and its service behavior," *Nano Energy*, vol. 16, pp. 329–338, Sep. 2015.

[18] Q. Liang, X. Yan, X. Liao, S. Cao, S. Lu, X. Zheng, and Y. Zhang, "Integrated active sensor system for real time vibration monitoring.," *Sci. Rep.*, vol. 5, p. 16063, Jan. 2015.

[19] W. Tang, C. B. Han, C. Zhang, and Z. L. Wang, "Cover-sheet-based nanogenerator for charging mobile electronics using low-frequency body motion/vibration," *Nano Energy*, vol. 9, pp. 121–127, 2014.

[20] C. Bao, C. Zhang, X. Hui, and L. Zhang, "Self-powered velocity and trajectory tracking sensor array made of planar triboelectric nanogenerator pixels," *Nano Energy*, vol. 9, pp. 1–9, 2014.

[21]   F.-R. Fan, Z.-Q. Tian, and Z. Lin Wang, "Flexible triboelectric generator," *Nano Energy*, vol. 1, no. 2, pp. 328–334, Mar. 2012.

[22]   R. Zhang, L. Lin, Q. Jing, W. Wu, Y. Zhang, Z. Jiao, L. Yan, R. P. S. Han, and Z. L. Wang, "Nanogenerator as an active sensor for vortex capture and ambient wind-velocity detection," *Energy Environ. Sci.*, vol. 5, no. 9, p. 8528, Aug. 2012.

[23]   J. Chen, J. Yang, Z. Li, X. Fan, Y. Zi, Q. Jing, H. Guo, Z. Wen, K. C. Pradel, S. Niu, and Z. L. Wang, "Networks of triboelectric nanogenerators for harvesting water wave energy: a potential approach toward blue energy.," *ACS Nano*, vol. 9, no. 3, pp. 3324–31, Mar. 2015.

[24]   H. Zhang, Y. Yang, Y. Su, J. Chen, K. Adams, S. Lee, C. Hu, and Z. L. Wang, "Triboelectric nanogenerator for harvesting vibration energy in full space and as self-powered acceleration sensor," *Adv. Funct. Mater.*, vol. 24, no. 10, pp. 1401–1407, 2014.

[25]   Z. L. Wang, "Triboelectric nanogenerators as new energy technology and self-powered sensors - principles, problems and perspectives.," *Faraday Discuss.*, vol. 176, pp. 447–58, Jan. 2014.

[26]   T.-H. Chang, Y.-W. Peng, C.-H. Chen, T.-W. Chang, J.-M. Wu, J.-C. Hwang, J.-Y. Gan, and Z.-H. Lin, "Protein-based contact electrification and its uses for mechanical energy harvesting and humidity detecting," 2016.

[27]   T.-W. Chang, C.-W. Wang, C.-H. Chen, Y.-C. Li, C.-L. Hsu, H.-T. Chang, and Z.-H. Lin, "Controlled synthesis of Se-supported Au/Pd nanoparticles with photo-assisted electrocatalytic activity and their application in self-powered sensing systems," 2016.

[28]   K. Y. Lee, J. Chun, J.-H. Lee, K. N. Kim, N.-R. Kang, J.-Y. Kim, M. H. Kim, K.-S. Shin, M. K. Gupta, J. M. Baik, and S.-W. Kim, "Hydrophobic sponge structure-based

triboelectric nanogenerator.," *Adv. Mater.*, vol. 26, no. 29, pp. 5037–42, Aug. 2014.

[29] K. Y. Lee, M. K. Gupta, and S.-W. Kim, "Transparent flexible stretchable piezoelectric and triboelectric nanogenerators for powering portable electronics," *Nano Energy*, Nov. 2014.

[30] W. Yang, J. Chen, X. Wen, Q. Jing, J. Yang, Y. Su, and G. Zhu, "Triboelectrification Based Motion Sensor for Human-Machine Interfacing," 2014.

CHAPTER - 7

Sustainable Biomechanical Energy Scavenger towards Self-Reliant Kids' Interactive Battery-Free Smart Puzzle

Graphical overview
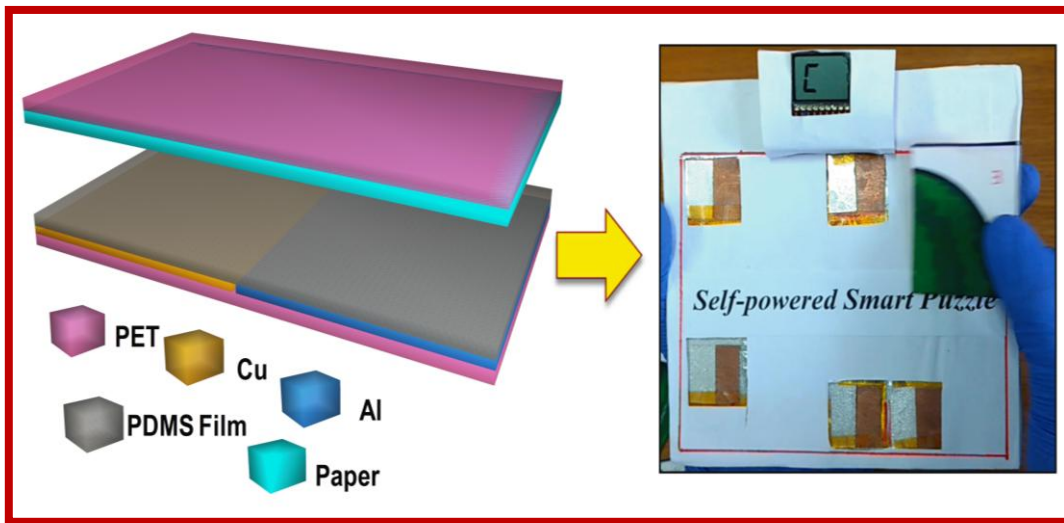
Highlights

- ➤ Biomechanical energy is a promising renewable energy source and, owing to the demand for portable and smart device power sources, has attracted the attention of researchers in a wide range of disciplines

- ➤ We present a smart puzzle triboelectric nanogenerator (SP-TENG) based on the contact and separation mode between a surface-modified polydimethylsiloxane film and a paper contact material

- ➤ The SP-TENG exhibits a simple structure (thin and lightweight), with an output voltage of 70 V and a current of 6.5 μA, which can drive a liquid crystal display at the press of a finger

- ➤ The SP-TENG also acts as an instantaneous force sensor with detection sensitivity of 2.605 μA kPa^{-1}

- ➤ We fabricated six SP-TENGs as puzzle pieces and formed a self-powered smart puzzle by connecting it to a simple logic circuit

- ➤ This approach improved a simple traditional puzzle, transforming it into an interactive smart puzzle

7.1. Introduction

The recent trend of interactive, low-power smart devices is a milestone of technological advancement, but it also presents significant challenges as the demand for compact, efficient, and robust technology grows. Smart devices must be well designed and user-friendly to fulfill a user's needs, which may include real-time health monitoring, interactive games, and the execution of voice commands. Interactive games are particularly attractive to children, but require power for uninterrupted operation. Worldwide, researchers are working to find solutions to this via energy harvesting and energy storage. Several innovative approaches using solar cells[1] and supercapacitors[2]–[6] have exhibited sought-after features, such as cost-effectiveness, stability, reliability, and eco-friendliness. Viable alternatives to satisfy the present requirements are devices that scavenge biomechanical energy, such as piezoelectric nanogenerators,[7]–[11] electromagnetic generators,[12], [13] or triboelectric nanogenerators.[14]–[19] Recently, triboelectric nanogenerators (TENGs) have attracted the attention of scientists in respect to future energy harvesting applications. TENG devices have the potential to scavenge energy from a range of sources including human activity,[20]–[23] vibration,[24] wind,[25] and water.[26] Furthermore, the potential for these device to be used in the field of biocompatible nanogenerators has also drawn attention.[27], [28]

Zhang,[29] Kim,[30] and Choi[31] experimentally demonstrated valuable innovations in the field of TENGs and potential self-powered applications. However, most TENG devices are complex in design or have undesirable weight and thickness, restricting their application in various sectors. Our approach to TENGs is to use the coupled effects of contact electrification and electrostatic induction to scavenge biomechanical energy with eco-friendly materials, thus

reducing environmental pollution. The research also addresses the problems that occur due to the relative structural complexity of other TENGs.

We present an innovative approach for fabricating an eco-friendly TENG device that is capable of scavenging biomechanical energy. A surface-modified polydimethylsiloxane (PDMS) film was used as an active layer, where the surface modification procedure can be applied to recycled plastic Petri dishes, discarded after laboratory use. The smart puzzle TENG (SP-TENG), fabricated using the PDMS film, could be bent up to a 1-cm curvature radius, and had a weight of 1.022 g and a thickness of 0.69 mm. In the proposed SP-TENG, charge generation occurs during the interaction between the PDMS film and the paper during applied human motion. To investigate the energy harvesting and charging behavior of the SP-TENG, tests were performed under controlled mechanical motion instead. The output voltage and current reached 70 V and 6.5 μA, respectively, and the device had the ability to act as a force sensor to measure instantaneous force. Furthermore, preliminary results imply that there is a high likelihood that the SP-TENG could be used as a sustainable self-powered smart puzzle. This opens up new applications for self-powered TENGs. This work describes a promising technology for scavenging biomechanical energy and its impact on the future generation of self-powered smart toys.

7.2. Experimental methods

7.2.1. Surface treatment of the polymer Petri dish

A polymer Petri dish was cleaned with ethanol and deionized water, then blown dry with compressed nitrogen gas to remove dust particles. The Petri dish was then submerged in acetone for 120 s, washed with deionized water and ethanol, and then dried in a hot air oven at 60ºC for

one hour (detailed discussion regarding ABS plastic reaction with acetone is presented in the supporting information).

7.2.2. SP-TENG fabrication

PDMS monomer and cross-linker (10:1) were mixed with a magnetic stirrer for 20 min, transferred to the surface-modified Petri dish, and degassed to remove air bubbles. After degassing, the PDMS was spin-coated at 600 rpm for 30 s and solidified by baking at 70ºC for 40 min. Next, copper (12×30 mm) and aluminum (12×30 mm) electrodes were attached with a fine gap between the electrodes as shown in **Figure 7.1 (a-d)**. Finally, a polyethylene terephthalate (PET) sheet was attached to the bottom as a supporting layer for the SP-TENG.
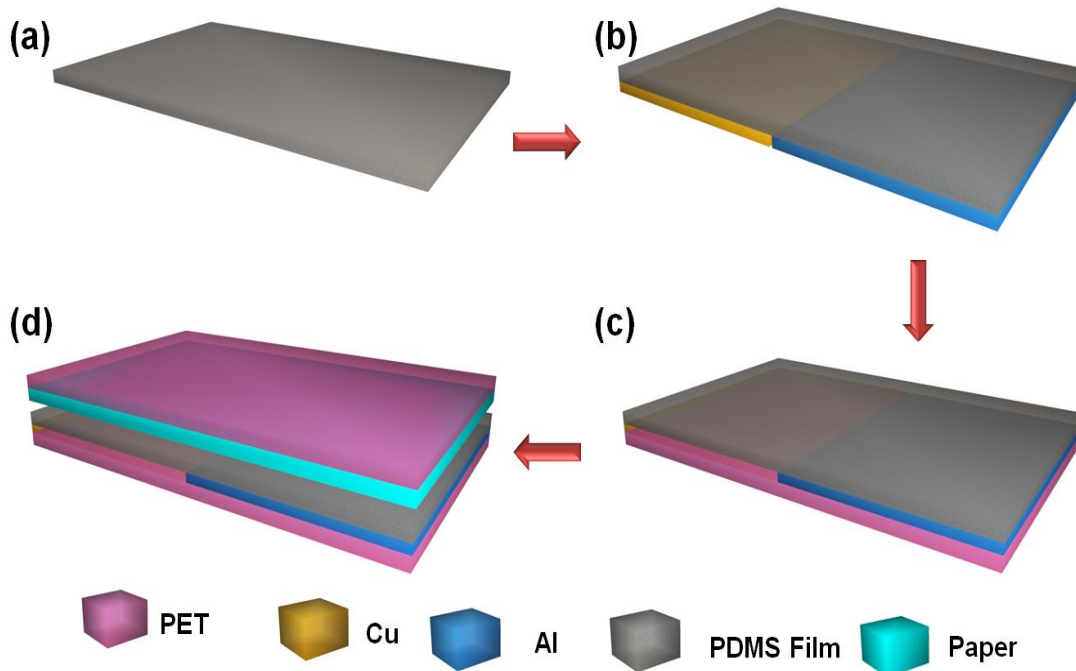
Figure 7.1 The fabrication and assembly process of the SP-TENG. (a) PDMS film, (b) attaching with the electrodes, (c) adhere with the supporting substrate, and (d) attaching paper with a PET.

7.2.3. Self-powered smart puzzle fabrication

A small piece of paper on the back side of a puzzle piece was positioned opposite to the SP-TENG base frame. The logic circuit was assembled using thin copper wire and a mini bread board.

7.3. Measurement systems

The surface morphology analysis for the surface-modified PDMS film and paper was performed using a field emission scanning electron microscope (FE-SEM) (Zeiss Supra 55VP). To measure the electrical output, a force was applied using a commercial linear motor (LinMot, Inc.). The output voltage and short circuit current of the SP-TENG were measured using an electrometer (Keithley 6514). Before carrying out the electrical measurements, the device and the contact material were heat-treated (in a hot air oven) at 60ºC for 40 min to remove any water residue. To prevent external noise in the measurement signals, all electrical measurements were performed inside a Faraday cage. Software built on LabVIEW was used for real-time data acquisition, control, and analysis.

7.4. Results and discussion

7.4.1. SP-TENG design

The two key parts of the SP-TENG were: the PDMS film with copper and aluminum electrodes (stationary); and the paper attached to PET (moving). **Figure 7.2 (a)** illustrates a 3D schematic representation of the SP-TENG. The PDMS film was chosen as an active layer due to its higher tendency to gather electrons,[14], [32]–[34] and paper was chosen as a contact material to provide electrons.[35] PET was selected as a supporting substrate for SP-TENG and the

제주대학교 중앙도서관
JEJU NATIONAL UNIVERSITY LIBRARY

contact material (paper) due to its high flexibility and toughness. **Figure 7.2 (b)** presents a digital photograph of the SP-TENG (25 × 30 mm) and **Figure 7.2 (c)** shows that the SP-TENG can bend with a curvature radius of up to 1 cm, demonstrating its potential as a flexible energy harvesting device. **Figure 7.2 (d)** shows that the weight of the device with electrodes was 1.02 g, meaning that this device is a promising candidate for lightweight energy harvesting applications. The thickness of the SP-TENG is 0.69 mm, as shown in **Figure 7.2 (e)**. As the thickness is less than 1 mm, the device could be considered thin enough to accommodate portable and wearable electronic applications.
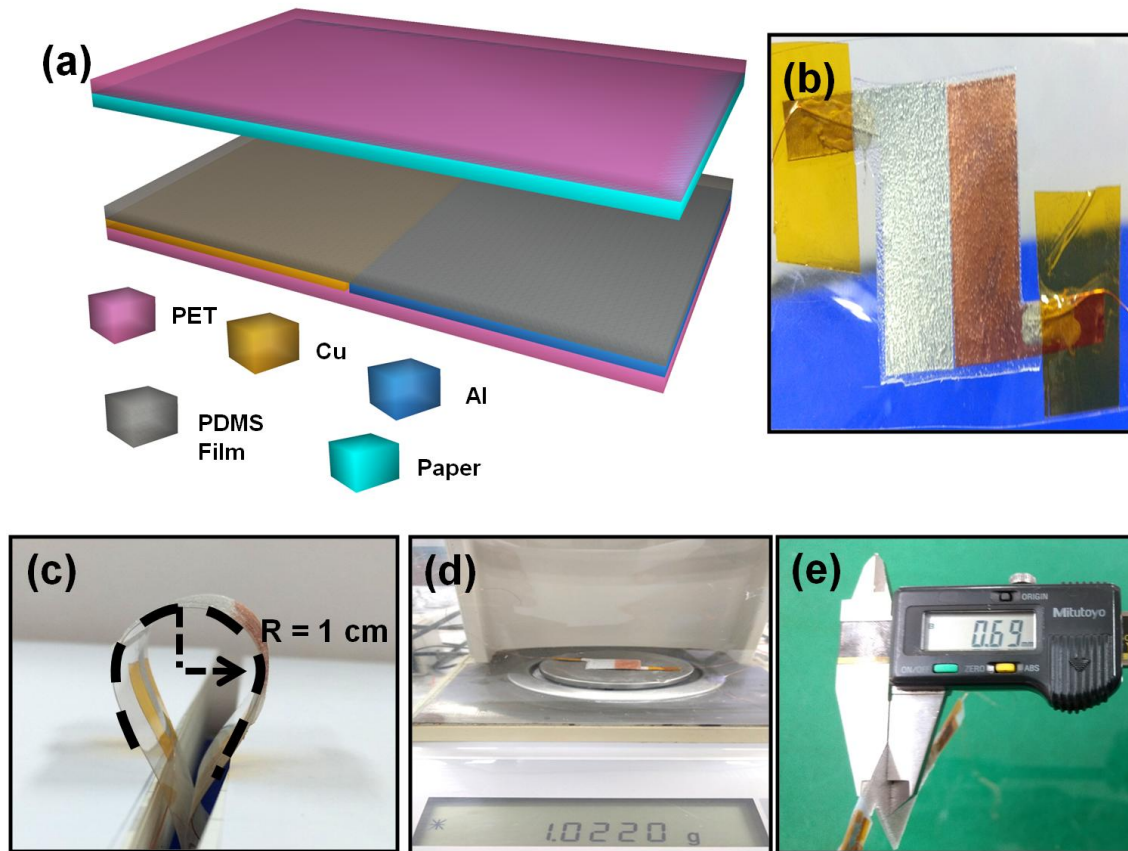
Figure 7.2 (a) Schematic illustration of the SP-TENG and (b) Digital image. (c) Photograph of the SP-TENG bending test with a radius of 1 cm, (d) weight of the SP-TENG and (e) Digital image of SP-TENG thickness.

139

7.4.2. Morphology analysis of negative and positively charged layers

Here, the Figure 1(a) shows the FE-SEM image of PDMS film triboelectric active layer and Figure 1(b) shows the surface of paper. Paper and PDMS are eco-friendly and bio-compactable materials.
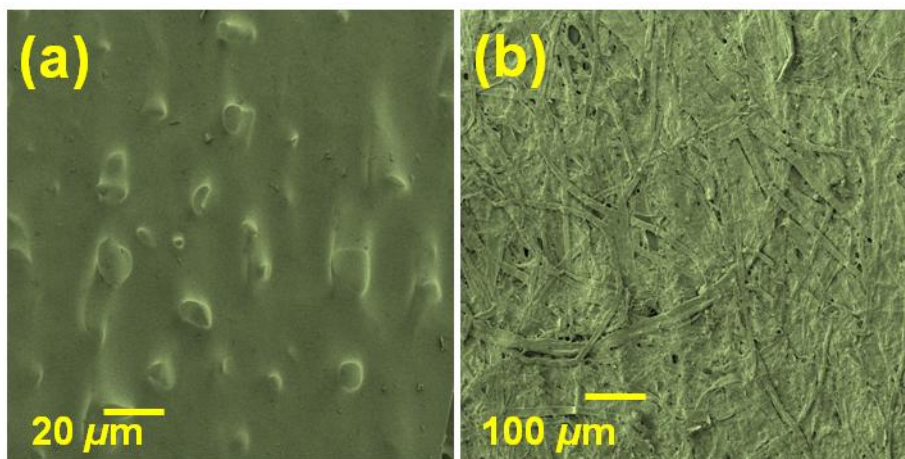
Figure 7.3 FE-SEM images of (a) surface-modified PDMS film and (b) paper.

7.4.3. Working mechanism of SP-TENG

The mechanism of the SP-TENG is shown in **Figure 7.4** , which involves the interaction of paper (contact material) with the PDMS film, producing a combination of electrostatic induction[17], [30], [36] and the triboelectric effect.[37]–[39] First, the contact material (paper) comes into contact with the PDMS film, as shown in **Figure 7.4 (a)**. Next, owing to the influence of external motion, the surfaces separate and a potential difference is created across the electrodes. This operation induces a flow of electrons from the aluminum electrode to the copper electrode through the external circuit shown in **Figure 7.4 (b)**, ultimately reaching an electrostatic equilibrium state, shown in **Figure 7.4 (c)**. This process contributes towards the

positive half-cycle of the AC signal; the negative half-cycle is attained when the contact material approaches the upper surface of the PDMS film, causing a flow of electrons in the reverse direction, as shown in **Figure 7.4 (d)**.
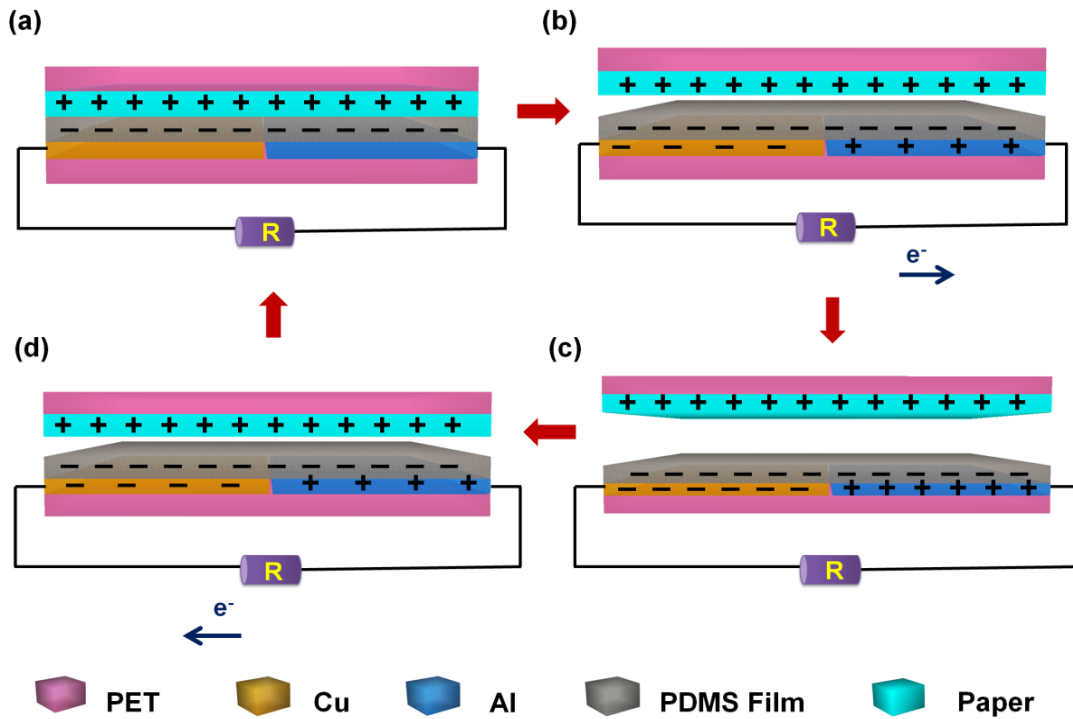
Figure 7.4 Schematic diagram of a SBP-TENG energy harvesting mechanism during contact and separation motion. (a) Initial stage, (b) releasing, (c) equilibrium state, and (d) pressing.

7.4.4. Electrical analysis of SP-TENG

Figure 7.5 (c, d) shows the rectified output voltage and short circuit current of the SP-TENG during the interaction with paper. The rectified output voltage profile reached 70 V and the corresponding current profile reached 6.5 µA during external motion of 0.5 m/s. When the external motion increased from 0.1 to 0.5 m/s, the output current from the SP-TENG increased, leading to the conclusion that increased external motion also led to a greater impact force. The

141

larger force contributes to a tighter contact between the PDMS film and paper, leading to better triboelectrification and greater current amplitude.[17]
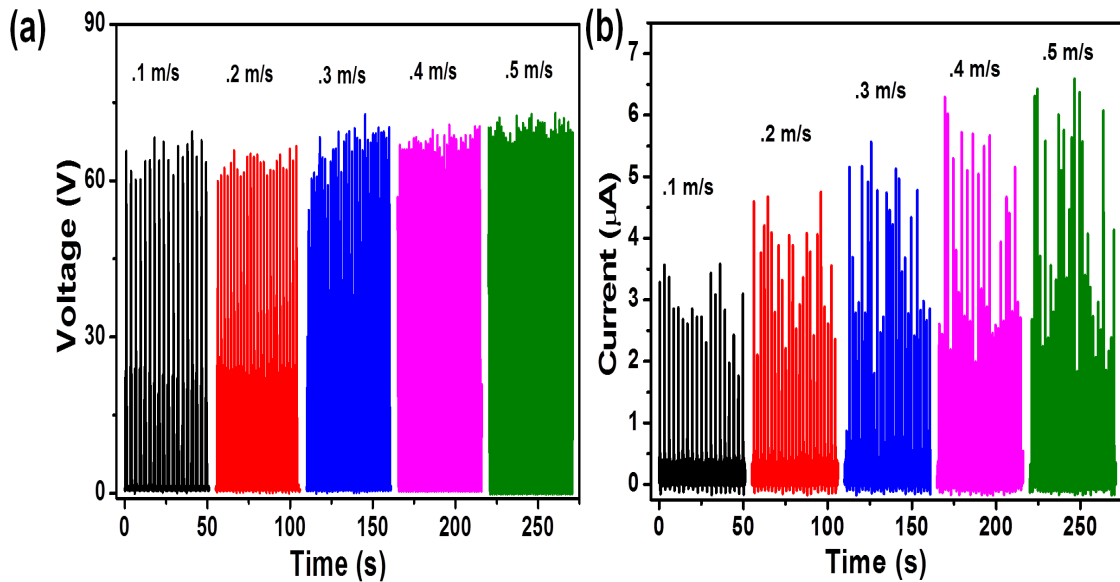
Figure 7.5 (a) Output voltage measurements and (b) short circuit current measurements of SP-TENG.

For the effective characterization of the SP-TENG as a standalone electronic device, the output voltage was measured at a series of load resistances. **Figure 7.6 (a)** shows the output voltage with respect to load resistance, where the instantaneous peak power was maximized at a load resistance of 1 MΩ, corresponding to a peak power of 643 µW and power density of 8.53 µW/m^2. This experiment illustrates that the SP-TENG is an electronic device suitable for steady current applications. To verify the charging ability of the SP-TENG, the alternating current (AC) output was converted into a pulsating direct current (DC) signal with a bridge rectifier and connected to a capacitor circuit. **Figure 7.6 (b)** shows the measured voltage curve across different load capacitors (0.1 to 0.44 µF). These results demonstrate the proficiency of the SP-

제주대학교 중앙도서관
JEJU NATIONAL UNIVERSITY LIBRARY

TENG as a DC power source to drive low-power electronic devices. To investigate the cumulative induced charge with respect to external motion, the DC electrical output from the SP-TENG was measured. **Figure 7.6 (c)** presents the rate of charge accumulation; it was found to be directly proportional to the external motion. Since an increased velocity of contact and separation movements (forward and backward) increased the triboelectric charge generation, higher charge accumulation resulted. For commercial applications, it is essential to demonstrate the device over a long period of activity; hence, we performed a stability test over 2500 cycles. Figure 7.6 (d) shows the electrical signal obtained during the cyclic stability test, where the performance of the SP-TENG remained stable over the period of operation with negligible fluctuations of the electrical signal. To verify the real-time energy harvesting and charging efficiency of the SP-TENG, the electrical output was connected to a bridge rectifier circuit, which charged a capacitor when the paper was pressed onto, and released from, the device.
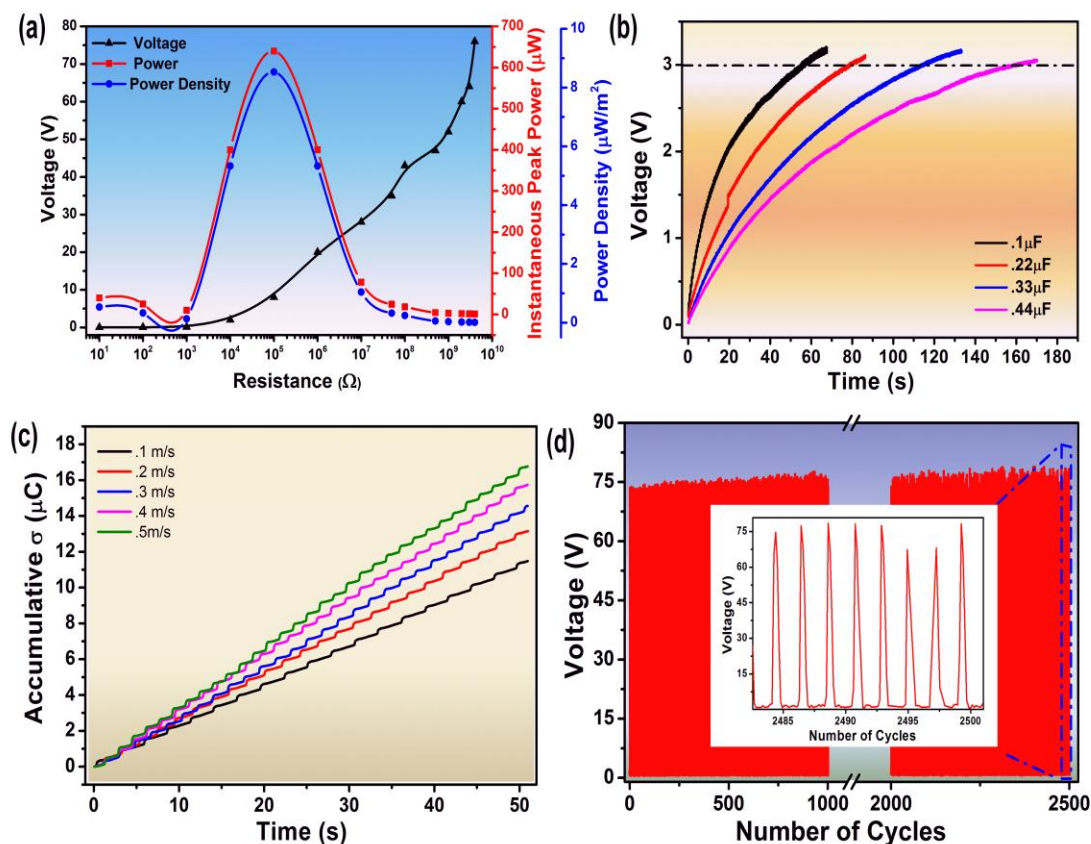
Figure 7.6 Electrical performance of the SP-TENG as an energy harvester. (a) Relationship between voltage (black), peak power (red), and power density (blue) with respect to load resistance. (b) Measured voltage curve of load capacitors from 0.1 to 0.44 µF. (c) Cumulative charge produced by the SP-TENG during external motion. (d) Output voltage of the SP-TENG during applied external motion for 2500 cycles. Inset: Magnified view of the voltage signal at the end of the stability test.

Figure 7.7 (a) shows the charging and discharging voltage curve of the 0.1-µF capacitor for various frequencies of hand presses and **Figure 7.7 (b)** shows the charge stored in the capacitor during the real-time motion. This experiment confirms the low-frequency human-motion energy harvesting capability of the SP-TENG.
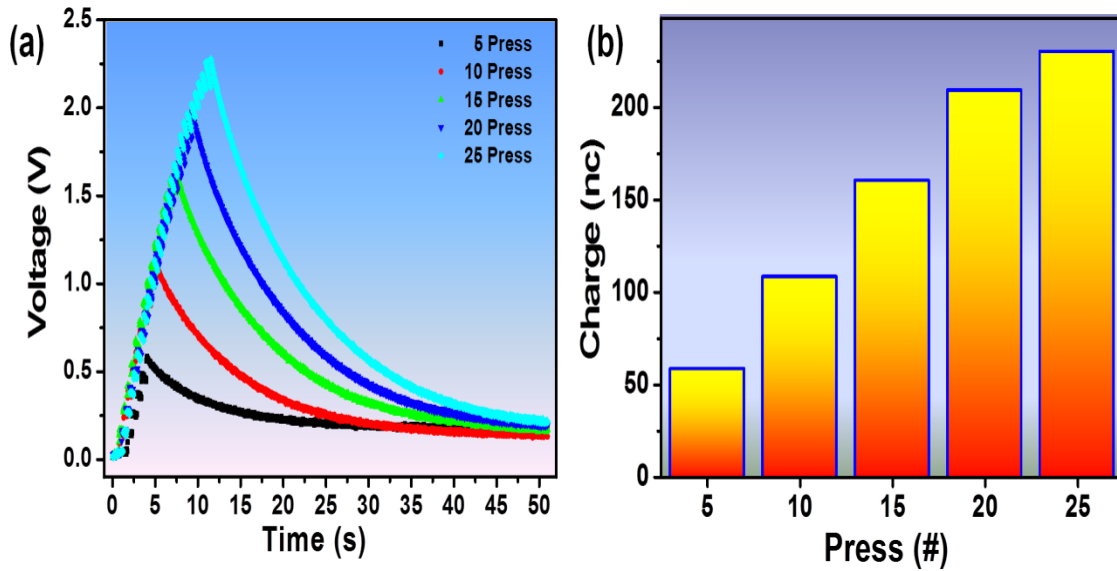
Figure 7.7 (a) The charging and discharging voltage curve of the 0.1-µF capacitor charged by the SP-TENG and (b) stored charge by hand pressing.

7.4.5. SP-TENG for Self-powered application

7.4.5.1. Self-powered pressure sensor

To demonstrate the SP-TENG as an instantaneous force sensor for self-powered sensing applications, we used an SP-TENG with dimensions of 15 × 30 mm under different instantaneous pressures. The resultant current profile for a range of pressures applied to the device is shown in **Figure 7.8 (a)**, where a clear relationship between the applied force and the output current was found. The linear relationship with detection sensitivity of 2.605 µA kPa^{-1} is plotted in **Figure 7.8 (b)**, which indicates that the SP-TENG can be used as an effective force sensor for practical applications.

제주대학교 중앙도서관
JEJU NATIONAL UNIVERSITY LIBRARY
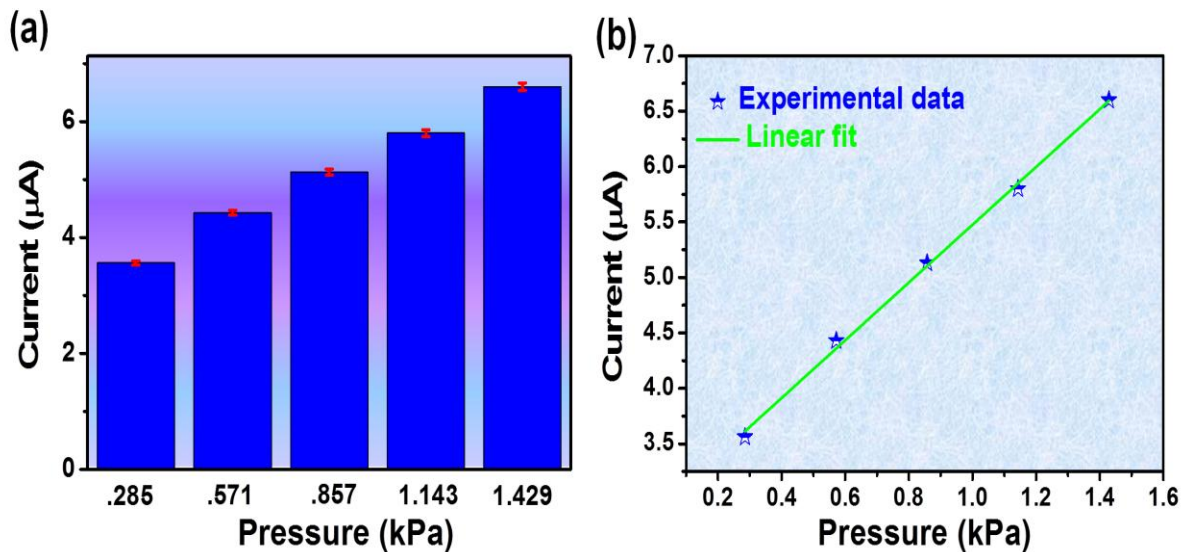
Figure 7.8 (a) Output current of the SP-TENG under external forces of 0.285 to 0.1429 kPa. (b) Relationship between the output current and the applied pressure.

7.4.5.2. Self-powered smart puzzle

Recent demands for smart gadgets and smart toys such as mini robots, mini drones, and other toys motivated us to develop an innovative design for a self-powered smart puzzle TENG (SPSP-TENG). A six-piece picture puzzle was fabricated with the image of a watermelon, which consisted of two key parts: the base, which had a logic circuit connected to SP-TENGs placed in different locations of the puzzle; and the paper moving piece attached to the rear of a puzzle piece, as shown in **Figure 7.9 (a, b)**. The paper behind the puzzle piece was adhered in such a way that it only came into contact with the SP-TENG surface if the puzzle piece was exactly matched to that position. **Figure** 7.9 **(c)** shows a digital photograph of the SPSP-TENG base and LCD. A detailed logic circuit diagram of the SPSP-TENG and a photograph of the LCD display showing "C" when the puzzle piece was matched with the correct position are shown in Figure S4. When the puzzle piece was in the correct location, the paper fixed on the backside of the

puzzle piece came into contact with the SP-TENG on the base. The interaction between the paper and PDMS then produced a charge transfer mechanism, which was collected across the two electrodes and connected to the LCD via the simple logic circuit. This changed the display to alphanumeric "C" denoting "Correct" when the piece was placed in the correct location. **Figure** 7**.**9 **(d)** shows the working model of the SPSP-TENG, where the number "3" puzzle piece was attempted at various positions and the LCD only displayed "C" when the puzzle piece was matched to the correct location. This demonstrates that the SPSP-TENG is a promising solution for energy harvesting and self-powering applications, as clearly demonstrated by its capacity for use in a self-powered toy.
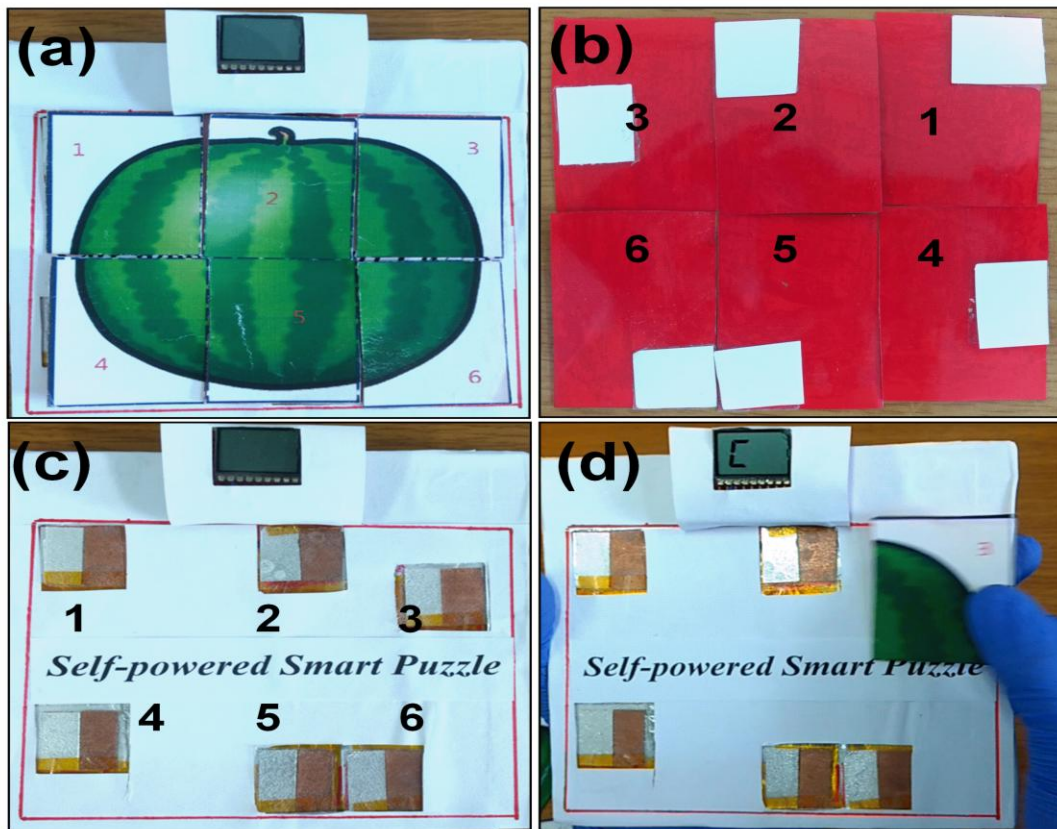
Figure 7.9 (a) Photograph of the fully assembled self-powered smart puzzle, (b) reverse side of the puzzle pieces with attached paper (contact material), and (c) base of the self-powered smart puzzle. (d) Digital photograph of the LCD displaying "C" during operation of the self-powered smart puzzle.

7.5. Conclusion

In summary, we have developed an innovative design for scavenging biomechanical energy using an eco-friendly approach and materials. The SP-TENG was demonstrated as an energy harvesting device by utilizing PDMS as active material and paper as contact material. The SP-TENG was shown to charge a capacitor rapidly, namely, within a few seconds of operation, and the long-term operation of the SP-TENG was demonstrated by stability tests, confirming that the degradation of the electrical signal was negligible. Finally, the SP-TENG was integrated to form a self-powered smart puzzle by connecting it to a simple logic circuit. This approach demonstrated that a traditional puzzle can be transformed into a smart puzzle, opening up a new approach in the field of commercializing battery-less smart toys.

7.6. References

[1] K.-W. Ko, M. Lee, S. S. Sekhon, S. K. Balasingam, C.-H. Han, and Y. Jun, "Efficiency Enhancement of Dye-Sensitized Solar Cells by the Addition of an Oxidizing Agent to the TiO_2 Paste," *ChemSusChem*, vol. 6, no. 11, pp. 2117–2123, Nov. 2013.

[2] S. K. Balasingam, A. Thirumurugan, J. S. Lee, Y. Jun, N. Shinya, L.-C. Qin, Y. M. Jung, T. J. Park, S. W. Khang, W. S. Kim, J. Kong, and H. S. Park, "Amorphous MoS_x thin-film-coated carbon fiber paper as a 3D electrode for long cycle life symmetric supercapacitors," *Nanoscale*, vol. 8, no. 23, pp. 11787–11791, 2016.

[3] S. K. Balasingam, J. S. Lee, Y. Jun, D. R. Dreyer, C. W. Bielawski, R. S. Ruoff, K. S. Suh, S. Yang, Z. Jiang, D. Zhao, G. D. Stucky, M. Kuno, V. V. Plashnitsa, R. D. Robinson, R. S. Ruoff, S. Salahuddin, J. Shan, L. Shi, M. G. Spencer, M. Terrones, W. Windl, and J. E.

Goldberger, "Molybdenum diselenide/reduced graphene oxide based hybrid nanosheets for supercapacitor applications," *Dalt. Trans.*, vol. 45, no. 23, pp. 9646–9653, 2016.

[4]   S. K. Balasingam, M. Lee, B. H. Kim, J. S. Lee, Y. Jun, J. Xiao, C. X. Wang, Y. X. Tong, G. W. Yang, Q. Zhang, R. Vajtai, and P. M. Ajayan, "Freeze-dried MoS $_2$ sponge electrodes for enhanced electrochemical energy storage," *Dalt. Trans.*, vol. 46, no. 7, pp. 2122–2128, 2017.

[5]   A. Ramadoss and S. J. Kim, "Improved activity of a graphene–TiO2 hybrid electrode in an electrochemical supercapacitor," *Carbon N. Y.*, vol. 63, pp. 434–445, Nov. 2013.

[6]   A. Ramadoss and S. J. Kim, "Enhanced supercapacitor performance using hierarchical TiO2 nanorod/Co(OH)2 nanowall array electrodes," *Electrochim. Acta*, vol. 136, pp. 105–111, Aug. 2014.

[7]   Z. L. Wang and J. Song, "Piezoelectric nanogenerators based on zinc oxide nanowire arrays.," *Science*, vol. 312, no. 5771, pp. 242–6, Apr. 2006.

[8]   R. Yang, Y. Qin, L. Dai, and Z. L. Wang, "Power generation with laterally packaged piezoelectric fine wires.," *Nat. Nanotechnol.*, vol. 4, no. 1, pp. 34–9, Jan. 2009.

[9]   A. Ramadoss, B. Saravanakumar, S. W. Lee, Y.-S. Kim, S. J. Kim, and Z. L. Wang, "Piezoelectric-driven self-charging supercapacitor power cell.," *ACS Nano*, vol. 9, no. 4, pp. 4337–45, Apr. 2015.

[10]   N. R. Alluri, B. Saravanakumar, and S. J. Kim, "Flexible-Hybrid Piezoelectric Film (BaTi(1-x)ZrxO3)-PVDF Nanogenerator as a Self-Powered Fluid Velocity Sensor.," *ACS Appl. Mater. Interfaces*, Apr. 2015.

[11] B. Saravanakumar, R. Mohan, K. Thiyagarajan, and S.-J. Kim, "Fabrication of a ZnO nanogenerator for eco-friendly biomechanical energy harvesting," *RSC Adv.*, vol. 3, no. 37, p. 16646, Aug. 2013.

[12] K. C. Aw and S. V. Praneeth, "Low frequency vibration energy harvesting from human motion using IPMC cantilever with electromagnectic transduction," *8th Annu. IEEE Int. Conf. Nano/Micro Eng. Mol. Syst.*, vol. 1, pp. 645–648, 2013.

[13] H. Guo, Z. Wen, Y. Zi, M.-H. Yeh, J. Wang, L. Zhu, C. Hu, and Z. L. Wang, "A Water-Proof Triboelectric-Electromagnetic Hybrid Generator for Energy Harvesting in Harsh Environments," *Adv. Energy Mater.*, vol. 6, no. 6, p. 1501593, Mar. 2016.

[14] T. C. Hou, Y. Yang, H. Zhang, J. Chen, L. J. Chen, and Z. Lin Wang, "Triboelectric nanogenerator built inside shoe insole for harvesting walking energy," *Nano Energy*, vol. 2, no. 5, pp. 856–862, 2013.

[15] J. H. Lee, R. Hinchet, S. K. Kim, S. Kim, and S.-W. Kim, "Shape memory polymer-based self-healing triboelectric nanogenerator," *Energy Environ. Sci.*, vol. 8, no. 12, pp. 3605–3613, Nov. 2015.

[16] Q. Liang, X. Yan, Y. Gu, K. Zhang, M. Liang, S. Lu, X. Zheng, and Y. Zhang, "Highly transparent triboelectric nanogenerator for harvesting water-related energy reinforced by antireflection coating.," *Sci. Rep.*, vol. 5, p. 9080, Jan. 2015.

[17] A. Chandrasekhar, N. R. Alluri, B. Saravanakumar, S. Selvarajan, and S.-J. Kim, "Human Interactive Triboelectric Nanogenerator as a Self-Powered Smart Seat.," *ACS Appl. Mater. Interfaces*, vol. 8, no. 15, pp. 9692–9, Apr. 2016.

[18] F.-R. Fan, Z.-Q. Tian, and Z. Lin Wang, "Flexible triboelectric generator," *Nano Energy*, vol. 1, no. 2, pp. 328–334, Mar. 2012.

[19] A. Chandrasekhar, N. R. Alluri, M. S. P. Sudhakaran, Y. S. Mok, S.-J. Kim, H. Si, S. Lu, Y. Zhang, M. K. Gupta, J. M. Baik, and S.-W. Kim, "A smart mobile pouch as a biomechanical energy harvester towards self-powered smart wireless power transfer applications," *Nanoscale*, vol. 47, pp. 1–10, 2017.

[20] Z. L. Wang, "Triboelectric nanogenerators as new energy technology and self-powered sensors - principles, problems and perspectives.," *Faraday Discuss.*, vol. 176, pp. 447–58, Jan. 2014.

[21] W. Tang, C. B. Han, C. Zhang, and Z. L. Wang, "Cover-sheet-based nanogenerator for charging mobile electronics using low-frequency body motion/vibration," *Nano Energy*, vol. 9, pp. 121–127, 2014.

[22] A. Chandrasekhar, N. R. Alluri, V. Vivekananthan, Y. Purusothaman, and S.-J. Kim, "Sustainable Freestanding Biomechanical Energy Harvesting Smart Back Pack as a Portable-Wearable Power Source," *J. Mater. Chem. C*, 2017.

[23] A. Chandrasekhar, N. R. Alluri, S. Balasubramaniam, S. Selvarajan, and S.-J. Kim, "Microcrystalline cellulose ingrained polydimethylsiloxane triboelectric nanogenerator as a self-powered locomotion detector," *J. Mater. Chem. C*, 2017.

[24] H. Zhang, Y. Yang, Y. Su, J. Chen, K. Adams, S. Lee, C. Hu, and Z. L. Wang, "Triboelectric nanogenerator for harvesting vibration energy in full space and as self-powered acceleration sensor," *Adv. Funct. Mater.*, vol. 24, no. 10, pp. 1401–1407, 2014.

[25] R. Zhang, L. Lin, Q. Jing, W. Wu, Y. Zhang, Z. Jiao, L. Yan, R. P. S. Han, and Z. L. Wang, "Nanogenerator as an active sensor for vortex capture and ambient wind-velocity detection," *Energy Environ. Sci.*, vol. 5, no. 9, p. 8528, Aug. 2012.

[26] Z.-H. Lin, G. Cheng, X. Li, P.-K. Yang, X. Wen, and Z. Lin Wang, "A multi-layered interdigitative-electrodes-based triboelectric nanogenerator for harvesting hydropower," *Nano Energy*, vol. 15, pp. 256–265, 2015.

[27] T.-H. Chang, Y.-W. Peng, C.-H. Chen, T.-W. Chang, J.-M. Wu, J.-C. Hwang, J.-Y. Gan, and Z.-H. Lin, "Protein-based contact electrification and its uses for mechanical energy harvesting and humidity detecting," 2016.

[28] T.-W. Chang, C.-W. Wang, C.-H. Chen, Y.-C. Li, C.-L. Hsu, H.-T. Chang, and Z.-H. Lin, "Controlled synthesis of Se-supported Au/Pd nanoparticles with photo-assisted electrocatalytic activity and their application in self-powered sensing systems," 2016.

[29] Q. Liang, X. Yan, X. Liao, S. Cao, X. Zheng, H. Si, S. Lu, and Y. Zhang, "Multi-unit hydroelectric generator based on contact electrification and its service behavior," *Nano Energy*, vol. 16, pp. 329–338, Sep. 2015.

[30] J. Chun, J. W. Kim, W. Jung, C.-Y. Kang, S.-W. Kim, Z. L. Wang, and J. M. Baik, "Mesoporous pores impregnated with Au nanoparticles as effective dielectrics for enhancing triboelectric nanogenerator performance in harsh environments," *Energy Environ. Sci.*, vol. 8, no. 10, pp. 3006–3012, Oct. 2015.

[31] S.-B. Jeon, D. Kim, M.-L. Seol, S.-J. Park, and Y.-K. Choi, "3-Dimensional broadband energy harvester based on internal hydrodynamic oscillation with a package structure,"

Nano Energy, vol. 17, pp. 82–90, Oct. 2015.

[32]   B. Meng, W. Tang, Z. Too, X. Zhang, M. Han, W. Liu, and H. Zhang, "A transparent single-friction-surface triboelectric generator and self-powered touch sensor," *Energy Environ. Sci.*, vol. 6, no. 11, p. 3235, Oct. 2013.

[33]   Y. Mao, D. Geng, E. Liang, and X. Wang, "Single-electrode triboelectric nanogenerator for scavenging friction energy from rolling tires," *Nano Energy*, vol. 15, pp. 227–234, Jul. 2015.

[34]   S.-Y. Shin, B. Saravanakumar, A. Ramadoss, and S. J. Kim, "Fabrication of PDMS-based triboelectric nanogenerator for self-sustained power source application," *Int. J. Energy Res.*, p. n/a-n/a, Jul. 2015.

[35]   P.-K. Yang, Z.-H. Lin, K. C. Pradel, L. Lin, X. Li, X. Wen, J.-H. He, and Z. L. Wang, "Paper-based origami triboelectric nanogenerators and self-powered pressure sensors.," *ACS Nano*, vol. 9, no. 1, pp. 901–7, Jan. 2015.

[36]   T.-C. Hou, Y. Yang, H. Zhang, J. Chen, L.-J. Chen, and Z. Lin Wang, "Triboelectric nanogenerator built inside shoe insole for harvesting walking energy," *Nano Energy*, vol. 2, no. 5, pp. 856–862, Sep. 2013.

[37]   L. E. Helseth and X. D. Guo, "Triboelectric motion sensor combined with electromagnetic induction energy harvester," *Sensors Actuators A Phys.*, May 2016.

[38]   K. Y. Lee, M. K. Gupta, and S.-W. Kim, "Transparent flexible stretchable piezoelectric and triboelectric nanogenerators for powering portable electronics," *Nano Energy*, Nov. 2014.

[39]   S. Li, S. Wang, Y. Zi, Z. Wen, L. Lin, G. Zhang, and Z. L. Wang, "Largely Improving the Robustness and Lifetime of Triboelectric Nanogenerators through Automatic Transition between Contact and Noncontact Working States," *ACS Nano*, vol. 9, no. 7, pp. 7479–7487, Jul. 2015.

CHAPTER – 8

Summary and suggestion for the future work

8.1 Summary

This chapter discusses the main conclusion of the overall thesis and the future works related to this research. This thesis mainly focuses towards the development of portable/wearable triboelectric nanogenerator for commercialization. For this, the research was focused on the portable gadgets such as mobile pouch, bag, shoe, toys and so on.

➤ First **two Chapters** discussed about the brief introduction about the TENG and fabrication and characterization techniques used in the research. The TENG devices were prepared according to the real time applications and its energy harvesting potential was investigated in detail.

➤ Human interactive triboelectric nanogenerator as a self-powered smart seat was fabricated as a lightweight, flexible, cost effective and robust, single electrode device and discussed in the **Chapter- 3**. It is an effective method for harvesting biomechanical energy from human motion utilizing widely adaptable everyday contact materials (newspaper, denim, polyethylene covers, and bus cards). The performance of SS-TENG was about 52 V and 5.2 μA for a multi-unit and it includes two self-powered applications self-powered passenger seat number indicator and a STOP-indicator using LEDs, using a simple logical circuit.

➤ Next in **Chapter - 4** presented an innovative device Smart mobile pouch as a biomechanical energy harvester towards self-powered smart wireless power transfer applications. The device harvest energy in two operational modes: lateral sliding and vertical contact and separation. A wireless power transmission setup integrated with SMP-TENG was developed and sucessfully tranfered the harvested energy for short distance. SMP-TENG is a

promising eco-friendly approach for scavenging biomechanical energy for powering next generation intelligent devices and smart phones.

➢ Microcrystalline cellulose ingrained polydimethylsiloxane triboelectric nanogenerator as a self-powered locomotion detector was proposed in **Chapter – 5**. In this chapter the device with a composite film of 5 wt% generates an open circuit voltage of 28 V and a short circuit current of 2.8 µA with an instantaneous peak power of 576 µW. The C-TENG demonstrated to be a feasible power source that can commute instantaneous operation of LEDs. Also it can act as a self-powered locomotion detector for security applications and it can be used as a wearable power source with an in-built lithium ion battery charging circuit during a range of human motion

➢ **Chapter – 6** presented a novel approach for developing sustainable freestanding biomechanical energy harvesting smart back pack as a portable-wearable power source. It is a new approach to creating irregular surfaces on polydimethylsiloxane (PDMS) film is demonstrated by recycling a plastic petri dish discarded after laboratory usage. The SBP-TENG relies on contact and separation electrification between the PDMS film and the contact materials (wool, paper, cotton, denim and polyethylene). Also the fabricated SBP-TENG can be used as self-powered emergency flash light.

➢ Smart puzzle triboelectric nanogenerator (SP-TENG) based on the contact and separation mode between a surface-modified polydimethylsiloxane film and a paper contact material was developed and discussed in **Chapter – 7**. The SP-TENG also acts as an instantaneous force sensor with detection sensitivity of 2.605 µA kPa^{-1}. A six piece SP-TENGs as puzzle was fabricated and formed a self-powered smart puzzle by connecting it to a simple logic

156

circuit. This approach improved a simple traditional puzzle, transforming it into an interactive smart puzzle

8.2 Suggestions for future work

The current research work has laid a strong foundation for the development of portable and wearable TENG and self-powered applications. This study further opens a path for commercialization of TENG in various applications such as

- To develop a TENG device by incorporating the biocompatible TENG with the traditional toys to develop battery-free toys. This is a cost-effective method for scavenging biomechanical energy which can be utilized to transform a traditional toy into a smart toy. By this approach, we can convert a clapping toy into the smart clapping toy (SCT-TENG) and duck toy into the smart duck toy (SDT-TENG). Both the SCT-TENG and SDT-TENG are based on contact and separation (CS) mode between the active layer and the upper electrode.

- A self-powered smart fishing net tracking buoy for identifying the fishing net via integration of Smart Buoy-Triboelectric Nanogenerator (SB-TENG), a power management unit, Arduino, and Bluetooth controller using a smartphone. By combining SB-TENG with the Arduino, and Bluetooth controller, it act as a self-powered wireless control system. This work will demonstrates a effective method for scavenging blue energy and its potential application as self-powered smart fishing net tracking buoy featured being user-friendly, cost-effective and self-powered.

제주대학교 중앙도서관
JEJU NATIONAL UNIVERSITY LIBRARY

APPENDIX A: List of Publications

1. **Arunkumar Chandrasekhar**, Nagamalleswara Rao Alluri, Venkateswaran Vivekananthan, Jung Hwan Park, and Sang-Jae Kim, Sustainable biomechanical energy scavenger towards self-reliant kids' interactive battery-free smart puzzle, **ACS Sustainable Chem. Eng,** 2017, 5,7310-7316.   **(I.F= 5.951)**

2. **Arunkumar Chandrasekhar**, Nagamalleswara Rao Alluri, M.S.P Sudhakaran, Young Sun Mok, Sang-Jae Kim, smart mobile pouch as a biomechanical energy harvester towards self-powered smart wireless power transfer applications, **Nanoscale,** 2017, 9, 9818-9824. **(I.F= 7.367)**

3. **Arunkumar Chandrasekhar**, Nagamalleswara Rao Alluri, Venkateswaran Vivekananthan, Yuvasree Purusothaman, Sang-Jae Kim, Sustainable freestanding biomechanical energy harvesting smart backpack as a portable –wearable power source, **J. Mater. Chem. C**, 2017, 5, 1488-1493. **(I.F= 5.256)**

4. **Arunkumar Chandrasekhar**, Nagamalleswara Rao Alluri, Balasubramaniam Saravanakumar, Sophia Selvarajan, Sang-Jae Kim, Microcrystalline cellulose ingrained polydimethylsiloxane triboelectric nanogenerator as a self-powered locomotion detector, **J. Mater. Chem. C**, 2017, 5, 1810-1815. **(I.F= 5.256)**

5. **Arunkumar Chandrasekhar**, Nagamalleswara Rao Alluri, Balasubramaniam Saravanakumar, Sophia Selvarajan, Sang-Jae Kim, Human interactive triboelectric nanogenerator as a self-powered smart seat, **ACS applied materials & interfaces**, 2016, 8, 9692-9699. **(I.F= 7.501)**

6. Yuvasree Purusothaman, Nagamalleswara Rao Alluri, **Arunkumar Chandrasekhar**, Venkateswaran Vivekananthan, Sang-Jae Kim, Regulation of charge carrier in ZnO micro-

architecture based UV/ Visible photo detector via photonic-strain induced effects, **Small,** 2017, **(I.F= 8.315)**

7. Nagamalleswara Rao Alluri, Venkateswaran Vivekananthan, **Arunkumar Chandrasekhar**, Sang-Jae Kim, Adaptable piezoelectric hemispherical composite strips using scalable groove technique for self-powered muscle monitoring system, **Nanoscale,** 2017, (**DOI:** 10.1039/C7NR06674K). **(I.F= 7.367)**

8. Nagamalleswara Rao Alluri, Yuvasree Purusothaman, **Arunkumar Chandrasekhar,** Sang-Jae Kim, Self-powered wire type UV sensor using in-situ radial growth of $BaTiO_3$ and TiO_2 nanostructures on human hair sized single Ti-wire, Chemical Engineering Journal, 2017,(**DOI:** 10.1016/j.cej.2017.11.149). **(I.F= 6.216)**

9. Venkateswaran Vivekananthan, Nagamalleswara Rao Alluri, Yuvasree Purusothaman, **Arunkumar Chandrasekhar**, A flexible, planar energy harvesting device for scavenging roadside waste mechanical energy via synergistic piezoelectric response of K 0.5 Na 0.5 NbO_3 -$BaTiO_3$ /PVDF composite films, **Nanoscale,** 2017, 9, 15122-15130. **(I.F= 7.367)**

10. Sophia Selvarajan, Nagamalleswara Rao Alluri, **Arunkumar Chandrasekhar**, Sang-Jae Kim, Unconventional, active biosensor made of piezoelectric $BaTio_3$ nanoparticles for biomolecule detection, **Sensors and Actuators B: Chemical**, 2017.1180-1187. **(I.F= 5.401)**

11. Ganesh Kumar Veerasubramani, **Arunkumar Chandrasekhar**, Sudhakaran M. S. P, Mok Young Sun and Sang-Jae Kim, Liquid electrolyte mediated flexible pouch-type hybrid supercapacitor based on binder-less core-shell nanostructures congregated with honeycomb-like porous carbon, **J. Mater. Chem. A**, 2017, **5**, 11100-11113 **(I.F= 8.867)**

12. Nagamalleswara Rao Alluri, **Arunkumar Chandrasekhar**, Ji Hyun Jeong and Sang-Jae Kim, Enhanced electroactive β-phase of the sonication-process-derived PVDF-activated carbon

composite film for efficient energy conversion and a battery-free acceleration sensor, **J. Mater. Chem. C**, 2017, 5, 4833- 4844. **(I.F= 5.256)**

13. Yuvasree Purusothaman, Nagamalleswara Rao Alluri, **Arunkumar Chandrasekhar** and Sang-Jae Kim, Harnessing low frequency-based energy using K0.5Na0.5NbO3 (KNN) pigmented piezoelectric paint system, **J. Mater. Chem. C**, 2017, (**DOI:** 10.1039/C7TC00846E). **(I.F= 5.256)**

14. Nagamalleswara Rao Alluri, **Arunkumar Chandrasekhar,** Venkateswaran Vivekananthan, Yuvasree Purusothaman, Sophia Selvarajan, Ji Hyun Jeonga and Sang-Jae Kim, Scavenging biomechanical energy using high-performance, flexible $BaTiO_3$ Nanocube/PDMS composite films**, ACS Sustainable Chemistry and Engineering,** 2017,4730-4730. **(I.F= 5.951)**

15. Nagamalleswara Rao Alluri, Sophia Selvarajan, **Arunkumar Chandrasekhar**, Balasubramaniam Saravanakumar, Ji Hyun Jeong, Sang-Jae Kim, Piezoelectric $BaTiO_3$ /alginate spherical composite beads for energy harvesting and self-powered wearable flexion sensor, **Composites Science, and Technology,** 2017, Pages 65–78. **(I.F= 4.873)**

16. Sophia Selvarajan, Nagamalleswara Rao Alluri, **Arunkumar Chandrasekhar**, Sang-Jae Kim, Direct detection of cysteine using functionalized $BaTiO_3$ nanoparticles film based self-powered biosensor, **Biosensors and Bioelectronics** (2017) 203–210. **(I.F= 7.780)**

17. Yuvasree Purusothaman, Nagamalleswara Rao Alluri, **Arunkumar Chandrasekhar**, Sang-Jae Kim, Elucidation of the unsymmetrical effect on the piezoelectric and semiconducting properties of Cd-doped 1D-ZnO nanorods, **J. Mater. Chem. C**, 2017, **5**, 415-426. **(I.F= 5.256)**

18. Sophia Selvarajan, Nagamalleswara Rao Alluri, **Arunkumar Chandrasekhar**, Sang-Jae Kim, BaTiO$_3$ nanoparticles as biomaterial film for self-powered glucose sensor application, **Sensors and Actuators B: Chemical**, 2016, 234, 395-403. **(I.F= 5.401)**

19. Nagamalleswara Rao Alluri, Sophia Selvarajan, **Arunkumar Chandrasekhar**, Balasubramaniam Saravanakumar, Gae Myoung Lee, Ji Hyun Jeong, Sang-Jae Kim, Worm structure piezoelectric energy harvester using ionotropic gelation of barium titanate-calcium alginate composite, **Energy,** (2016) 1146–1155. **(I.F= 4.52)**

20. Nagamalleswara Rao Alluri, Sophia Selvarajan, **Arunkumar Chandrasekhar**, Saravanakumar Balasubramaniam, Ji Hyun Jeong, Sang-Jae Kim, Self-powered pH sensor using piezoelectric composite worm structures derived by ionotropic gelation approach, **Sensors and Actuators B: Chemical**, 2016, 237, 534-544. **(I.F= 5.401)**

List of Submitted manuscripts

1. **Arunkumar Chandrasekhar**, Gaurav Khandelwal, Nagamalleswara Rao Alluri, Venkateswaran Vivekananthan, Sang-Jae Kim, Battery-free electronic smart toys: a step towards the commercialization of sustainable triboelectric nanogenerator.

2. **Arunkumar Chandrasekhar**, Nagamalleswara Rao Alluri, Venkateswaran Vivekananthan, Gaurav Khandelwal, Sang-Jae Kim, Portable smart buoy as a blue energy scavenger towards self-powered smart fishing net tracker to assist fishers.

3. Gaurav Khandelwal, **Arunkumar Chandrasekhar**, Nagamalleshwar Rao Alluri, Venketeswaran Vievekananthan, Sang Jae Kim, Trash to energy: a facile robust and cheap approach for mitigating environment pollutant using household triboelectric nanogenerator

APPENDIX B: Conference Presentations

International Conferences [Oral Presentation]

1. **Arunkumar Chandrasekhar**, Nagamalleswara Rao Alluri, Venkateswaran Vivekananthan, Sang-Jae Kim, Portable-Wearable Triboelectric Nanogenerators for Self-Powered Systems, **4th ICAE**, Nov. 21~ 24, 2017, Jeju, Korea.

2. **Arunkumar Chandrasekhar**, Nagamalleswara Rao Alluri, Sang-Jae Kim, Microcrystalline cellulose ingrained PDMS for intensifying triboelectric nanogenerator performance and a self-powered locomotion detector, **3rd International conference on Nanogenerators and Piezotronics** (**NGPT-2016**), 2016, June 15 ~ 17, Italy.

3. **Arunkumar Chandrasekhar**, Nagamalleswara Rao Alluri, Sang-Jae Kim, Freestanding Triboelectric Nanogenerator as a Mobile Cover and its self-powered Applications, ISPSA-2016, July 3~7, Jeju Island, Korea.

4. **Arunkumar Chandrasekhar**, Nagamalleswara Rao Alluri, Balasubramaniam Saravanakumar**,** Sophia Selvarajan, Sang-Jae Kim, Triboelectric Energy harvesting From daily life materials and the human interactive self-powered smart seat, **14th ICMR**, Nov. 23~ 25, 2015, ICC Jeju, Korea.

5. Nagamalleswara Rao Alluri, **Arunkumar Chandrasekhar**, Sang-Jae Kim, Boosted Energy Conversion via Piezo-Triboelectric Coupling in Irregular Composite Film for Self-powered Systems, NENS2017, Oct 21~23, 2017, Beijing, China.

6. Nagamalleswara Rao Alluri, Sophia Selvarajan, **Arunkumar Chandrasekhar**, Ji Hyun Jeong, Sang-Jae Kim, Hybrid Nanogenerator as a Self-Powered Air Pressure Sensor, **ICAMR-2017**, Jan 20~22, 2017, Hong Kong. [**Best Oral presentation**]

7. Nagamalleswara Rao Alluri, Sophia Selvarajan, **Arunkumar Chandrasekhar**, Ji Hyun Jeong, Sang-Jae Kim, Beads-Worm microstructures using BTO nanoparticles functionalized by Ca-Alginate biopolymer for Piezoelectric nanogenerators, **14th IUMRS-International Conference on Advanced Materials**, October 25 ~ 29, 2015, ICC Jeju, Korea.

8. Nagamalleswara Rao Alluri, Sophia Selvarajan, **Arunkumar Chandrasekhar**, Ji Hyun Jeong, Sang-Jae Kim, BTO/Ca-Alginate Linear Worm based piezoelectric nanogenerator and its self-powered application**, The 3rd International Conference on Advanced Electromaterials,** November, 17 ~ 20, 2015, ICC Jeju, Korea.

9. Nagamalleswara Rao Alluri, **Arunkumar Chandrashekar**, Sophia Selvarajan, Ji Hyun Jeong, Sang Jae Kim, High Performance Piezoelectric-Triboelectric Nanogenerator using Irregular Surface Morphology, **ISPSA-2016**, July 3 ~ 7, Jeju, Korea.

10. Sophia Selvarajan, Nagamalleswara Rao Alluri, **Arunkumar Chandrasekhar,** Sang-Jae Kim, Nonenzymatic self-powered glucose sensor based on polycrystalline thick film of BaTiO$_3$ nanoparticles, **3rd ICMR-2015,** Nov. 23 ~ 25, Jeju, Korea.

International Conferences [Poster Presentation]

1. **Arunkumar Chandrasekhar,** Nagamalleswara Rao Alluri, Venkateswaran Vivekananthan, Gaurav Khandelwal Sang-Jae Kim, Smart Puzzle Toy: A Step towards the Commercialization of Triboelectric Nanogenerator, **10th ICAMD-2017**, Dec 05~08, 2017, Jeju Island, Korea.

2. **Arunkumar Chandrasekhar**, Ananthakumar Ramadoss, Nagamalleswara Rao Alluri, Sang-Jae Kim, Human Interactive Self-Powered Smart Table for Scavenging Biomechanical Energy, **4th ICAE**, Nov. 21~ 24, 2017, Jeju, Korea. [**Awarded as a best poster**]

3. **Arunkumar Chandrasekhar,** Nagamalleswara Rao Alluri, Venkateswaran Vivekananthan, Yuvasree Purusothaman, Sang-Jae Kim, Freestanding Triboelectric Nanogenerator as Smart Back Pack, **MCARE-2017**, Feb.20~24, 2017, Jeju Island, Korea.

4. **Arunkumar Chandrasekhar**, Alluri Nagamalleswara Rao, Sudhakaran M. S. P, Young Sun Mok, Sang-Jae Kim, Human Interactive Smart Mobile Pouch Triboelectric Nanogenerator and its Self-powered Applications, **International Conference on Electronic Materials and Nanotechnology for Green Environment (ENGE 2016)**, Nov 6 ~ 9, Jeju, South Korea. [**Awarded as a best poster**]

5. **Arunkumar Chandrasekhar,** Nagamalleswara Rao Alluri, Sophia Selvarajan, Ji Hyun Jeong, Sang-Jae Kim, Piezoelectric Composite Wavy Pattern Worm Nanogenerator for Self-Powered pH Sensor, **NGPT 2016**, June 15 ~ 17, 2016, Rome, Italy.

6. **Arunkumar Chandrasekhar,** Nagamalleswara Rao Alluri, Balasubramaniam Saravanakumar**,** Sophia Selvarajan, Sang-Jae Kim, Human interactive Self-powered smart seat by Triboelectric nanogenerator, **The 3rd ICAE,** November**,** 17 ~ 20, 2015, ICC Jeju, Korea.

7. Gaurav Khandelwal, **Arunkumar Chandrasekhar** , Nagamalleswara Rao Alluri , Venkateswaran Vivekananthan, Nirmal Prashanth Maria Joseph Raja , Sang-Jae Kim, Ionic Conductor: Imparting Stretchability, Transparency and high Electrical Performance to Triboelectric Nanogenerator for Energy Harvesting Applications, **10th ICAMD-2017,** 05 ~08, 2017 Jeju, Korea.

8. Sophia Selvarajan, Nagamalleswara Rao Alluri, **Arunkumar Chandrasekhar**, Sang-Jae Kim, Multifunctional biosensor for monitoring protein-drug interactions with potential in theranostics, **10th ICAMD-2017,** 05 ~08, 2017 Jeju, Korea. [**Awarded as a best poster**]

9. Nagamalleswara Rao Alluri, Venkateswaran Vivekananthan, **Arunkumar Chandrasekhar**, Sang-Jae Kim, Enhanced output performance of piezoelectric BaTiO3 Nanocubes/PDMS composite film, **10th ICAMD-2017,** 05 ~08, 2017 Jeju, Korea.

10. Yuvasree Purusothaman, Nagamalleswara Rao Alluri, **Arunkumar Chandrasekhar**, Venkateswaran Vivekananthan, Sang-Jae Kim, Synergistic Effect on Self-Integration of PVDF/ZnO Nanorods for Enhanced Photodetector Performance, **10th ICAMD-2017**, 05 ~08, 2017 Jeju, Korea.

11. Venkateswaran Vivekananthan, Nagamalleswara Rao Alluri, Yuvasree Purusothaman, **Arunkumar Chandrasekhar**, and Sang-Jae Kim, Flexible, Planar Piezoelectric Composite Films: A Solution to Harness Waste Mechanical energy in Society, **10th ICAMD-2017,** 05 ~08, 2017 Jeju, Korea.

12. Nirmal Prashanth Maria Joseph Raj, Nagamalleswara Rao Alluri, Gaurav Khandelwal Venkateswaran Vivekananthan**, Arunkumar Chandrasekhar,** Sang-Jae Kim**,** Harnessing Waste Biomechanical Energy using Bismuth Titanate Nanoparticales/ PDMS Composite Thin films applications, **10th ICAMD-2017,** 05 ~08, 2017 Jeju, Korea.

13. Ananthakumar Ramadoss, **Arunkumar Chandrasekhar**, Saravanakumar Balasubramaniam, Nagamalleswara Rao Alluri, Sang-Jae Kim, A Rectification-Free Self-Charging Hybrid Supercapacitor Power Cell: Energy Conversion and Energy Storage, **4th ICAE**, Nov. 21~ 24, 2017, Jeju, Korea.

14. Nagamalleswara Rao Alluri, **Arunkumar Chandrasekhar**, Sang-Jae Kim, Realization of Self-Powered Acceleration Sensor using PVDF Polymer/Activated Carbon Composite Film, **4th ICAE**, Nov. 21~ 24, 2017, Jeju, Korea.

15. Gaurav Khandelwal, **Arunkumar Chandrasekhar**, Nagamalleswara Rao Alluri, Venkateswaran Vivekananthan, Sang-Jae Kim, Triboelectric Nanogenerator: An Approach Towards Utilization of Waste Material for Scavenging Biomechanical Energy, **4**[th] **ICAE**, Nov. 21~ 24, 2017, Jeju, Korea.

16. Sophia Selvarajan, Nagamalleswara Rao Alluri, **Arunkumar Chandrasekhar**, Sang-Jae Kim, Casein Micelle based Biocompatible Electronic Platform for Monitoring Protein-Drug Interactions, **4**[th] **ICAE**, Nov. 21~ 24, 2017, Jeju, Korea.

17. Yuvasree Purusothaman, Nagamalleswara Rao Alluri, **Arunkumar Chandrasekhar**, Venkateswaran Vivekananthan, Sang-Jae Kim, Significance of ZnO Micro-Architectures in Photosensing Performance Modulated by Piezo-Phototronic Effect, **4**[th]**ICAE**, Nov. 21~ 24, 2017, Jeju, Korea.

18. Venkateswaran Vivekananthan, Nagamalleswara Rao Alluri, Yuvasree Purusothaman, **Arunkumar Chandrasekhar**, and Sang-Jae Kim, Structural and piezoelectric analysis of flexible (1-x) KNN-xBTO/PVDF composite films for energy harvesting applications, **4**[th]**ICAE**, Nov. 21~ 24, 2017, Jeju, Korea.

19. Nirmal Prashanth Maria Joseph Raj, Nagamalleswara Rao Alluri, Venkateswaran Vivekananthan**, Arunkumar Chandrasekhar,** Sang-Jae Kim**,** Facile, cost-effective approach for piezoelectric Bi4Ti3O12 films for energy conversion applications, **4**[th] **ICAE**, Nov. 21~ 24, 2017, Jeju, Korea.

20. Nagamalleswara Rao Alluri, Sophia Selvarajan, **Arunkumar Chandrasekhar**, Ji Hyun Jeong, Sang-Jae Kim, Chemically synthesized $BaTiO_3$ nanostructures-polymer interfaces for self-powered devices, **MCARE-2017**, Feb.20-24, 2017, Jeju Island, Korea.

21. Ganeshkumar Verrasubramanian, **Arunkumar Chandrasekhar**, M.S.P Sudhakaran, Young Sun Mok, Sang-Jae Kim, Flexible Pouch-type Hybrid Supercapacitor **MCARE-2017**, Feb.20 ~ 24, 2017, Jeju Island, Korea.

22. Sophia Selvarajan, Alluri Nagamalleswara Rao, **Arunkumar Chandrasekhar**, Sang-Jae Kim, BaTiO3 film based nanogenerator as a self-powered/active biosensor for glucose detection, **MCARE-2017**, Feb.20 ~ 24, 2017, Jeju Island, Korea.

23. Nagamalleswara Rao Alluri, **Arunkumar Chandrasekhar,** Sophia Selvarajan, Ji Hyun Jeong, Gae Myoung Lee Sang Jae Kim, Piezoelectric-Triboelectric Hybrid Nanogenerator as a Self-Powered Air Pressure Sensor, **International Conference on Electronic Materials and Nanotechnology for Green Environment (ENGE-2016)**, Nov 6 ~ 9, Jeju, South Korea.

24. Yuvasree Purusothaman, Alluri Nagamalleswara Rao, **Arunkumar Chandrasekhar**, Sang-Jae Kim, Tuning of Piezoelectric-Semiconducting behavior of 1D-ZnO nanorods by cadmium dopant for self-powered UV sensor, **International Conference on Electronic Materials and Nanotechnology for Green Environment (ENGE 2016)**, Nov 6 ~ 9, Jeju, South Korea.

25. Sophia Selvarajan, Alluri Nagamalleswara Rao, **Arunkumar Chandrasekhar**, Sang-Jae Kim, Biothiol Responsive Film based self-powered sensor for Non-invasive analysis, **International Conference on Electronic Materials and Nanotechnology for Green Environment (ENGE 2016)**, Nov 6 ~ 9, Jeju, South Korea.

26. Nagamalleswara Rao Alluri, **Arunkumar Chandrashekar,** Sophia Selvarajan, Ji Hyun Jeong, Sang Jae Kim, Radial growth of BaTiO$_3$ nanostructures-polymer interfaces for self-powered devices, **MRS-2016 Fall Meeting**, Nov 27 ~ Dec 2, Boston, USA.

27. Sophia Selvarajan, Alluri Nagamalleswara Rao, **Arunkumar Chandrasekhar**, Sang-Jae Kim, Self-powered biosensor for direct detection of cysteine using functionalized $BaTiO_3$ Nanoparticles, **13th International Conference on Nanotek and Expo**, 2016, December 05 ~ 07, USA. [**Awarded as a best poster**]

28. Sophia Selvarajan, Nagamalleswara Rao Alluri, **Arunkumar Chandrasekhar**, Sang-Jae Kim, Self-Powered reaction based cysteine sensor and its application for sensing in Urine sample, **ISPSA-2016**, July 3~ 7, Jeju Island, Korea. [**Awarded as a best poster**]

Domestic Conferences

1. **Arunkumar Chandrasekhar,** Nagamalleswara Rao Alluri, Venkateswaran Vivekananthan, Sang-Jae Kim, Multifunctional NE-TENG for Biomechanical Energy Scavenging and Self-Powered Health Monitoring Systems, Joint symposium of Jeju National University and Nagasaki University on Science and Technology (JSST 2017) [**Award as a best paper**]

2. **Arunkumar Chandrasekhar,** Nagamalleswara Rao Alluri, Venkateswaran Vivekananthan, Sang-Jae Kim, Nickel electrode based portable triboelectric nanogenerator for scavenging bio-mechanical energy, **KMEMS 2017**, 30.3.2017 ~ 01.04.2017, Jeju Island, Korea.

3. **Arunkumar Chandrasekhar,** Nagamalleswara Rao Alluri, Venkateswaran Vivekananthan, Sang-Jae Kim, Development of Interactive Self-Reliant Smart Puzzle, Micro/Nano Engineering 2017 Spring Conference, May 25 ~ 26. , Busan, Korea.

4. Nagamalleswara Rao Alluri, **Arunkumar Chandrasekhar,** Sang-Jae Kim, Composite Piezoelectric Nanogenerator as Self-Powered Acceleration Sensor, Joint symposium of Jeju National University and Nagasaki University on Science and Technology (JSST 2017) 25.05.2017, Jeju Island, Korea. [**Award as a best paper**]

5. Venkateswaran Vivekananthan, Nagamalleswara Rao Alluri, **Arunkumar Chandrasekhar**, Yuvasree Purusothaman, Structural and Piezoelectric Analysis of Flexible (1-x)KNN-xBTO/PVDF Composite films for Energy Harvesting Applications. Joint symposium of Jeju National University and Nagasaki University on Science and Technology (JSST 2017) 25.05.2017, Jeju Island, Korea. [**Award as a best paper**]

6. Ganeshkumar Verrasubramanian, **Arunkumar Chandrasekhar**, M.S.P Sudhakaran, Young Sun Mok, Sang-Jae Kim, 유연파우치형 슈퍼커패시터의 제작, **KMEMS 2017**, Mar 30 ~ Apr 01, Jeju Island, Korea.

7. Nagamalleswara Rao Alluri, Sophia Selvarajan, **Arunkumar Chandrasekhar**, Ji Hyun Jeong, Sang-Jae Kim, Eco-Friendly Hybrid Piezoelectric Structures for Utilization of Wind and Vibration Energy, **KMEMS 2017**, Mar 30 ~ Apr 01, Jeju Island, Korea.

8. Venkateswaran Vivekananthan, Nagamalleswara Rao Alluri, **Arunkumar Chandrasekhar**, Yuvasree Purusothaman, Sang-Jae Kim, Fabrication of lead-free piezoelectric 0.96 (K0.5Na0.5) NbO3-0.04 BaTiO3 composite nanogenerator, **KMEMS 2017**, Mar 30 ~ Apr 01, Jeju Island, Korea.

9. Kim Gwan Yong, Oh Gil Seop, Kim Tae Beom, **Arunkumar Chandrasekhar**, Sang-Jae Kim, 하이브리드 마찰형 나노발전기를 이용한 블루에너지수확 Smart Buoy 의 제작, **KMEMS 2017**, Mar 30 ~ Apr 01, Jeju Island, Korea.

10. Sophia Selvarajan, Nagamalleswara Rao Alluri, **Arunkumar Chandrasekhar**, Sang-Jae Kim, Piezoelectric nanogenerators for energy harvesting and biosensing applications, **KMEMS 2017**, Mar 30 ~ Apr 01, Jeju Island, Korea.

11. Yuvasree Purusothaman, Nagamalleswara Rao Alluri, **Arunkumar Chandrasekhar,** Fabrication of low-frequency vibration sensor using K0.5Na0.5NbO3 (KNN) piezoelectric paint, **KMEMS 2017**, Mar 30 ~ Apr 01, Jeju Island, Korea.

International Workshop and School

1. The 1st school on "Nanoenergy and Nanosystems", NGPT 2016, June 15~ 17, 2016, Rome, Italy.

APPENDIX C: Patents

1. Self-Powered Child's Toy - 10-2017-0176565 (Processing).

2. Pouch Type Triboelectric Nanogenerator and Manufacturing Method of the Same- 10-2017-0155943 (Processing).

3. Self-Powered Puzzle Comprising Triboelectric Nanogenerators and Preparing Method of the Same 10-2017-0140491 (Processing).

APPENDIX C: Cover Page

Nanoscale

rsc.li/nanoscale

ROYAL SOCIETY
OF CHEMISTRY
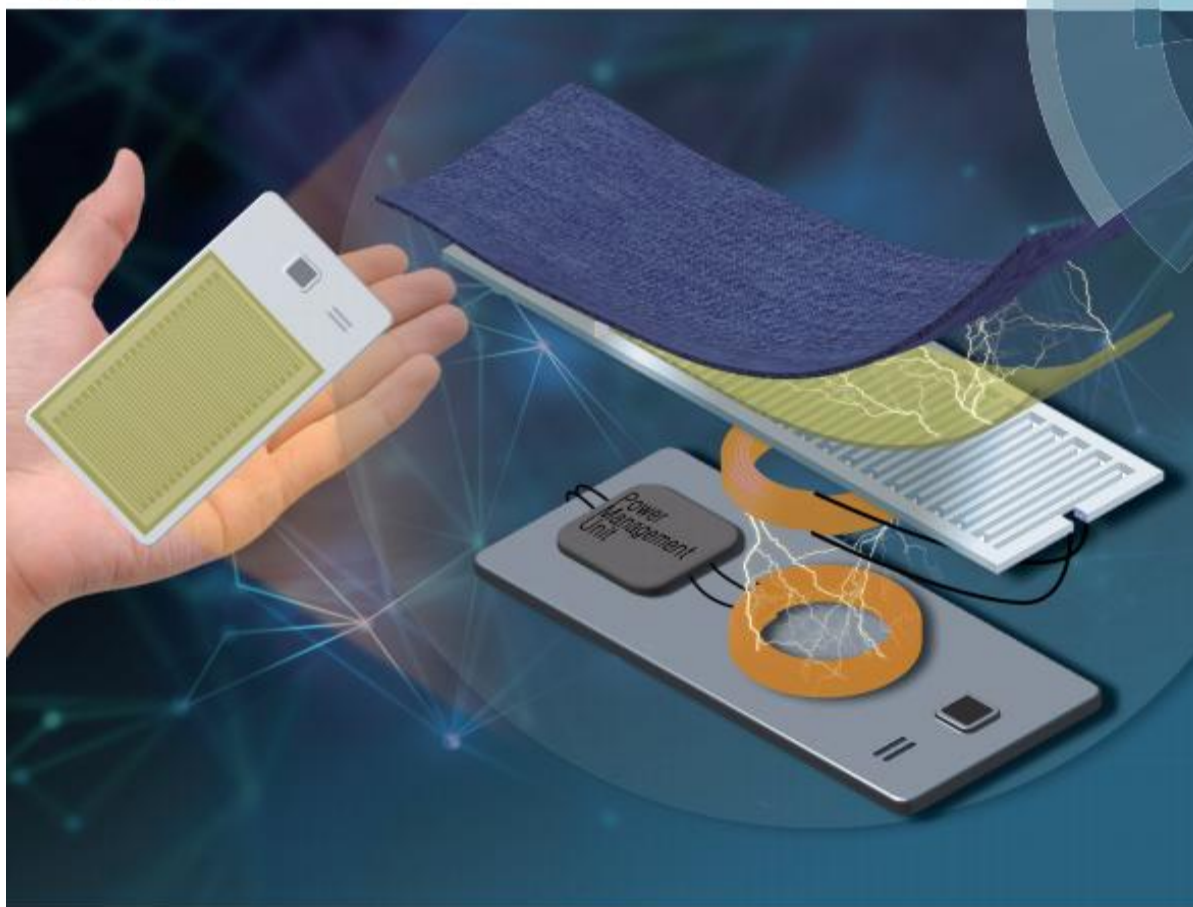
PAPER
Sang-Jae Kim et al.
A smart mobile pouch as a biomechanical energy harvester towards
self-powered smart wireless power transfer applications

NCNST

Declaration

I **Arunkumar Chandrasekhar**, hereby declare that the thesis entitled **"Triboelectric Nanogenerator for Powering Portable/Wearable Devices and its Smart Self-powered Applications"**, submitted to the Jeju National University, in partial fulfillment of the requirement for the award of the **Degree of Doctor of Philosophy in Department of Mechatronics Engineering** is a record of original and independent research work done and published by me during the period September 2014 to Feb 2018 under the supervision and guidance of **Prof. Sang Jae Kim**, Department of Mechatronics Enginnering, Jeju National University. This thesis solely based on our publication in reputed journals, and it has not been formed for the award of any other Degree/ Diploma/ Associateship/ Fellowship to any candidate of any University.

Arunkumar Chandrasekhar